

Dipartimento di Chimica Industriale “Toso Montanari”

Corso di Laurea Magistrale in

Chimica Industriale

Classe LM-71 - Scienze e Tecnologie della Chimica Industriale

**Light-Driven Birch Reduction Catalyzed by a
New Organic Photoreductant**

Tesi di laurea sperimentale

CANDIDATA

Magdalena Medrzycka

RELATORE

Chiar.mo Prof. Paolo Melchiorre

CORRELATORE

Chiar.mo Prof. Giorgio Bencivenni

Riassunto della Tesi

La riduzione di Birch, consentendo la trasformazione di semplici molecole aromatiche planari in strutture tridimensionali parzialmente saturate, ha una notevole utilità per la chimica farmaceutica. La complessità strutturale è infatti rilevante nello sviluppo di nuovi farmaci, in quanto composti tridimensionali hanno maggiore probabilità di interagire produttivamente e selettivamente con target proteici. Tradizionalmente, la riduzione di Birch avviene ad opera di un metallo alcalino (sodio, litio, o potassio) disciolto in ammoniaca liquida (Figura 1). Tuttavia, questa procedura non è sostenibile dal punto di vista ambientale e richiede temperature criogeniche per mantenere l'ammoniaca allo stato liquido. Inoltre, i metalli alcalini sono piroforici e necessitano di un'atmosfera inerte per evitare reazioni indesiderate causate dall'umidità.

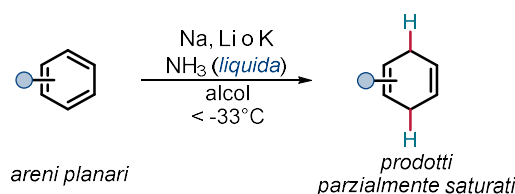


Figura 1. Riduzione di Birch tradizionale.

Per superare tali problematiche, negli ultimi decenni sono state sviluppate metodologie alternative, tra cui le più promettenti si basano su approcci meccanochimici, elettrochimici, e fotocatalitici. Tuttavia, i metodi moderni restano limitati in efficienza e tolleranza verso gruppi funzionali. In particolare, risulta difficile l'attivazione fotocatalitica di areni elettron-ricchi, a causa dei loro potenziali di riduzione altamente negativi ($E_{\text{red}} < -3.0 \text{ V vs SCE}$).

In questa tesi viene presentata una nuova metodologia fotocatalitica per effettuare la riduzione di Birch su composti aromatici elettron-ricchi in condizioni blande e con buona tolleranza di gruppi funzionali. Basandoci sui nostri studi precedenti, che avevano portato allo sviluppo del versatile fotocatalizzatore organico altamente riducente **C1** ($E_{\text{red}} = -3.38 \text{ V vs SCE}$), abbiamo disegnato ed ottimizzato un nuovo derivato indolo tiolato che promuovesse la riduzione di Birch in modo efficiente e selettivo (Figura 2a). Sebbene **C1** fosse efficace nella riduzione di derivati naftalenici, la sua applicabilità a substrati aromatici monociclici risultava fortemente limitata. Mantenendo la struttura centrale dell'indolo tiolato, l'introduzione di un gruppo benzilico in posizione α alla tionammide ha portato allo sviluppo del fotocatalizzatore **C2**. Approfonditi studi di ottimizzazione delle condizioni di reazione hanno riguardato parametri quali solvente, base, sorgenti protoniche e ammine organiche, evidenziando come la combinazione di

dimetilformammide (DMF), K_3PO_4 , metanolo e *N,N'*-dimetiletilendiammina (DMEDA) fosse la più efficace, ottenendo a partire da anisolo **1a** il prodotto selettivamente ridotto **2a** con una resa del 64% (Figura 2b).

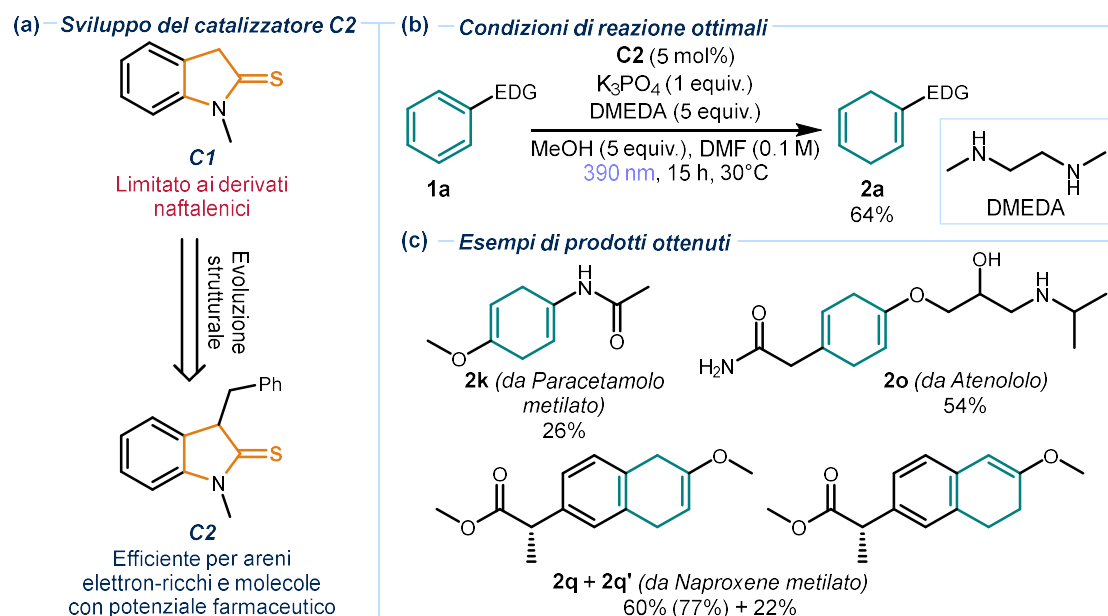


Figura 2. (a) Sviluppo del catalizzatore **C2** a partire dalla piattaforma catalitica **C1**. (b) Condizioni ottimizzate per la riduzione di Birch di areni elettron-ricchi. (c) Esempi di molecole farmaceuticamente rivelanti ridotte utilizzando la procedura mostrata.

La metodologia sviluppata è stata applicata a una vasta gamma di substrati elettron-ricchi, dimostrando una notevole tolleranza verso vari gruppi funzionali. È stato possibile ridurre ai rispettivi 1,4-diidrocicloesadieni composti aromatici semplici, come anisolo, benzene e toluene, o funzionalizzati con alcoli, ammine libere e protette, ammidi, carbamati e acetali. Particolarmente rilevante è il successo ottenuto nella riduzione di derivati farmaceutici di interesse clinico come *Paracetamolo* (**2k**), *Atenololo* (**2o**) e *Naproxene* (isomeri **2q** e **2q'**) (Figura 2c). Infine, è stata dimostrata la scalabilità della metodologia svolgendo la reazione su una scala di 3.5 mmol, senza diminuzione della resa.

Sui prodotti derivanti dalla riduzione di Birch contenenti opportune catene alcoliche, è stato possibile realizzare consecutivamente una spirociclizzazione, delineando una strategia sintetica efficace per ottenere composti spirociclici **5** strutturalmente complessi (Figura 3). Per svolgere la spirociclizzazione direttamente dopo la riduzione di Birch dei substrati **3** è stato sufficiente eliminare, per filtrazione, la base inorganica ed evaporare il solvente, senza la necessità di purificare i composti intermedi 1,4-diidroarenici **4**. In condizioni di catalisi acida con acido trifluorometansolfonico (TfOH), utilizzando cloroformio ($CHCl_3$) come solvente, è stato

possibile ottenere cicloesadieni β,γ -insaturi funzionalizzati con anelli a cinque termini eterici o acetalici **5**.

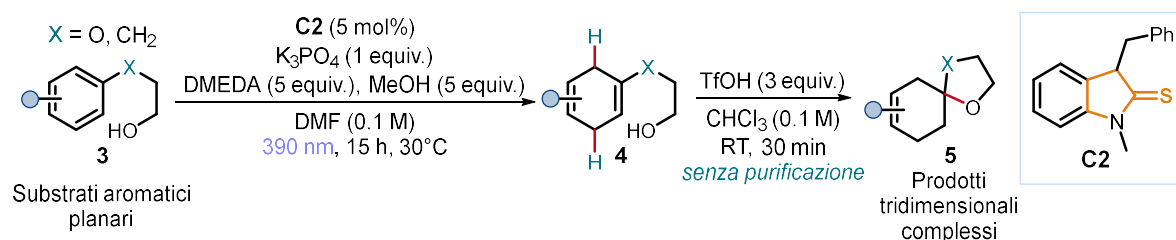


Figura 3. Spirociclizzazione che permette di trasformare areni planari **3** in prodotti tridimensionali con potenziale rilevanza farmaceutica **5**.

Dal punto di vista meccanicistico, la nostra riduzione di Birch fotocatalitica avviene tramite due trasferimenti monoelettronici (SET) seguiti da protonazione (Figura 4a). Inizialmente, il catalizzatore **C2** subisce una deprotonazione da parte della base K₃PO₄, generando l'anione tiolato **I** (Figura 4b). Sotto irradiazione luminosa di 390 nm, quest'ultimo raggiunge lo stato eccitato **I***, avente un potenziale di riduzione di -3.30 V vs. Ag/AgCl, sufficientemente negativo per ridurre tramite SET substrati aromatici **1**, portando alla formazione di radical anioni **III**. Dopo protonazione con metanolo si ottengono gli intermedi anionici **IV**, che in seguito a un secondo SET e una seconda protonazione portano alla formazione dei prodotti **2**. Il catalizzatore ossidato **II** si rigenera grazie a un trasferimento di atomo di idrogeno (HAT) promosso dalla DMEDA, complessata con un anione fosfato come mostrato nell'intermedio **VI**.

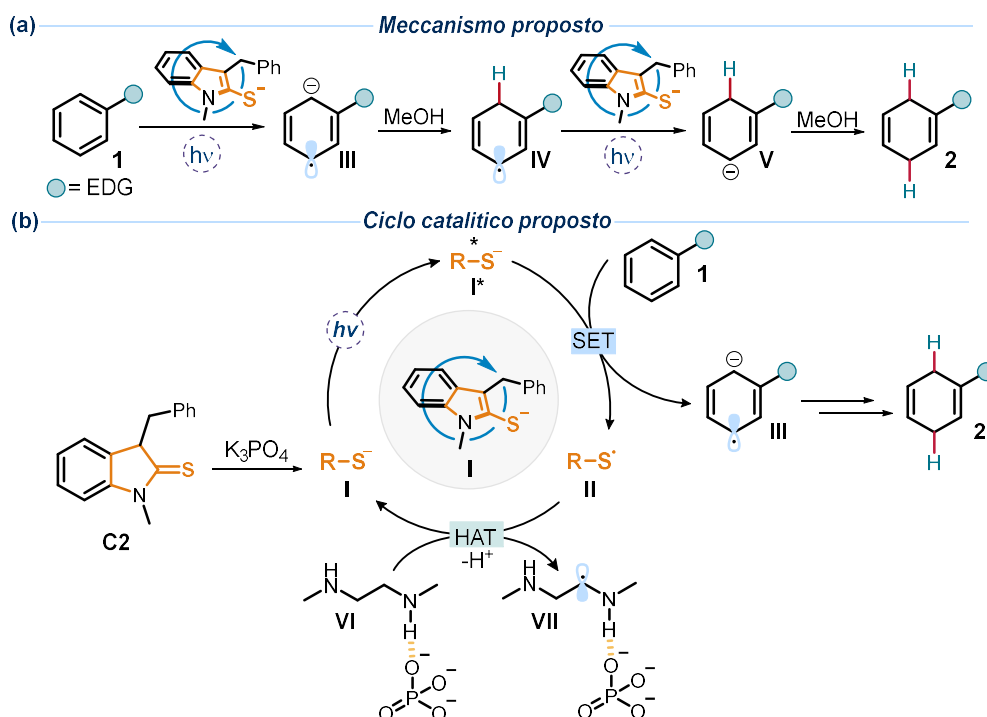


Figura 4. (a) Meccanismo (b) e ciclo catalitico proposti.

Table of Contents

1	Introduction.....	6
1.1	The Birch Reduction: Traditional Approach	7
1.2	Electrochemical Approaches to the Birch Reduction.....	9
1.3	Photocatalytic Approaches to the Birch Reduction.....	11
1.4	A New Organophotocatalytic Approach to the Birch Reduction	14
1.4.1	A Foundational Organophotocatalytic Platform from our Laboratory.....	15
2	Objectives of the Thesis	17
3	Results and Discussion	19
3.1	Optimization of the Reaction Conditions.....	19
3.2	Structural Development of the Photocatalyst.....	20
3.3	Further Optimization Studies	21
3.4	Scope of the Reaction.....	22
3.5	Sequential Spirocyclization.....	25
3.6	Mechanistic Investigations	27
3.6.1	Characterization of the Catalytic Photoactive Intermediate.....	27
3.6.2	Proposed Catalytic Cycle	28
4	Conclusions.....	30
5	Experimental Section	31
5.1	Synthesis of the Organic Photocatalysts	32
5.2	Experimental Procedures and Compound Characterization for the Birch Reduction of Benzene Derivatives.....	37
5.3	Experimental Procedures and Compound Characterization for Spirocyclization....	46
5.4	Photophysical Studies	48
5.5	Electrochemical Studies	51
5.6	Evaluation of the Excited-State Potential of the Deprotonated Photocatalyst C2 ...	52
5.7	Evidence of Hydrogen Bonding Interaction between DMEDA and K ₃ PO ₄	52
5.8	NMR Spectra.....	54

1 Introduction

The development of sustainable and efficient strategies to access key molecular scaffolds is a central goal of modern synthetic chemistry. In this context, the selective reduction of aromatic rings holds a privileged position, as it enables the conversion of readily available, planar aromatic compounds into partially saturated structures commonly found in natural products, pharmaceuticals, and agrochemicals.¹ Traditionally, this transformation has been achieved through the Birch reduction, which uses alkali metals in liquid ammonia to generate solvated electrons (Figure 1.1b).² The Birch reduction is a valuable tool in drug discovery, enabling the dearomatization of planar aromatic scaffolds. It has been proven that saturated, three-dimensional molecules tend to be more complementary to the structures of target proteins, enabling stronger protein–ligand interactions and improving drug selectivity (Figure 1.1a).³ While effective, the classical Birch protocol poses practical limitations, including harsh conditions and limited functional group tolerance. Great efforts have been made to overcome these shortcomings, including the use of alternative solvents, mechanochemistry, electrochemistry, and photocatalysis (Figure 1.1b).¹

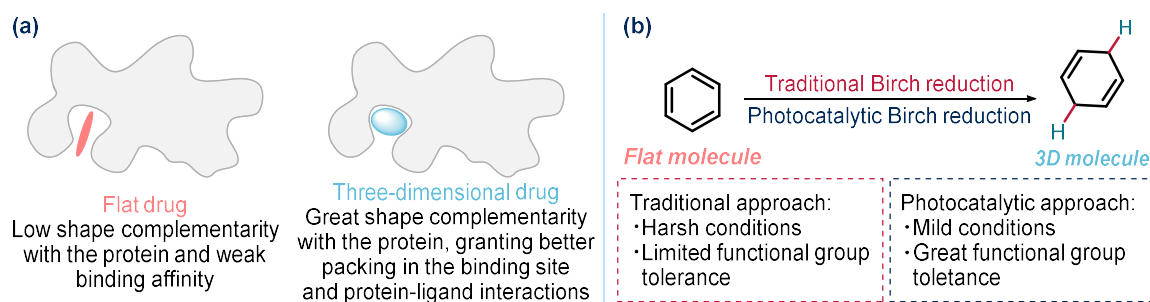


Figure 1.1. (a) Flat and three-dimensional drugs interacting with a protein. **(b)** Disadvantages of the traditional Birch reduction and the potential of a photocatalytic method.

In recent years, visible-light-induced single-electron transfer (SET) chemistry has emerged as a sustainable alternative to traditional redox processes.⁴ By harnessing light energy to trigger redox events under mild conditions, photocatalysis allows for the generation of open-shell

¹Liu, D.; Ma, J. Recent Advances in Dearomative Partial Reduction of Benzenoid Arenes. *Angew. Chem. Int. Ed.* **2024**, *63*, e202402819.

²Birch, A. J. Reduction by dissolving metals. *J. Chem. Soc.* **1944**, *66*, 430–436.

³Lovering, F.; Bikker, J.; Humblet, C. Escape from Flatland: Increasing Saturation as an Approach to Improving Clinical Success. *J. Med. Chem.* **2009**, *52*, 6752–6756.

⁴Stavness, D.; Bosque, I.; Stephenson, C. R. J. Free Radical Chemistry Enabled by Visible Light-Induced Electron Transfer. *Acc. Chem. Res.* **2016**, *49*, 2295–2306.

intermediates in a controlled fashion, opening new avenues for selective molecular activation.⁵ This thesis focuses on a photocatalytic approach to the Birch reduction, developed within the Melchiorre group as part of a broader effort to design strong organic photoreductants.⁶ During these studies, a specific catalyst was identified that could effectively promote the dearomatization of arenes under visible light. This discovery laid the foundation for the present project, which explores a sustainable, operationally simple alternative to the traditional Birch process, with a special focus on the reduction and activation of electron-rich arenes—substrates that are traditionally difficult for classical Birch conditions.

1.1 The Birch Reduction: Traditional Approach

When the Birch reduction was first introduced by the Australian chemist Artur Birch in 1944,² the reducing agent consisted of an alkali metal (sodium, lithium, or potassium) dissolved in liquid ammonia, generating a solution containing solvated electrons, metal cations, and an electride species ($[\text{Na}(\text{NH}_3)_6]^+ \text{e}^-$ when sodium was used). Alcohols were employed as cosolvents to act as proton sources (Figure 1.2).⁷

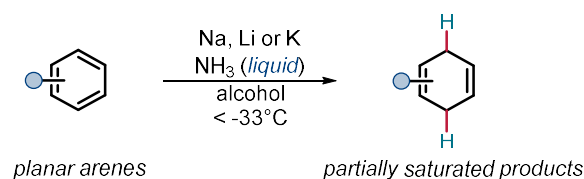


Figure 1.2. The traditional Birch reduction.

While very useful in organic synthesis, the reaction is considered hazardous and requires stringent procedures to maintain an inert atmosphere and cryogenic temperatures, necessary to keep ammonia in its liquid state. Moreover, ammonia is highly corrosive and irritating to the skin and eyes and acutely toxic if inhaled or ingested;⁸ sodium—the first metal utilized by Birch—is pyrophoric and reacts violently with water, generating flammable explosive hydrogen gas and sodium hydroxide.⁹

⁵Shaw, M. H.; Twilton, J.; MacMillan, D. W. C. Photoredox Catalysis in Organic Chemistry. *J. Org. Chem.* **2016**, *81*, 6898–6926.

⁶Wu, S.; Schiel, F.; Melchiorre, P. A General Light-Driven Organocatalytic Platform for the Activation of Inert Substrates. *Angew. Chem. Int. Ed.* **2023**, *62*, e202306364.

⁷Zimmerman, H. E. A Mechanistic Analysis of the Birch Reduction. *Chem. Res.* **2012**, *45*, 164–170.

⁸National Center for Biotechnology Information, **2025**, PubChem Compound Summary for CID 222, Ammonia.

⁹National Center for Biotechnology Information, **2025**, PubChem Compound Summary for CID 5360545, Sodium.

The mechanism of the Birch reduction exploits solvated electrons, which can reduce the arene **1**, forming the radical anion **I** (Figure 1.3a). This intermediate extracts a proton from the donor cosolvent, generating the radical **II**, which then undergoes a second SET reduction. The carbanion **III** is formed and, after a final protonation, the 1,4-dihydrocyclohexadiene product **2** is obtained.¹⁰

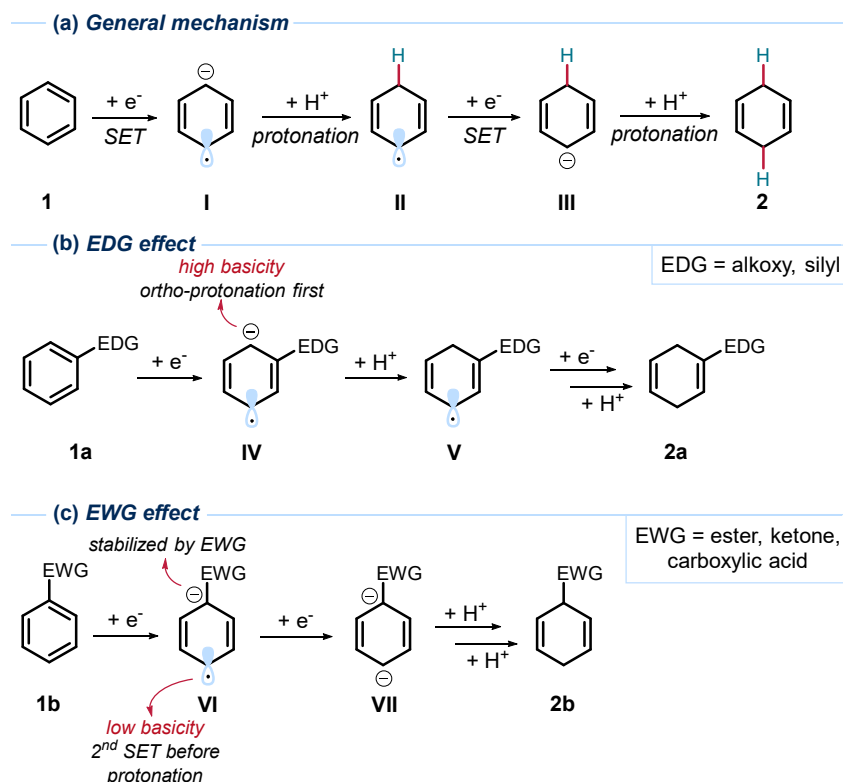


Figure 1.3. (a) General mechanism of the traditional Birch reduction. (b) Effects of electron-donating (EDG) and (c) electron-withdrawing (EWG) groups on the mechanism of the Birch reduction.

Birch observed that the reduction of a substituted aromatic ring to the corresponding 1,4-dihydro product **2** proceeds in a regioselective fashion. An electron-donating group (EDG) promotes the *ortho* and *meta* reduction (Figure 1.3b), while an electron-withdrawing group (EWG) favors reduction at the *ipso* and *para* positions (Figure 1.3c). When an EDG is present, the highest electron density of the delocalized radical anion **IV** is localized *ortho* to the EDG. This species is sufficiently basic to get protonated by an alcohol, selectively at the *ortho* position, forming the radical **V**. Then the second SET occurs, leading to a second protonation at the *meta* position, yielding product **2a**. On the other hand, the presence of an EWG stabilizes the radical anion **VI** formed in *ipso* position through electron delocalization, thus reducing its

¹⁰Brezina, K.; Jungwirth, P.; Marsalek, O. *J. Phys. Chem. Lett.* **2020**, *11*, 6032–6038.

basicity. The alcohol is not able to perform the protonation, so a second SET occurs first. The generated dianion **VII** is then selectively protonated at *para* and *ipso* positions, affording product **2b**.¹¹ This reaction works for benzene derivatives, heteroaromatic and polycyclic aromatic compounds. Depending on the structure, some of the latter suffer from either poor regioselectivity or over-reduction.¹² Other recurring problems are bond cleavage and reduction of substituent groups.

Due to the intrinsic hazards of the classic Birch reduction, chemists have been seeking safer alternatives. Benkeser *et al.* discovered that ammonia can be replaced by safer amine solvents, such as ethylamine or ethylenediamine, but their system proved less selective.¹³ In 2023, Ito *et al.* reported a mechanochemical version of the reaction.¹⁴ By employing ball milling, they conducted the reaction in solvent-free conditions. Unlike the previous procedures, this methodology tolerated aerobic conditions. However, it showed low functional group tolerance, as many groups were cleaved during the reaction, and more complex substrates often decomposed. Since none of these strategies surpassed the classic Birch reduction in efficiency, several new methods have been developed to address its practical limitations and enhance sustainability, including those based on electrochemistry and photocatalysis.

1.2 Electrochemical Approaches to the Birch Reduction

Artur Birch himself was the first to explore an electrochemical approach to his reduction.¹⁵ Subsequently, other chemists attempted to develop scalable electrochemical methods, but were limited by the narrow scope allowed under their reaction conditions.^{16,17} However, a recent study by Baran *et al.* successfully overcame these challenges.¹⁸ Their procedure employs 1,3-

¹¹Yao, S. Birch Reduction: Mechanism, Localization Effects, Products and Reaction Conditions. *Highlights in Science, Engineering and Technology* **2024**, *121*, 114–119.

¹²Rabideau, P. W.; Marcinow, Z. The Birch Reduction of Aromatic Compounds. *Organic Reactions* **1992**, *42*, 1–334.

¹³Benkeser, R. A.; Burrous, M. L.; Hazdra, J. J.; Kaiser, E. M. Reduction of Organic Compounds by Lithium in Low Molecular Weight Amines. VII. The Preparation of Dihydroaromatics. A Comparison of the Lithium-Amine and Birch Reduction Systems. *J. Org. Chem.* **1963**, *48*, 1094–1097.

¹⁴Gao, Y.; Kubota, K.; Ito, H. Mechanochemical Approach for Air-Tolerant and Extremely Fast Lithium-Based Birch Reductions in Minutes. *Angew. Chem. Int. Ed.* **2023**, *62*, e202217723.

¹⁵Birch, A. J. Electrolytic Reduction in Liquid Ammonia. *Nature* **1946**, *158*, 60.

¹⁶Benkeser, R. A.; Kaiser, E. M. An Electrochemical Method of Reducing Aromatic Compounds Selectively to Dihydro or Tetrahydro Products. *J. Am. Chem. Soc.* **1963**, *85*, 2858–2859.

¹⁷Swenson, K. E.; Zemach, D.; Nanjundiah, C.; Kariv-Miller, E. Birch reductions of methoxyaromatics in aqueous solution. *J. Org. Chem.* **1983**, *48*, 1777–1779.

¹⁸Peters, B. K.; Rodriguez, K. X.; Reisberg, S. H.; Beil, S. B.; Hickey, D. P.; Kawamata, Y.; Collins, M.; Starr, J.; Chen, L.; Udyavara, S.; Klunder, K.; Gorey, T.; Anderson, S. L.; Neurock, M.; Minter, S. D.; Baran, P. S. Scalable and safe synthetic organic electroreduction inspired by Li-ion battery chemistry. *Science* **2019**, *363*, 838–845.

dimethylurea (DMU) as the proton source, complexed with lithium cations derived from lithium bromide (Figure 1.4). The additive tri(pyrrolidin-1-yl)phosphine oxide (TPPA) provides overcharge protection for the electrodes, and tetrahydrofuran (THF) serves as the solvent. Two electrode setups have been employed for the reaction: an aluminum plate anode paired with a zinc plate cathode operating at -78°C , or a magnesium plate anode combined with a galvanized steel wire cathode functioning at ambient temperature. In both cases, the anode plays a sacrificial role.

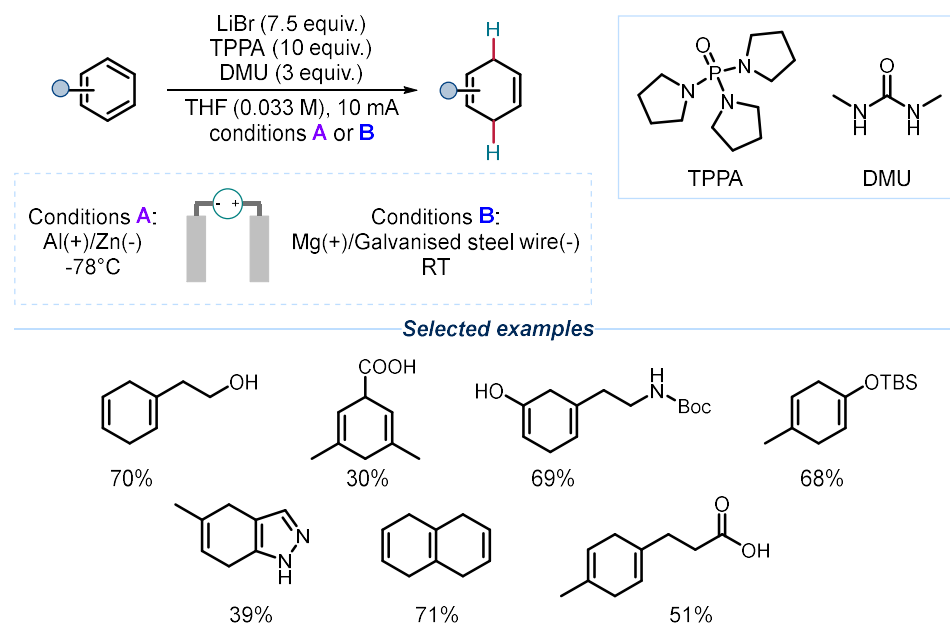


Figure 1.4. Electrochemical Birch reduction reported by Baran *et al.*

The reaction works efficiently on arenes bearing alcohol chains, carboxylic acids and alkyl, alkoxy, silyl, carbamate, or amide substituents. In substrates containing a ketone, both the aromatic ring and the ketone are reduced. For molecules containing both a carbocyclic and a heterocyclic ring, reduction selectively occurs on the carbocyclic ring. In polycyclic compounds, all aromatic rings undergo reduction (see selected examples in Figure 1.4).

Another electrochemical approach developed by the Baran laboratory was based on rapidly alternating the current's polarity (rAP), which increases chemoselectivity toward arenes while preserving other functional groups within the substrate (Figure 1.5).¹⁹ The reaction is carried out at ambient temperature in a mixture of THF and ethanol, using tetraalkylammonium

¹⁹Hayashi, K.; Griffin, J.; Harper, K. C.; Kawamata, Y.; Baran, P. S. Chemoselective (Hetero)Arene Electroreduction Enabled by Rapid Alternating Polarity. *J. Am. Chem. Soc.* **2022**, *144*, 5762–5768.

tetrafluoroborate as the electrolyte. Both electrodes are composed of reticulated vitreous carbon (RVC), while dimethylsulfide is employed as a sacrificial electron donor.

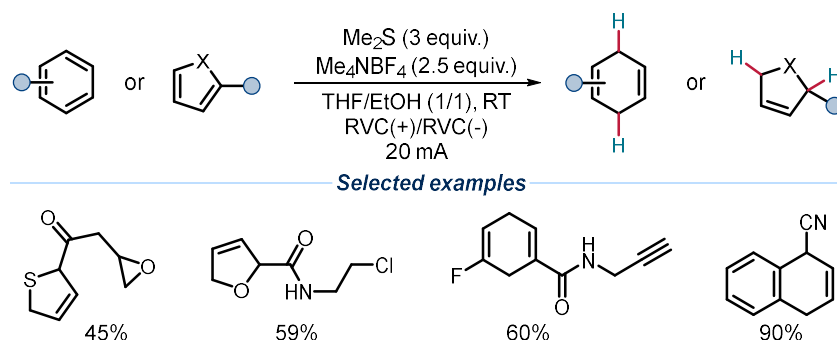


Figure 1.5. rAP electrochemical Birch reduction reported by Baran *et al.*

This methodology enables chemoselective reduction of substrates in which the arene has a higher reduction potential than other functional groups. As a result, electron-deficient arenes are more easily reduced than electron-rich ones. The rAP reduction is compatible with a broad range of functional groups on electron-poor heteroarenes (such as esters, nitriles, allyl groups, epoxides, and alkyl chlorides) and on electron-poor arenes (including allyl groups, alkynes, esters, boronate esters, alkyl chlorides, nitriles, and halogen atoms). However, it is ineffective on electron-neutral and electron-rich substrates, and chemoselective reduction fails in substrates bearing ketones, bromine atoms, or tosyl groups (selected examples of electron-deficient arenes and heteroarenes are shown in Figure 1.5).

1.3 Photocatalytic Approaches to the Birch Reduction

Photocatalysis offers a convenient alternative for organic syntheses, as light is a renewable and inexpensive energy source that permits mild reaction conditions. In 2019, König *et al.* reported a visible-light-driven methodology for arene reduction, combining energy transfer and electron transfer processes.²⁰ The reaction uses the photocatalyst Ir[dF(CF₃)ppy]₂(dtbpy)PF₆ and *N,N*-diisopropylethylamine (DIPEA) as both sacrificial electron donor and proton source for hydrogen atom transfer (HAT). The addition of MeNH₃Cl, serving as an extra proton donor, shortens the reaction time (Figure 1.6). Mechanistically, the photocatalyst is first excited by visible light and transfers its energy to the substrate **3a** via triplet energy transfer (EnT), generating the excited arene **VIII**. A second molecule of the same photocatalyst, previously excited and reduced by a sacrificial electron donor, then transfers an electron to **VIII** through a

²⁰Chatterjee, A.; König, B. Birch-Type Photoreduction of Arenes and Heteroarenes by Sensitized Electron Transfer. *Angew. Chem. Int. Ed.* **2019**, 58, 14289–14294.

SET, forming the radical anion **IX**. A HAT step converts **IX** into the more stable arene anion **X**, which is subsequently protonated to yield the 1,4-dihydro product **4a**.

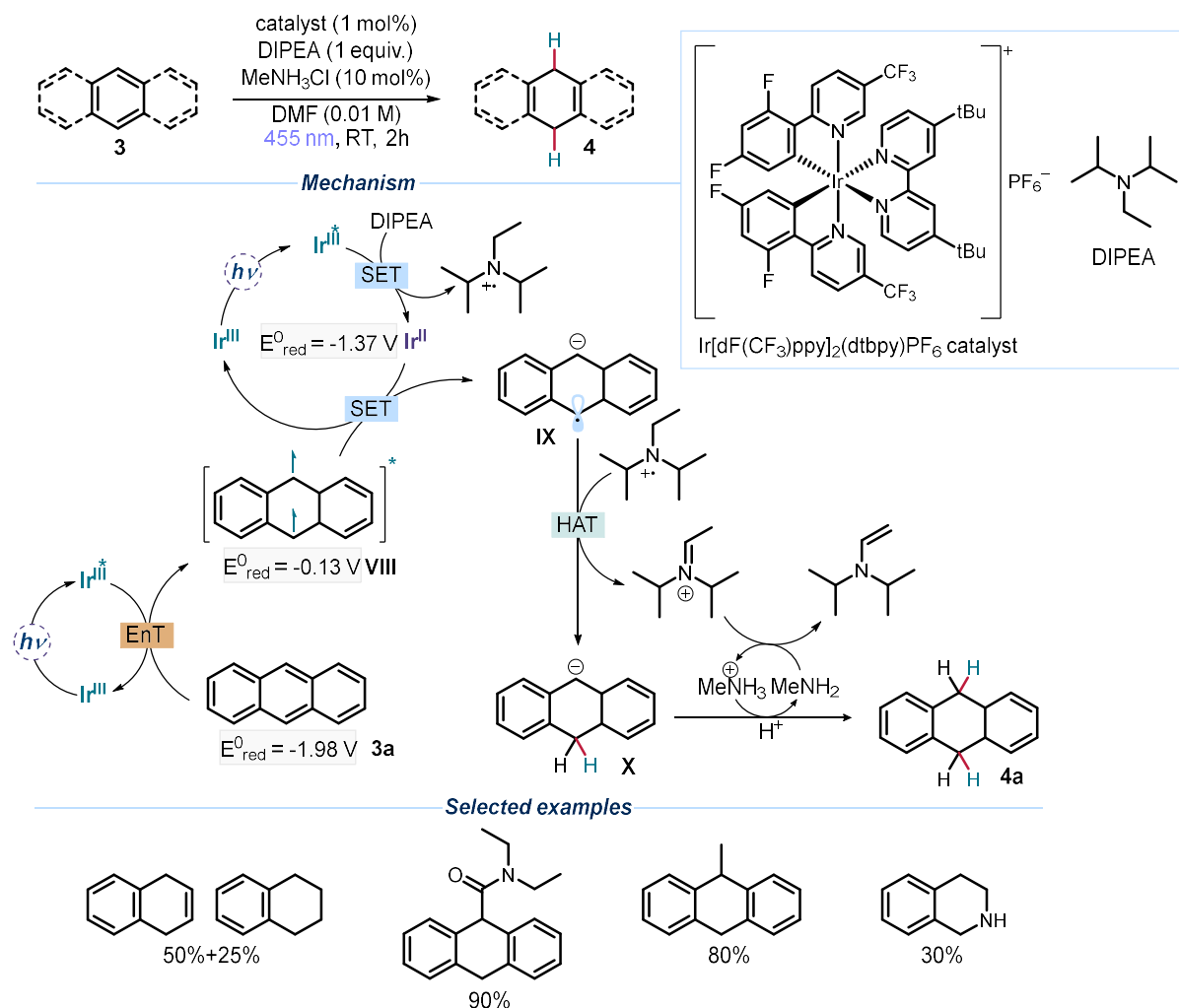


Figure 1.6. Photocatalytic Birch reduction reported by König *et al.*

This reaction is most effective on substrates that exhibit low aromatic stabilization energy and low triplet energy. Polycyclic compounds derived from anthracene and phenanthrene afford the highest yields. The reduction of naphthalene derivatives leads to a mixture of dihydro and tetrahydro products, while benzene derivatives cannot be reduced because of their high triplet energy. The reduction of anthracene-derived substrates tolerates the presence of both EDGs and EWGs, but halide and nitrile substituents are cleaved during the reduction. Heteroaromatic substrates containing nitrogen are well tolerated, especially when functionalized with EWGs (see selected examples in Figure 1.6).

Another photochemical methodology for the Birch reduction, where the catalytic cycle involves two photon absorption steps via a consecutive photoinduced electron transfer (ConPET), was

reported by Miyake *et al.*²¹ The reaction is carried out at ambient temperature in a solvent mixture of methanol and *tert*-amyl alcohol, with NMe₄OH as the proton donor and a benzo[*ghi*]perylene imide (BPI) as the photocatalyst (Figure 1.7).

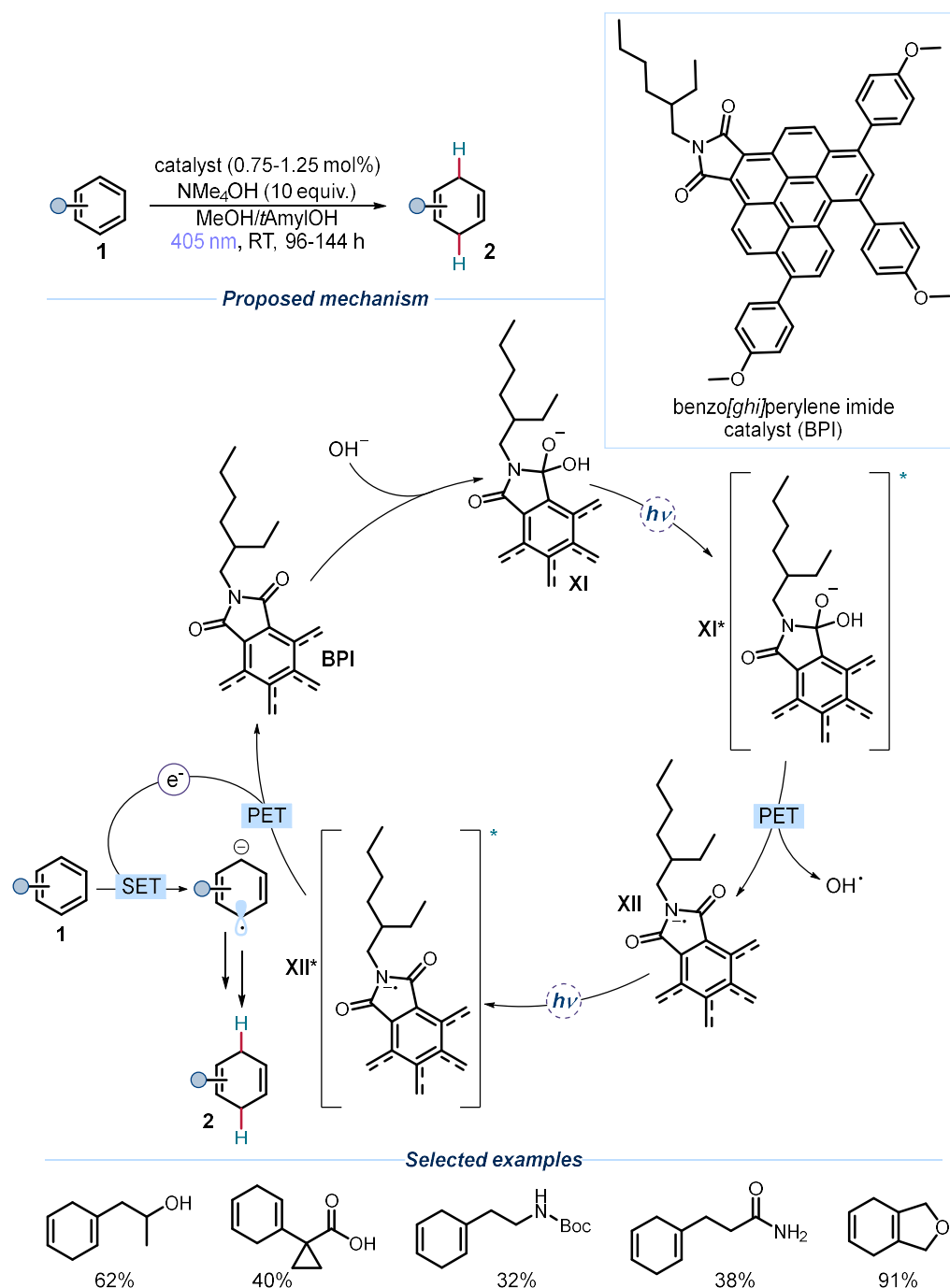


Figure 1.7. Photocatalytic Birch reduction reported by Miyake *et al.*

²¹Cole, J. P.; Chen, D. F.; Kudisch, M.; Pearson, R. M.; Lim, C. H.; Miyake, G. M. Organocatalyzed Birch Reduction Driven by Visible Light. *J. Am. Chem. Soc.* **2020**, *142*, 13573–13581.

BPI is a large, metal-free organic molecule that can undergo visible light excitation after a covalent association with a hydroxy group, which forms the anion **XI**. Upon cleavage of the C-O bond, a photoinduced electron transfer (PET) occurs, with an electron being transferred from the leaving hydroxy group to the excited photocatalyst **XI***, generating the radical anion **XII**. This species absorbs a second photon, leading to intermediate **XII***, which has acquired enough energy to release an electron for the Birch reduction of substrate **1** through a second PET. This solvated electron allows the reaction to proceed in the same manner as the classic Birch reduction, yielding the 1,4-dihydro product **2**. Under these conditions, the reaction proceeds efficiently on unsubstituted benzene and tolerates substituents such as alkyl chains, alcohols, carboxylic acids, amides, carbamates, and cyclopropane rings (selected examples are shown in Figure 1.7). However, electron-rich substrates are difficult to reduce, and compounds containing alkenes, alkynes, alkyl halides, unprotected amines, or alkoxy groups directly attached to the aromatic ring are unreactive. The method is also ineffective on nitrogen-containing heterocycles.

1.4 A New Organophotocatalytic Approach to the Birch Reduction

Despite overcoming the hazardous conditions of the classic Birch reduction, modern methodologies still suffer from significant limitations, including narrow substrate scope and low yields. In particular, current photocatalytic strategies remain ineffective for the reduction of electron-rich arenes. In this thesis, a novel photocatalytic approach is presented to address this limitation. The approach centers on a new organic photoreductant, rationally designed and optimized within the Melchiorre group, building upon their expertise in combining organocatalysis and photocatalysis.²² An organophotocatalytic platform, previously developed within our research laboratories,⁶ was adapted and optimized to function as an efficient catalyst for Birch-type reductions, with the specific goal of expanding reactivity to previously inaccessible, electron-rich aromatic substrates. During the writing of this thesis, another new effective photoreductant for the Birch reduction has been reported by Miyake *et al.*²³

²²Silvi, M.; Melchiorre, P. Enhancing the potential of enantioselective organocatalysis with light. *Nature* **2018**, *554*, 41–49.

²³Bains, A. K.; Sau, A.; Portela, B. S.; Kajal, K.; Green, A. R.; Wolff, A. M.; Patin, L. F.; Paton, R. S.; Damrauer, N. H.; Miyake, G. M. Efficient super-reducing organic photoredox catalysis with proton-coupled electron transfer mitigated back electron transfer. *Science* **2025**, *388*, 1294–1300.

1.4.1 A Foundational Organophotocatalytic Platform from our Laboratory

Building on evidence that excited-state sulfur anions can act as strong SET reductants capable of generating radicals by activation of difficult-to-reduce substrates,^{24,25} in 2023 the Melchiorre group developed a versatile indole thiolate organophotocatalyst **C1** (Figure 1.8).⁶ Upon excitation with 405 nm light, this catalyst reaches a highly reducing excited state, with a redox potential of -3.38 V vs SCE, enabling the reduction of substrates characterized by highly negative reduction potentials—features consistent with Birch-type reduction targets. Beyond arene reductions, this platform was also shown to promote hydrodechlorinations, hydrodefluorinations, reductive dephosphorylations, phosphorylations, and borylations on aromatic systems, as well as hydrodechlorination of aliphatic compounds.

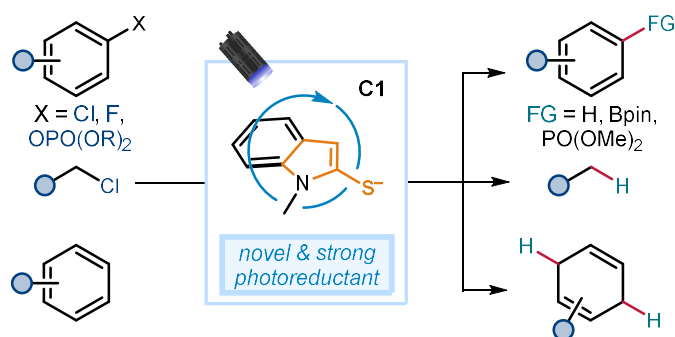


Figure 1.8. A new, versatile indole thiolate which acts as strong photoreductant upon excitation.

As depicted in Figure 1.9, the catalytically active species **XIII** is the anionic form of the photocatalyst **C1**, and therefore a base (Cs_2CO_3) was required for deprotonation. The reaction was conducted in *N*-methyl-2-pyrrolidone (NMP) with water as the proton donor. The deprotonated excited photocatalyst **XIII**^{*} performs a SET to substrate **5**, reducing it to the radical anion **XV**, which is then protonated to form intermediate **XVI**. The final 1,4-dihydroarene **6** is formed either via a second SET from the excited photocatalyst **XIII**^{*} or through a HAT from γ -terpinene. Moreover, γ -terpinene is essential for catalyst turnover, serving as the HAT partner that regenerates the photocatalyst from the thiyl radical **XIV**.

²⁴Wang, S.; Wang, H.; König, B. Light-Induced Single-Electron Transfer Processes involving Sulfur Anions as Catalysts; *J. Am. Chem. Soc.* **2021**, *143*, 15530–15537.

²⁵Wang, S.; Wang, H.; König, B. Photo-induced thiolate catalytic activation of inert C_{aryl}-hetero bonds for radical borylation; *Chem.* **2021**, *7*, 1653–1665.

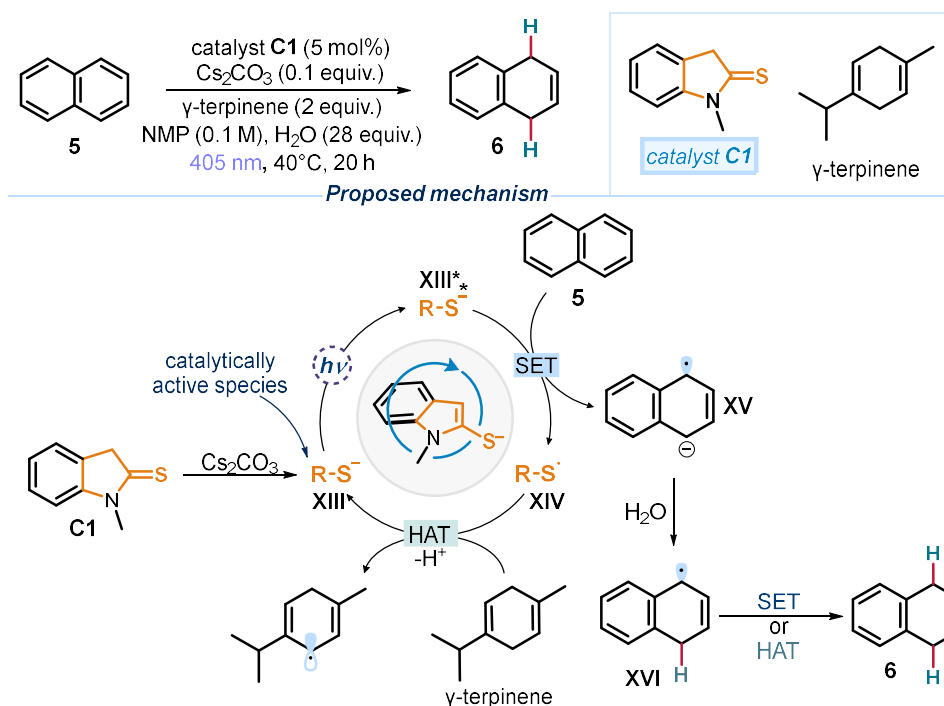


Figure I.9. Birch-type reduction using the novel, strong photoreductant **C1**: conditions and proposed mechanism.

The light-driven Birch-type reduction catalyzed by indole thiolate **C1** proved particularly effective on polyaromatic scaffolds such as naphthalene derivatives and phenanthrene; however, its effectiveness on simpler benzene-based arenes was limited.

While the method failed to activate electron-rich arenes, we considered that the strong reducing power and modular nature of this organophotocatalyst could offer a solid foundation to develop a new photocatalytic platform capable of tackling this limitation and expanding the scope of Birch-type reductions toward medically relevant substrates.

2 Objectives of the Thesis

Building on the previous limitations observed with the indole thiolate catalyst **C1**—i.e., its poor performance on electron-rich arenes—this thesis aimed to develop a next-generation organophotocatalyst capable of expanding the scope of Birch-type reductions. During my internship in the Melchiorre group, I contributed to the design and optimization of a new, bench-stable photocatalyst engineered to meet this challenge. The approach leveraged the modularity and strong reducing potential of the **C1** platform (Figure 1.8) to access reactivity with highly electron-rich aromatic substrates ($E_{\text{red}} < -3.0$ V vs SCE) via photoinduced SET, ultimately enabling their selective transformation into 1,4-dihydroarenes under mild conditions (Figure 2.1).

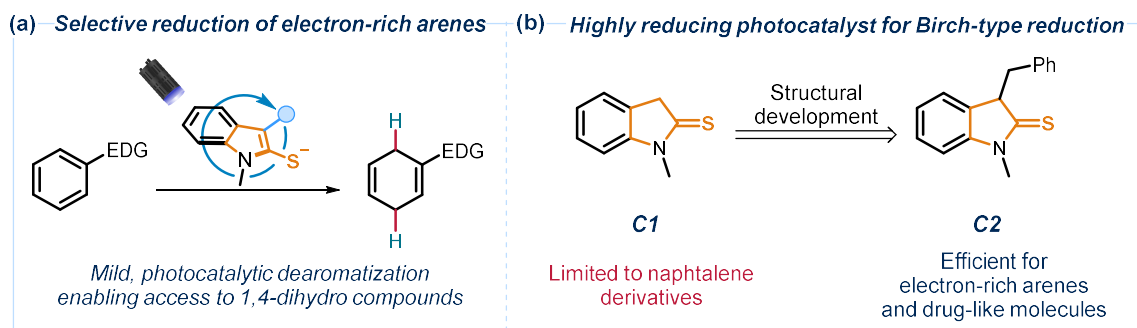


Figure 2.1. (a) Target of the thesis: selective Birch-type reduction of electron-rich arenes. (b) Evolution from the original indole thiolate platform **C1** to the newly designed photocatalyst **C2** developed in this thesis.

After optimizing the Birch-type reduction methodology, we shifted focus to broadening its scope, targeting biologically relevant and drug-like substrates. Furthermore, we performed a spirocyclization on 1,4-cyclohexadiene products bearing alcohol side chains (Figure 2.2).

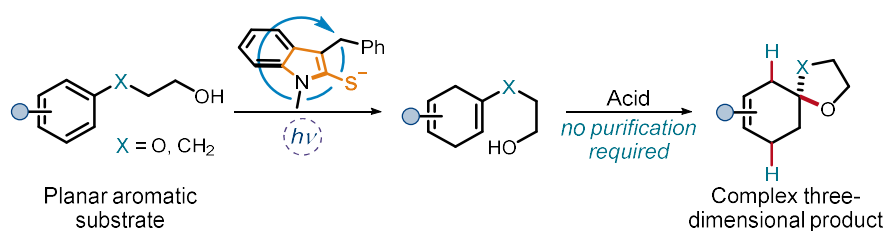


Figure 2.2. Spirocyclization to transform flat arenes into complex, three-dimensional scaffolds with enhanced structural diversity and potential pharmaceutical relevance.

Starting from planar aromatic scaffolds, these two sequential reactions provide straightforward access to architecturally spirocyclic frameworks. Considering that most biologically active natural products exhibit considerable molecular complexity, reactions that access this type of

structural diversity are potentially useful for drug design.²⁶ This part of the project was conducted in collaboration with *Johnson & Johnson* Toledo, particularly with Dr. Antonio Misale, with whom I maintained constant contact.

I was part of a team composed of a postdoctoral researcher (Dr. Andrea Palone) and three PhD students (Florian Schiel, Roberta Coccia, and Luca Di Martile). My main contributions involved investigating the substrate scope of the Birch reduction and developing the spirocyclization studies.

²⁶Arya, P.; Joseph, R.; Gan, Z.; Rakic, B. Exploring New Chemical Space by Stereocontrolled Diversity-Oriented Synthesis. *Chemistry & Biology* **2005**, *12*, 163–180.

3 Results and Discussion

Our recently reported photoreductant catalyst **C1** (discussed in the previous section 1.4.1) was effective to reduce unactivated arenes, such as naphthalene derivatives, to their corresponding 1,4-dihydro products. However, electron-rich substrates showed limited conversion, with appreciable yields only observed for benzene and anisole.²⁷ To address this limitation, we aimed to develop a more general and efficient photocatalytic system for the Birch-type reduction of electron-rich benzene derivatives.

3.1 Optimization of the Reaction Conditions

The following section outlines optimization studies aimed at improving the photocatalytic reduction of electron-rich benzene derivatives to their corresponding 1,4-dihydro products, using anisole **1a** as the model substrate. Under previously established conditions—utilizing photocatalyst **C1** (5 mol%), γ -terpinene (2 equivalents), and Cs_2CO_3 (0.1 equivalent) in NMP under 405 nm light irradiation—product **2a** was formed in 38% yield after 6 hours (Figure 3.1). However, **2a** displayed limited stability under these conditions, with prolonged reaction times resulting in substantial decomposition (<5% yield after 20 hours). Replacing γ -terpinene with *N,N'*-dimethylethylenediamine (DMEDA, 5 equivalents) and using methanol as a proton donor (5 equivalents) led to a significant improvement in the stability of product **2a** (Figure 3.1). The reaction was further optimized by switching to dimethylformamide (DMF) as the solvent and using K_3PO_4 (1 equivalent) as the base, with irradiation at 390 nm. Under these modified conditions, the yield of **2a** increased to 45% after 15 hours. The experiments were conducted in a temperature-controlled 3D-printed photoreactor maintained at 30 °C.²⁸

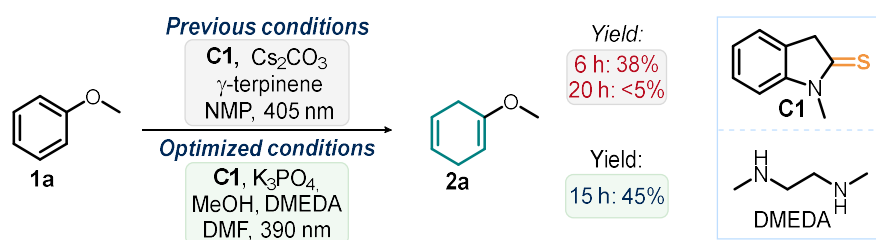


Figure 3.1. Comparison of the reaction conditions from the previous system based on catalyst **C1**,⁶ and the optimized conditions found for the reduction of benzene derivatives.

²⁷This work is still in progress and not published yet.

²⁸Schiel, F.; Peinsipp, C.; Kornigg, S.; Böse, D. A 3D-Printed Open Access Photoreactor Designed for Versatile Applications in Photoredox- and Photoelectrochemical Synthesis. *ChemPhotoChem* **2021**, 5, 431–437.

3.2 Structural Development of the Photocatalyst

The indole thiolate catalyst **C1** afforded the desired product **2a** in 45% yield (Figure 3.2, entry 1). We initially explored the impact of modifying the catalyst structure to improve efficiency. Introducing a benzyl group at the α -position of the thioamide (catalyst **C2**) proved beneficial for reactivity, leading to an improved yield of 64% (entry 2). In contrast, the α,α -dimethylated catalyst **C3** showed no catalytic activity, likely because it could not be deprotonated to generate the photoactive anionic species (entry 3). We then evaluated the electronic properties of the photocatalyst by introducing substituents on the benzyl moiety. The introduction of a *para*-methoxy substituent (catalyst **C4**) had minimal effect on performance, resulting in a 65% yield of **2a** (entry 4). On the other hand, electron-deficient variants—such as catalyst **C5** bearing a nitrile group or **C6** incorporating a naphthalene moiety—completely inhibited reactivity, with only the starting material recovered (entries 5–6). Substituting the benzyl group with an aliphatic chain (catalyst **C7**) or employing the fully saturated analogue of **C2** (catalyst **C8**) led to similar yields of 59–65% (entries 7–8), suggesting that aromaticity at the α -position is not essential for catalytic performance. The free thioamide catalyst **C9**, which also lacks an α -substituent, exhibited significantly reduced efficiency, affording product **2a** with only 25% yield (entry 9).

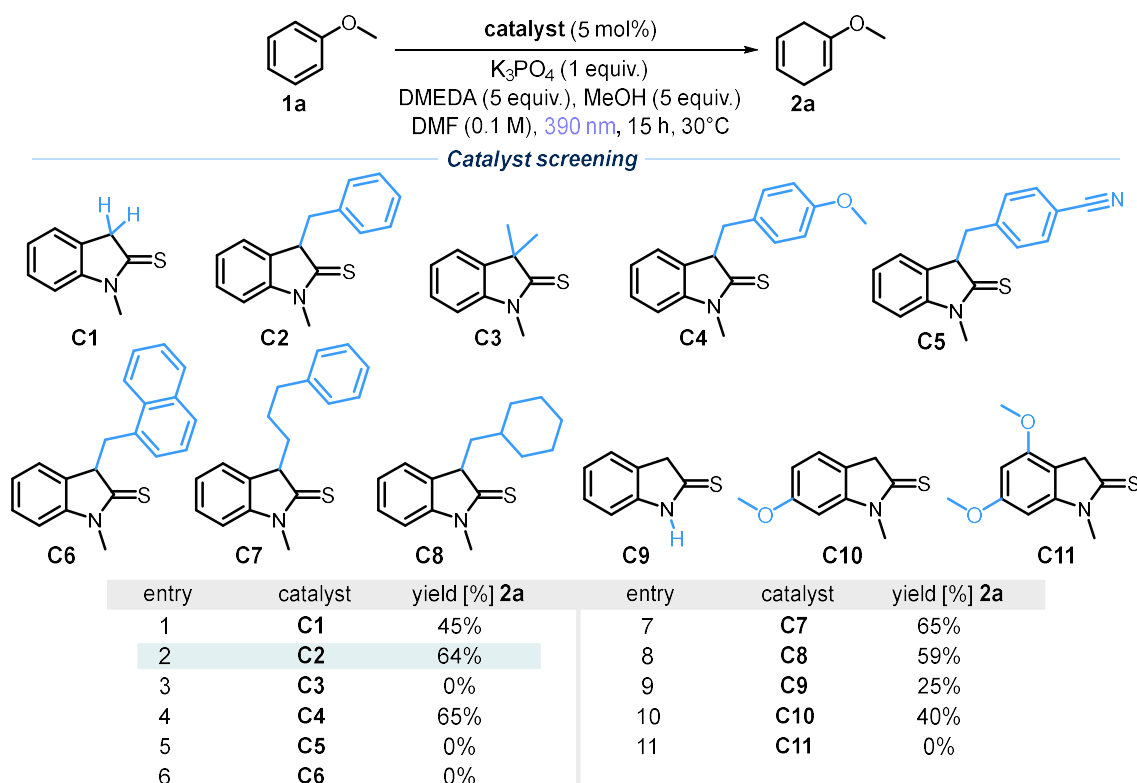


Figure 3.2. Catalyst screening for the Birch reduction of anisole **1a** performed on a 0.1 mmol scale. Yields of **2a** were determined by 1H NMR analysis of the crude mixtures using mesitylene as the internal standard.

Finally, we evaluated modifications to the indoline-2-thione core. Introducing a methoxy group to the arene moiety (catalyst **C10**) afforded **2a** in 40% yield (entry 10), comparable to that of **C1**. However, the presence of a second methoxy substituent (catalyst **C11**) completely suppressed catalytic activity, and no product was detected (entry 11).

Catalyst **C2** was ultimately selected for further investigations due to its straightforward and cost-efficient synthesis, which involves a simple condensation between *N*-methyl oxindole and readily available, inexpensive benzaldehyde, followed by thiation with Lawesson's reagent. This practical and efficient synthetic route is detailed in section 5.1.

3.3 Further Optimization Studies

Next, the influence of the organic amine used as an additive was investigated, using catalyst **C2** (Figure 3.3). The use of DMEDA (**A1**) proved most effective, affording a 64% yield of product **2a** (Figure 3.3, entry 1). Its analogues tetramethylethylenediamine (**A2**) and ethylenediamine (**A3**) delivered significantly lower yields of 21% (entry 2) and 29% (entry 3), respectively.

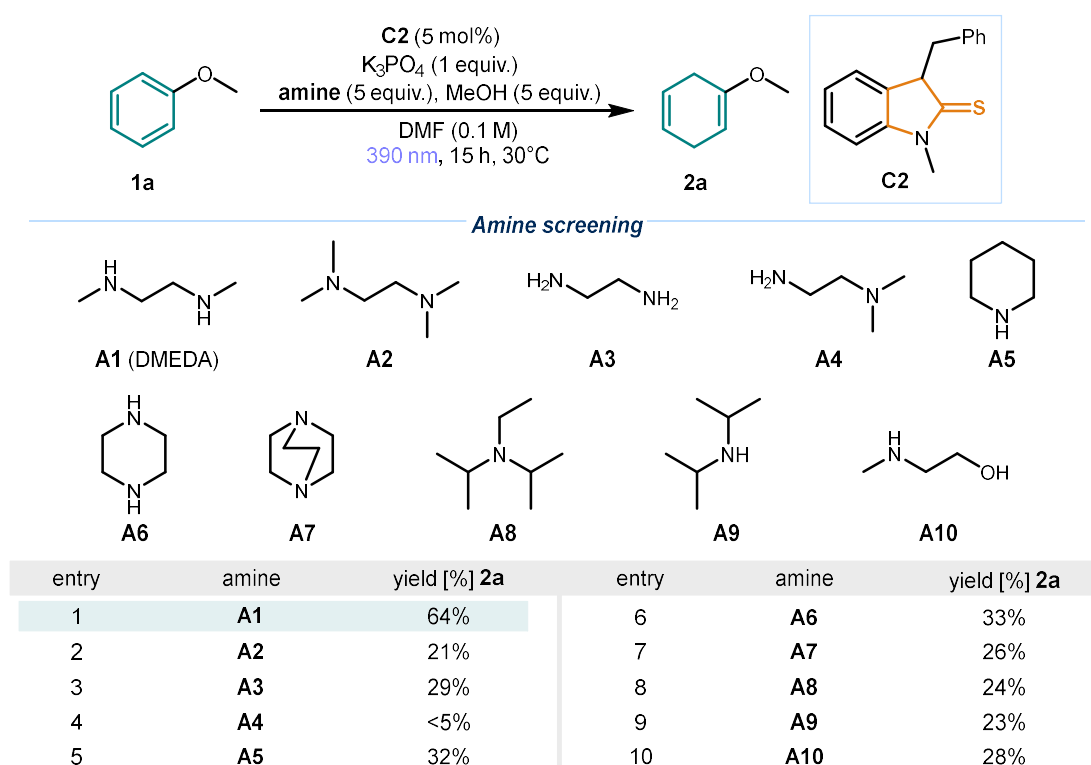


Figure 3.3. Organic amine screening for the Birch reduction of anisole **1a** performed on a 0.1 mmol scale. Yields of **2a** were determined by ¹H NMR analysis of the crude mixtures using mesitylene as internal standard.

The asymmetric *N,N*-dimethylethylenediamine (**A4**) afforded only traces of the product (entry 4). Cyclic organic amines, including piperidine (**A5**), piperazine (**A6**), and 1,4-diazabicyclo[2.2.2]octane (**A7**) afforded **2a** in yields ranging from 26% to 33% (entries 5–7).

Monoamines, such as diisopropylethylamine (**A8**), diisopropylamine (**A9**) and *N*-methylethanolamine (**A10**) were less effective, delivering yields between 23% and 28% (entries 8–10).

Subsequent optimization focused on evaluating the influence of the inorganic base, demonstrating that K_3PO_4 could be effectively replaced by Cs_2CO_3 or potassium methoxide (KOMe), which delivered comparable yields of product **2a** (57% and 66%, respectively, Figure 3.4, entries 1–3). Among the evaluated solvents, DMF proved essential for the reaction. No product formation was observed when using acetonitrile (ACN) or dimethyl sulfoxide (DMSO) as the solvent (entries 4–5). Control experiments were carried out to verify that all components were essential for the reactivity: the reaction did not occur without light, the photocatalyst, an inorganic base, an organic amine, or methanol (entries 6–10).

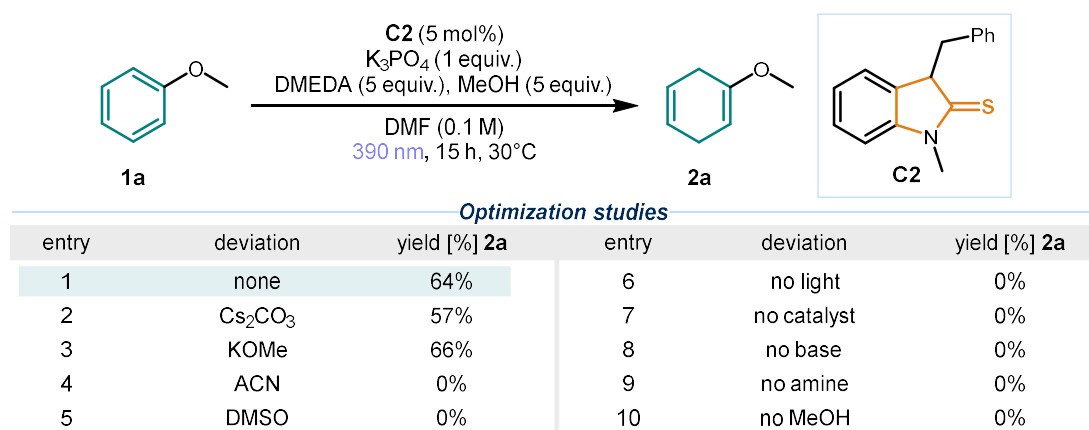


Figure 3.4. Further reaction optimization for the anisole reduction performed on a 0.2 mmol scale. Yields of **2a** determined by 1H NMR analysis of the crude mixture using mesitylene as internal standard.

3.4 Scope of the Reaction

With the optimized conditions in hand (Figure 3.4, entry 1), the scope of the Birch reduction was explored (Figure 3.5). Catalyst **C2** enabled the reduction of simple aromatic molecules—such as benzene (product **2b**), toluene (**2c**), and indane (**2d**)—into the respective 1,4-dihydrocyclohexadienes, with yields ranging from 52% to 58%. Free alcohols were tolerated as well (products **2e**, **2f**), affording comparable yields. The reaction was successful when an amine group was present on the substrate—both free (**2g**, 52% yield) and protected with a *tert*-butoxycarbonyl (Boc) group (**2h**, 55% yield). Compounds containing an amide were selectively reduced on the arene ring (products **2i–2k**), including a derivative of the analgesic and antipyretic drug *Paracetamol* (**2k**). The reduction of a chiral enantiopure amine led to the chiral product **2l** in 49% yield, with full retention of stereochemistry at both stereocenters,

indicating that no racemization occurred. The reaction tolerated the presence of a carbamate and an acetal protecting group, affording products **2m** and **2n** in 54% and 43% yields, respectively.

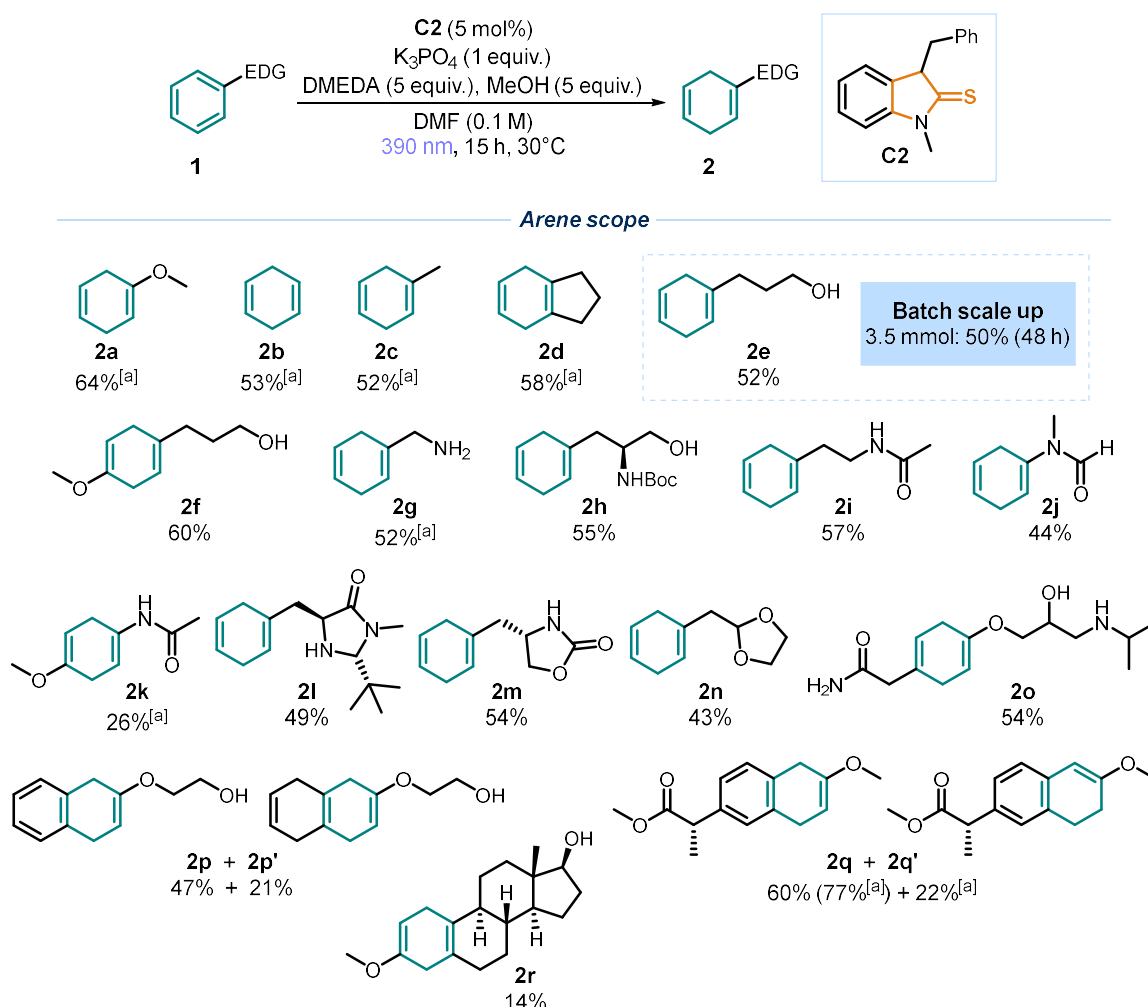


Figure 3.5. Scope of the Birch reduction performed on a 0.2 mmol scale using photocatalyst **C2** (5 mol%) in a temperature-controlled 3D-printed photoreactor²⁸ at 30°C under illumination by two Kessil lamps at 390 nm for 15 hours. Yields of products **2** refer to isolated compounds. ^[a] Yields determined by ¹H NMR analysis of the crude mixtures using mesitylene as internal standard.

We then evaluated the possibility to use our organic platform to reduce drug-relevant molecules. *Atenolol*, used as β -blocker to treat hypertension, containing an unprotected amide, alcohol and amine group, was reduced successfully to the corresponding product **2o** in 54% yield. The reduction of a naphthalene derivative led to a mixture of the 1,4-dihydro product **2p** (47% yield) and the over-reduced compound **2p'** (21% yield). A methylated derivative of the anti-inflammatory drug *Naproxen* was reduced successfully, delivering the isomers **2q** and **2q'** in yields of 60% and 22%. Finally, a derivative of the steroid hormone *Estradiol* was converted to the corresponding product **2r** in 14% yield.

A batch scale-up of the reaction using catalyst **C2** was performed on a 3.5 mmol scale using substrate **1e**, employing the same photoreactor as used for the 0.2 mmol small-scale procedure (see the experimental section 5.2 for details on the set-up). The only notable modification was an extended reaction time, increased from 15 to 48 hours. The reduced product **2e** was obtained in 50% yield, closely matching the 52% yield achieved on the small-scale procedure.

While the protocol demonstrated wide applicability, certain substrates remained unreactive under the optimized conditions, highlighting current limitations (Figure 3.6). Benzene derivatives bearing electron-withdrawing groups (EWGs) on the aromatic ring—such as amides (**1s**), esters (**1t**), and carboxylic acids (**1u**)—showed no conversion, with only the starting materials recovered. Although the reduction of these arenes should be thermodynamically easier (for example, $E_{\text{red}}(\mathbf{1t}) = -2.11 \text{ V vs. SCE}$) compared to electron-rich derivatives ($E_{\text{red}}(\mathbf{1b}) = -3.4 \text{ V vs. SCE}$), the lack in reactivity can be explained by an unfavourable protonation step with methanol, as indicated by the relatively high pK_a of the corresponding radical anion (radical anion of **1t**, $\text{pK}_a = 5.5$, see Figure 1.9 for the mechanism, protonation step of intermediate **XV** to afford **XVI**).²⁹ This likely results in an unproductive back-electron transfer (BET), regenerating the starting material.

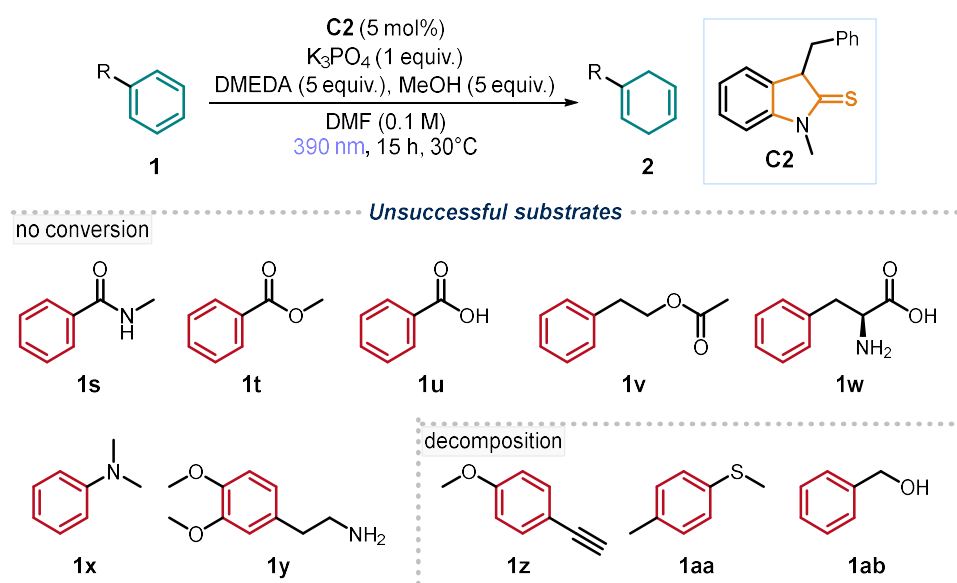


Figure 3.6. Unsuccessful substrates.

Compounds bearing ester (**1v**) and carboxylic acid (**1w**) functionalities on side chains showed no conversion, with these groups remaining intact. Also highly electron-rich benzene

²⁹Wei, D.; Bu, J.; Zhang, S.; Chen, S.; Yue, L.; Li, X.; Liang, K.; Xia, C. Light-Driven Stepwise Reduction of Aliphatic Carboxylic Esters to Aldehydes and Alcohols. *Angew. Chem. Int. Ed.* **2025**, 64, e202420084.

derivatives, such as anilines (**1x**) and more substituted arenes (**1y**), proved unreactive under the reaction conditions. Additionally, substrates containing sensitive groups, such as aromatic alkynes (**1z**), thioethers (**1aa**), or benzylic alcohols (**1ab**), underwent decomposition.

3.5 Sequential Spirocyclization

During the purification of substrate **3a**, the desired 1,4-dihydro product **4a** was not detected. Instead, the spiro cyclized compound **5a** was identified as the only product (Figure 3.7a). We hypothesized that the mildly acidic nature of SiO₂ used during column chromatography facilitated this cyclization. This unexpected result motivated further exploration of the reaction, as it provides access to interesting spirocyclic structures that are otherwise challenging to synthesize or require elaborated synthetic methods. The only available procedure was found in a patent for the synthesis of product **5b**, using classic Birch conditions and high temperature under vacuum to cyclize the Birch reduction product **4b** (Figure 3.7b).³⁰

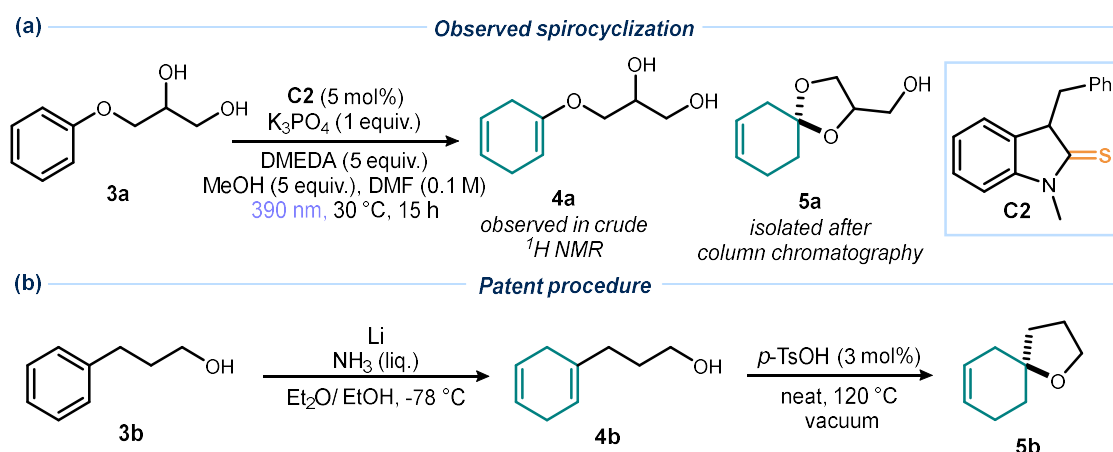


Figure 3.7. (a) Observed spiro-cyclization product **5a** after purification. (b) Previous Birch reduction/spirocyclization procedure reported in a patent.

Optimization experiments using **3b** as the model substrate yielded the targeted cyclization product **5b** under the patent's conditions; however, the procedure lacked reproducibility, with yields varying between 40 and 85%. Reliable and efficient cyclization was achieved by employing trifluoromethanesulfonic acid (TfOH, 3 equivalents) in chloroform (CHCl₃), producing **5b** in 76% yield (Figure 3.8a, entry 1). The reaction proceeded at ambient temperature and reached completion within 30 minutes. The Birch reduction and cyclization steps were performed sequentially without isolating the intermediate 1,4-dihydro product; only

³⁰Kazuyuki, T.; Yoshitaka, N.; Yu, O.; Sae, I. Aminocyclohexane Derivative and Pharmaceutical Use Thereof. WO 2023277116A1, January 5, 2023.

filtration of the inorganic base and solvent removal were required before adding TfOH and CHCl_3 . Reducing the equivalents of TfOH significantly lowered the yield to 40% (entry 2), while other acids failed to promote the cyclization effectively (entries 3–5). Attempts to conduct the reaction in DMF were unsuccessful, with no product formation observed even when heated to 80 °C (entry 6).

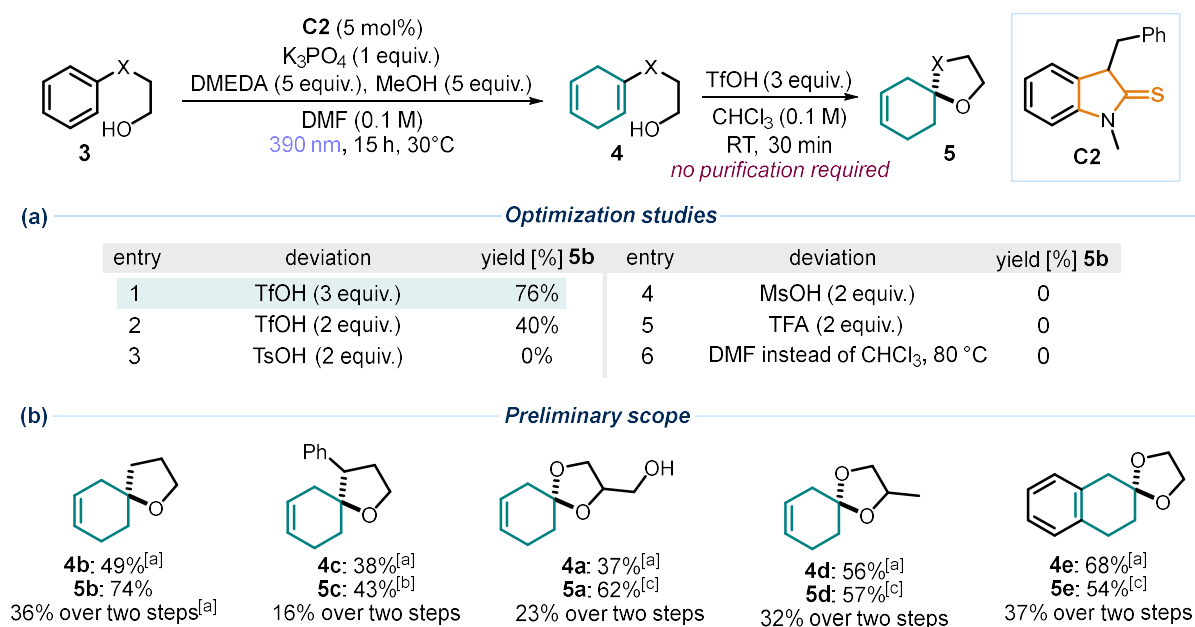


Figure 3.8. (a) Optimization studies: yields of **5b** were determined by ^1H NMR analysis of the crude mixtures using CH_2Br_2 as internal standard, calculated only on the spirocyclization step, relatively to corresponding 1,4-dihydro product **4b**. (b) Preliminary scope of the spirocyclization: reported yields over two steps refer to the isolated products **5**. Filtration and solvent evaporation were carried out prior to the cyclization. ^[a] Yields determined by ^1H NMR analysis of the crude mixtures using CH_2Br_2 as internal standard. ^[b] Reaction conducted at 70 °C for 16 hours. ^[c] TFA was used instead of TfOH.

With the two-step procedure in hand, a preliminary scope was investigated (Figure 3.8b). The five-membered ether products **5b** and **5c** were obtained in 36% and 16% yield over two steps, respectively. The cyclization was also successful in synthesizing the acetals **5a**, **5d** and **5e**, with yields ranging from 23% to 37%. Although acetals can be easily synthesized through the condensation of the appropriate diol with a carbonyl compound, the direct access to products containing a double bond in β,γ position from arenes is not straightforward. Overall, this approach allows for the efficient construction of complex, three-dimensional structures starting from simple, planar aromatic scaffolds.

3.6 Mechanistic Investigations

3.6.1 Characterization of the Catalytic Photoactive Intermediate

To verify the photoactivity of the deprotonated catalyst **I** under 390 nm light, its photophysical and electrochemical characteristics were examined using UV-Vis spectroscopy and cyclic voltammetry. The UV-Vis absorption spectrum of the thiolate **I**, formed in-situ by deprotonation of pre-catalyst **C2** with K₃PO₄ (3 equiv.), was measured in DMF, showing an absorption maxima of **I** at 357 nm (Figure 3.9a). In addition, the absorption profile of deprotonated **I** differed slightly from that of the parent pre-catalyst **C2**. The emission spectrum of **I** was recorded after excitation with a 355 nm laser, resulting in the detection of an emission peak at 410 nm, indicating that the deprotonated catalyst **I** can reach an electronically excited state (Figure 3.9b). Based on the intersection of the absorption and emission spectra at 384 nm, the 0-0 transition energy (E_{0-0}) was estimated to be 3.2 eV.³¹ Cyclic voltammetry (CV) was used to investigate the ground-state redox behavior of the deprotonated catalyst **I** (Figure 3.9c, purple line). An irreversible oxidation peak appeared at -0.07 V vs. Ag/AgCl in DMF, attributed to the conversion of the thiolate into a sulfur-centered radical. The lack of reversibility is likely due to the rapid formation of an S-S dimer, which gives rise to a new irreversible reduction peak at 0.95 V vs. Ag/AgCl. To support this hypothesis, we prepared an authentic sample of the S-S dimer of catalyst **C2**, which shows a comparable CV profile to the one observed with **C2** (Figure 3.9c, red line). The redox potential of the excited thiolate $E(\mathbf{I}^{\bullet}/\mathbf{I}^{*-})$ was calculated to be -3.30 V vs. Ag/AgCl according to the Rehm-Weller formalism ($E(\mathbf{Pc}^{\bullet}/\mathbf{Pc}^*) = E(\mathbf{Pc}^{\bullet}/\mathbf{Pc}^-) - E_{0-0}(\mathbf{Pc}^*)/(\mathbf{Pc}^-)$).³² Stern-Volmer analysis demonstrated an effective interaction between the excited state of the deprotonated catalyst **I** and anisole **1a**, yielding a quenching constant of 0.004 M⁻¹ (Figure 3.9d).

³¹Buzzetti, L.; Crisenza, G. E. M.; Melchiorre, P. Mechanistic Studies in Photocatalysis *Angew. Chem., Int. Ed.* **2019**, 58, 3730–3747.

³²Kavarnos, G. J. Fundamentals of Photoinduced Electron Transfer. chap. 1, pp. 29, VCH Publishers, **1993**.

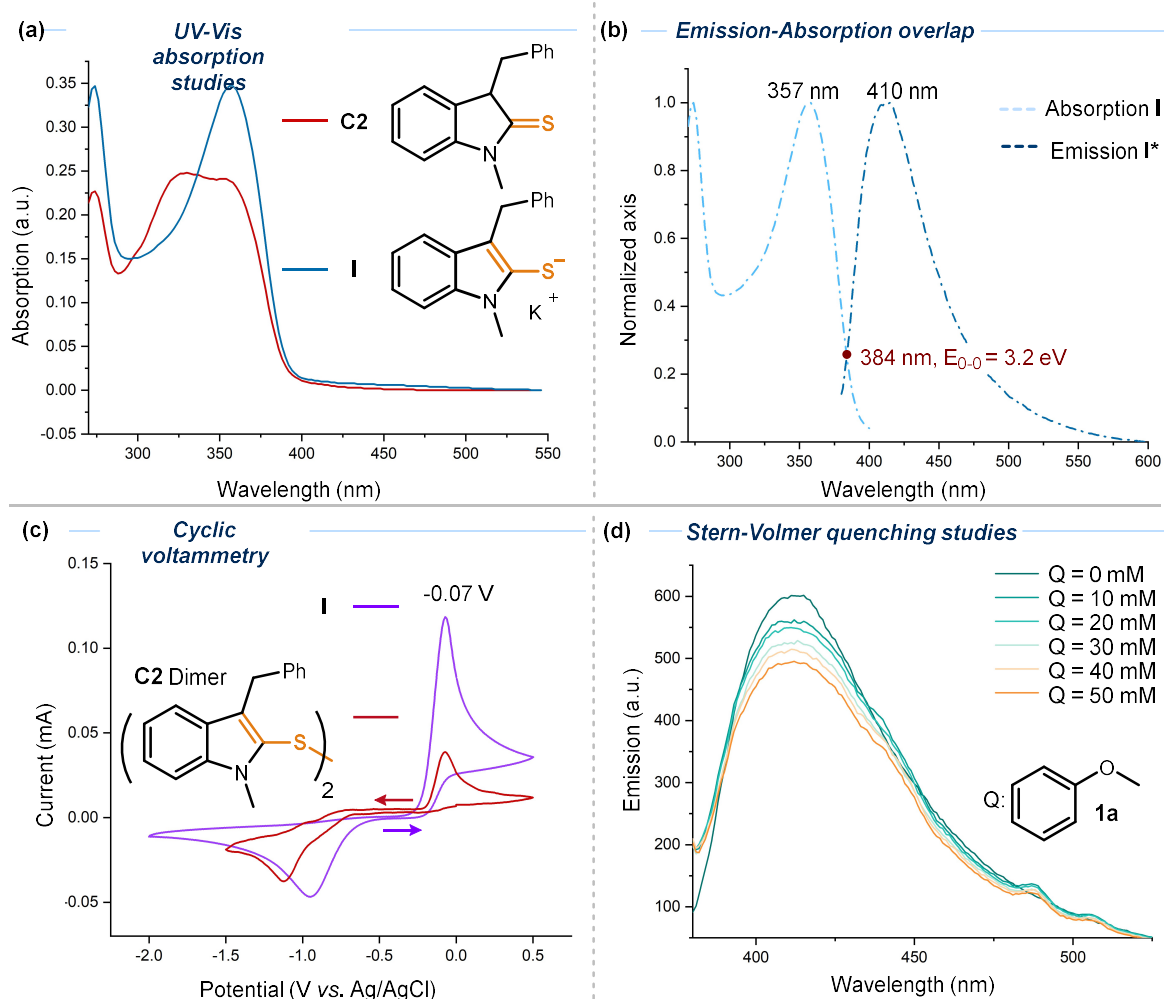


Figure 3.9. Characterization studies of thiolate **I**. **(a)** UV-Vis absorption spectra of catalyst **C2** and thiolate **I** in DMF. **(b)** Absorption and emission spectra of the excited thiolate **I*** in DMF (upon irradiation at 355 nm), intercepting at 384 nm, with a 0-0 transition energy (E_{0-0}) of 3.2 eV. **(c)** Cyclic voltammetry measurements of the thiolate **I** (oxidation first) and the S-S dimer of catalyst **C2** (reduction first) carried out in DMF vs. Ag/AgCl at a scan rate of 100 mV/V. **(d)** Stern-Volmer quenching study of the excited thiolate **I** with anisole **1a**.

3.6.2 Proposed Catalytic Cycle

Mechanistically, we propose that the light-driven reduction follows the traditional Birch reduction pathway, consisting of two successive SET and protonation steps (Figure 3.10a). The proposed catalytic cycle starts with the deprotonation of catalyst **C2**, followed by the excitation of the thiolate anion **I** with 390 nm light (Figure 3.10b). The excited intermediate **I*** has an estimated reduction potential of -3.30 V vs. Ag/AgCl, thermodynamically able to reduce arenes via SET. The turn-over of the oxidized catalyst **II** is proposed to occur by hydrogen atom transfer (HAT) from DMEDA. The substantial difference in bond dissociation energies (BDE)—a key parameter in evaluating HAT efficiency—between thiophenols (~75–80

kcal/mol)³³ and aliphatic amines (BDE \sim 88-92 kcal/mol),³⁴ indicates that a HAT is energetically disfavored. However, we propose that the inorganic base K_3PO_4 could engage in hydrogen bonding with DMEDA (depicted as intermediate **VI** in Figure 3.10b). Such interactions are known to enhance the reactivity of $\alpha(C-H)$ bonds in alcohols by increasing the electron density on the heteroatom, thereby facilitating HAT.^{35,36} Furthermore, the HAT from intermediate **VI** to the sulfur-centered radical **II** may be favored by polarization effects and polarity-matched reactivity between the electrophilic radical **II** and the nucleophilic $\alpha-C-H$ of the amine.³⁷ This step is essential for regenerating the active photocatalyst and completing the catalytic cycle.

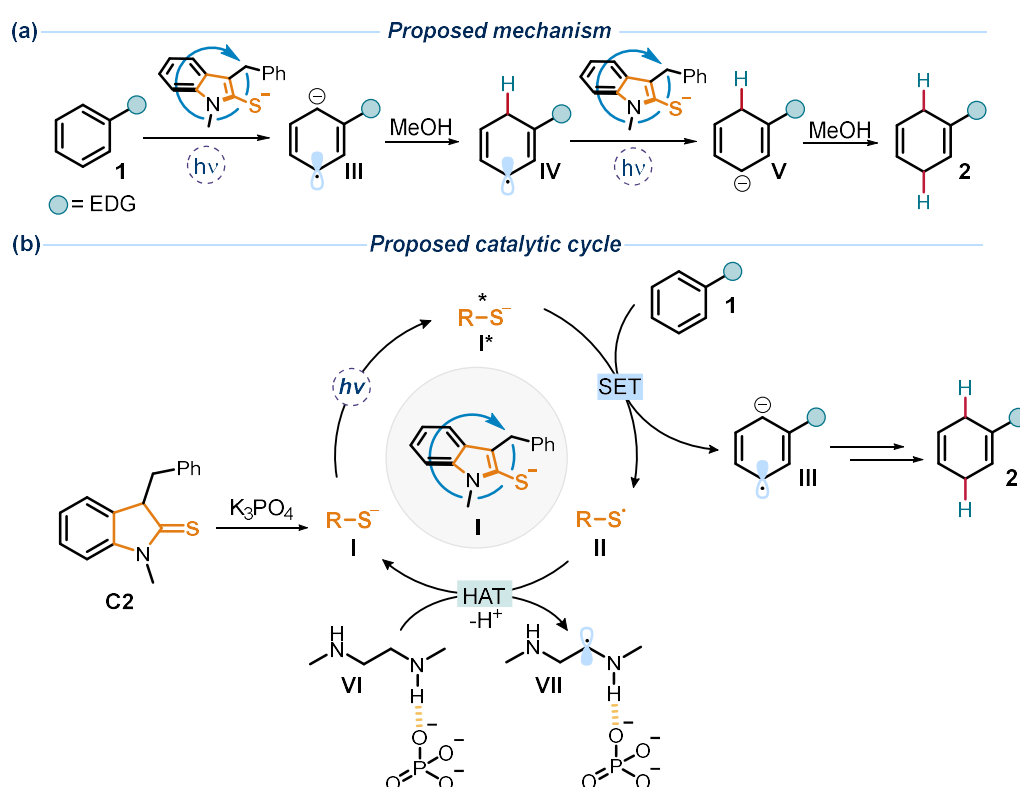


Figure 3.10. (a) Proposed mechanism and (b) catalytic cycle of the Birch reduction of electron-rich arenes.

³³Fu, Y.; Lin, B.; Song, K.; Liu, L.; Guo, Q. Substituent effects on the S–H bond dissociation energies of thiophenols. *J. Chem. Soc., Perkin Trans.* **2002**, 2, 1223–1230.

³⁴Lalevee, J.; Allonas, X.; Fouassier, J. N–H and $\alpha(C-H)$ Bond Dissociation Enthalpies of Aliphatic Amines. *J. Am. Chem. Soc.* **2002**, 124, 9613–9621.

³⁵Bietti, M. Activation and Deactivation Strategies Promoted by Medium Effects for Selective Aliphatic C–H Bond Functionalization. *Angew. Chem. Int. Ed.* **2018**, 57, 16618–16637.

³⁶Jeffrey, J. L.; Terrett, J. A.; MacMillan, D. W. C. O–H hydrogen bonding promotes H-atom transfer from a C–H bonds for C-alkylation of alcohols. *Science* **2015**, 349, 1532–1536.

³⁷Garwood, J. J. A.; Chen, A. D.; Nagib, D. A. Radical Polarity. *J. Am. Chem. Soc.* **2024**, 146, 28034–28059.

4 Conclusions

In conclusion, we have developed an efficient and scalable photocatalytic protocol for the Birch reduction, employing a newly designed and readily available indole-2-thione organocatalyst that operates under mild reaction conditions. Our new methodology provides a practical and simple pathway for the reduction of a broad range of electron-rich aromatic substrates. Moreover, we established a straightforward strategy for spirocyclization of the 1,4-dihydro reduced scaffolds, granting access to structurally sophisticated β,γ -unsaturated cyclohexadienes bearing five-membered ether or acetal rings, without the need for intermediate isolation. Notably, our protocol enables late-stage reduction of functionalized biologically relevant molecules, opening a new avenue for potential applications in pharmaceutical synthesis.

Mechanistic investigations and Stern-Volmer quenching studies confirmed that the catalytically photoactive intermediate, capable of performing a SET toward electron-rich arenes, is the deprotonated thiolate anion.

5 Experimental Section

General Information

The NMR spectra were recorded at 400 MHz and 600 MHz for ^1H and 101 or 126 MHz for ^{13}C . The chemical shifts (δ) for ^1H and ^{13}C are given in ppm relative to residual signals of the solvents (CHCl_3 at 7.26 ppm ^1H NMR and 77.16 ppm ^{13}C NMR). Coupling constants are given in Hertz. The following abbreviations are used to indicate the multiplicity: s, singlet; d, doublet; q, quartet; m, multiplet; br, broad signal.

High resolution mass spectra (HRMS) were obtained from the HRMS unit on MicroTOF Focus and Maxis Impact (Bruker Daltonics) with electrospray ionization (ESI) and Atmospheric-pressure chemical ionization (APCI).

UV-Vis measurements were carried out on an Agilent Cary 60 UV-Vis spectrophotometer equipped with two silicon diode detectors, double beam optics and Xenon pulse light. Fluorescence measurements were carried out on an Aminco-Bowman Series 2 Luminescence spectrofluorimeter equipped with a high voltage PMT detector and continuum Xe light source.

Cyclic voltammetry measurements were carried out on a Princeton Applied Research PARSTAT 2273 potentiostat, offering compliance voltage up to ± 100 V (available at the counter electrode), ± 10 V scan range and ± 2 A current range.

General Procedures

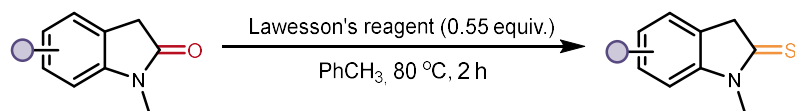
All reactions were set up under an argon atmosphere. Synthesis grade solvents were used as purchased and anhydrous solvents were taken from a commercial SPS solvent dispenser. Chromatographic purifications of products were accomplished using forced-flow chromatography (FC) on silica gel (230-400 mesh). For thin layer chromatography (TLC) analysis Merck pre-coated TLC plates (silica gel 60 GF254, 0.25 mm) were employed, using UV light as the visualizing agent and an acidic mixture of vanillin or basic aqueous potassium permanganate (KMnO_4) stain solutions, and heat as developing agents. Organic solutions were concentrated under reduced pressure on a Büchi rotatory evaporator.

Materials

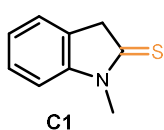
Commercial grade reagents and solvents were purchased at the highest quality from commercial suppliers and used as received, unless otherwise stated.

5.1 Synthesis of the Organic Photocatalysts

General procedure for the synthesis of catalysts C1, C9-C11 (A):



To a round bottom flask equipped with a stirring bar, oxindole (1 equiv.), Lawesson's reagent (0.55 equiv.) and toluene (0.1 M) were added. The mixture was purged with argon and then stirred at 80 °C for 1 h. The resulting solution was concentrated in vacuo and the crude mixture was purified by flash column chromatography on silica gel to afford the photocatalyst.



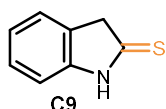
1-Methylindoline-2-thione (C1)

Synthesized according to the general procedure A using 1-methylindolin-2-one (1 equiv., 5 mmol, 736 mg). The crude mixture was purified by flash column chromatography on silica gel (hexane/EtOAc 10:1) to afford catalyst **C1** as a yellow solid (620.5 mg, 76% yield).

¹H NMR (400 MHz, CDCl₃): δ 7.37 – 7.28 (m, 2H), 7.16 (td, J = 7.5, 1.0 Hz, 1H), 6.97 (d, J = 7.9 Hz, 1H), 4.11 (s, 2H), 3.63 (s, 3H).

¹³C NMR (101 MHz, CDCl₃): δ 201.3, 146.8, 129.3, 128.0, 124.5, 124.1, 109.7, 49.2, 31.4.

Matching reported literature data.³⁸



Indoline-2-thione (C9)

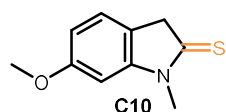
Synthesized according to the general procedure A using 2-oxindole (1 equiv., 2 mmol, 226 mg). The crude mixture was purified by flash column chromatography on silica gel (hexane/EtOAc 10:1) to afford catalyst **C9** as a yellow solid (220 mg, 74%).

¹H NMR (400 MHz, CDCl₃): δ 9.93 (br s, 1H), 7.30 – 7.23 (m, 2H), 7.15 – 7.09 (m, 1H), 6.98 (d, J = 7.8 Hz, 1H), 4.08 (s, 2H).

¹³C NMR (101 MHz, CDCl₃): δ 204.0, 144.3, 130.5, 128.2, 124.4, 124.2, 110.1, 49.2.

³⁸Ransborg, L. K.; Albrecht, L.; Weise, C. F.; Bak, J. R.; Jørgensen, K. A. Optically Active Thiophenes via an Organocatalytic One-Pot Methodology. *Org. Lett.* **2012**, *14*, 724–727.

Matching reported literature data.³⁹



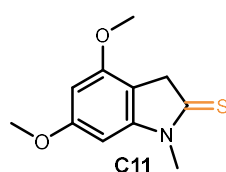
6-Methoxy-1-methylindoline-2-thione (C10)

Synthesized according to the general procedure **A** using 6-methoxy-1-methylindolin-2-one (1 equiv., 4 mmol, 709 mg). The crude mixture was purified by flash column chromatography on silica gel (hexane/EtOAc 10:1) to afford catalyst **C10** as a white solid (160 g, 21% yield).

¹H NMR (500 MHz, CDCl₃): δ 7.17 (dt, *J* = 8.1, 1.1 Hz, 1H), 6.67 (dd, *J* = 8.1, 2.3 Hz, 1H), 6.54 (d, *J* = 2.2 Hz, 1H), 4.06 – 4.01 (m, 2H), 3.84 (s, 3H), 3.60 (s, 3H).

¹³C NMR (126 MHz, CDCl₃): δ 202.6, 160.3, 148.0, 124.4, 121.0, 108.7, 97.5, 55.9, 48.6, 31.4.

HRMS (ESI⁺) C₁₀H₁₂NOS [M+H]⁺: found 194.0637, required 194.0634.



4,6-Dimethoxy-1-methylindoline-2-thione (C11)

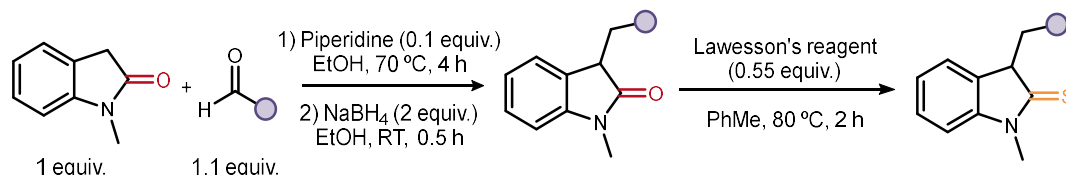
Synthesized according to the general procedure **A** using 4,6-dimethoxy-1-methylindolin-2-one (1 equiv., 2.5 mmol, 518 mg). The crude mixture was purified by flash column chromatography on silica gel (hexane/EtOAc 10:1) to afford catalyst **C11** as a white solid (78 mg, 14% yield).

¹H NMR (500 MHz, CDCl₃): δ 6.26 (d, *J* = 1.9 Hz, 1H), 6.20 (d, *J* = 2.0 Hz, 1H), 3.96 (s, 2H), 3.85 (s, 3H), 3.84 (s, 3H), 3.58 (s, 3H).

¹³C NMR (126 MHz, CDCl₃): δ 202.6, 161.9, 155.6, 148.5, 108.0, 94.3, 89.5, 55.9, 55.7, 46.7, 31.7.

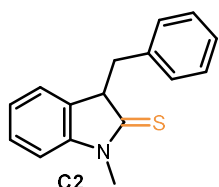
HRMS (ESI⁺) C₁₁H₁₃NO₂SNa [M+Na]⁺: found 246.0563, required 246.0559.

General procedure for the synthesis of catalysts **C2**, **C4-C8 (B)**:



³⁹Lopes, A. B.; Choury, M.; Wagner, P.; Gulea, M. Tandem Double-Cross-Coupling/Hydrothiolation Reaction of 2-Sulfonyl Benzimidazoles with Boronic Acids. *Org. Lett.* **2019**, *21*, 5943–5947.

In a round bottom flask equipped with a stirring bar, 1-methylindolin-2-one (1 equiv.), aldehyde (1.1 equiv.), and piperidine (0.1 equiv.) were dissolved in ethanol (0.1 M), then shortly purged with argon and stirred for 4 h at 70 °C. After the solution was cooled to ambient temperature, NaBH₄ (2 equiv.) was added and the reaction mixture was stirred for another 0.5 h. The reaction was quenched with water. The product was extracted with EtOAc, dried over anhydrous MgSO₄ and concentrated in vacuo. The crude mixture was purified by flash column chromatography on silica gel (hexane/EtOAc 10:1). To a round bottom flask equipped with a stirring bar the intermediate (1 equiv.), Lawesson's reagent (0.55 equiv.) and toluene (0.1 M) were added. The mixture was purged with argon and then stirred at 80 °C for 1 h. The solution was concentrated in vacuo and the crude mixture was purified by flash column chromatography on silica gel to afford the photocatalyst.



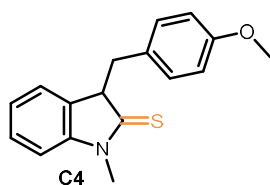
3-Benzyl-1-methylindoline-2-thione (C2)

Synthesized according to the general procedure **B** using 1-methylindolin-2-one (1 equiv., 15 mmol, 2.2 g) and benzaldehyde (1.1 equiv., 16.5 mmol, 1.67 mL). The crude mixture was purified by flash column chromatography on silica gel (hexane/EtOAc 30:1) to afford catalyst **C2** as an orange solid (3.32 g, 87% yield over all 3 steps).

¹H NMR (500 MHz, CDCl₃): δ 7.29 – 7.21 (m, 4H), 7.20 – 7.17 (m, 2H), 7.00 (td, *J* = 7.5, 1.0 Hz, 1H), 6.93 (d, *J* = 7.9 Hz, 1H), 6.69 (dd, *J* = 7.4, 0.9 Hz, 1H), 4.09 (dd, *J* = 9.7, 4.6 Hz, 1H), 3.82 (dd, *J* = 13.6, 4.6 Hz, 1H), 3.60 (s, 3H), 2.86 (dd, *J* = 13.6, 9.7 Hz, 1H).

¹³C NMR (126 MHz, CDCl₃): δ 204.9, 145.7, 138.1, 133.2, 129.7, 128.4, 128.2, 126.8, 124.8, 123.9, 109.5, 58.9, 41.0, 31.5.

HRMS (ESI⁺) C₁₆H₁₆NS [M+H]⁺: found 254.1002, required 254.0998.



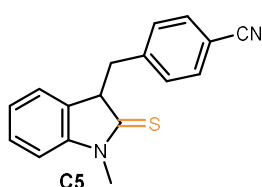
3-(4-Methoxybenzyl)-1-methylindoline-2-thione (C4)

Synthesized according to the general procedure **B** using 1-methylindolin-2-one (1 equiv., 1 mmol, 147 mg) and *p*-anisaldehyde (1.1 equiv., 1.1 mmol, 134 μL). The crude mixture was purified by flash column chromatography on silica gel (hexane/EtOAc 20:1) to afford catalyst **C4** as an orange solid (150 mg, 53% yield over all 3 steps).

¹H NMR (500 MHz, CDCl₃): δ 7.29 – 7.25 (m, 1H), 7.10 – 7.06 (m, 2H), 7.02 (td, *J* = 7.6, 1.0 Hz, 1H), 6.92 (d, *J* = 7.9 Hz, 1H), 6.79 – 6.74 (m, 3H), 4.05 (dd, *J* = 9.4, 4.6 Hz, 1H), 3.78 (s, 3H), 3.74 (dd, *J* = 13.7, 4.6 Hz, 1H), 3.58 (s, 3H), 2.85 (dd, *J* = 13.7, 9.4 Hz, 1H).

¹³C NMR (126 MHz, CDCl₃): δ 204.9, 158.5, 145.8, 133.3, 130.7, 130.0, 128.1, 124.8, 123.9, 113.7, 109.5, 59.2, 55.3, 40.1, 31.5.

HRMS (ESI⁺) C₁₇H₁₇NOSNa [M+Na]⁺: found 306.0933, required 306.0923.



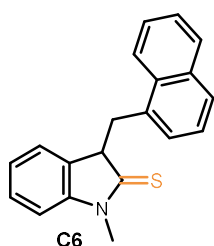
4-((1-Methyl-2-thioxoindolin-3-yl)methyl)benzonitrile (C5)

Synthesized according to the general procedure **B** using 1-methylindolin-2-one (1 equiv., 1 mmol, 147 mg) and 4-cyanobenzaldehyde (1.1 equiv., 1.1 mmol, 144 mg). The crude mixture was purified by flash column chromatography on silica gel (hexane/EtOAc 20:1) to afford catalyst **C5** as a yellow solid (261 mg, 94% yield over all 3 steps).

¹H NMR (500 MHz, CDCl₃): δ 7.51 – 7.45 (m, 2H), 7.30 (t, *J* = 7.7 Hz, 1H), 7.26 – 7.21 (m, 2H), 7.07 (td, *J* = 7.5, 1.0 Hz, 1H), 6.92 (d, *J* = 7.9 Hz, 1H), 6.87 (d, *J* = 7.4 Hz, 1H), 4.12 (dd, *J* = 8.3, 4.7 Hz, 1H), 3.75 (dd, *J* = 13.7, 4.8 Hz, 1H), 3.55 (s, 3H), 3.18 (dd, *J* = 13.6, 8.2 Hz, 1H).

¹³C NMR (126 MHz, CDCl₃): δ 203.9, 145.8, 143.3, 132.3, 132.0, 130.5, 128.7, 124.3, 124.2, 119.0, 110.8, 109.8, 58.3, 40.4, 31.5.

HRMS (ESI⁺) C₁₇H₁₄N₂SSNa [M+Na]⁺: found 301.0767, required 301.0770.



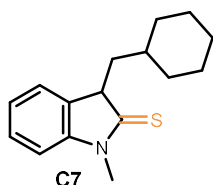
1-Methyl-3-(naphthalen-1-ylmethyl)indoline-2-thione (C6)

Synthesized according to the general procedure **B** using 1-methylindolin-2-one (1 equiv., 1 mmol, 147 mg) and 1-naphthaldehyde (1.1 equiv., 1.1 mmol, 149 μL). The crude mixture was purified by flash column chromatography on silica gel (hexane/EtOAc 20:1) to afford catalyst **C6** as a white solid (94 mg, 32% yield over all 3 steps).

¹H NMR (500 MHz, CDCl₃): δ 8.43 (d, *J* = 8.4 Hz, 1H), 7.93 (dt, *J* = 8.2, 0.9 Hz, 1H), 7.85 (d, *J* = 8.2 Hz, 1H), 7.62 (ddd, *J* = 8.4, 6.8, 1.4 Hz, 1H), 7.55 (ddd, *J* = 8.1, 6.8, 1.2 Hz, 1H), 7.44 (dd, *J* = 8.3, 6.9 Hz, 1H), 7.30 – 7.24 (m, 2H), 7.01 (d, *J* = 7.8 Hz, 1H), 6.91 (td, *J* = 7.5, 1.0 Hz, 1H), 6.35 (d, *J* = 7.5 Hz, 1H), 4.54 (dd, *J* = 13.8, 3.7 Hz, 1H), 4.22 (dd, *J* = 11.5, 3.7 Hz, 1H), 3.71 (s, 3H), 2.84 (dd, *J* = 13.8, 11.5 Hz, 1H).

¹³C NMR (126 MHz, CDCl₃): δ 205.3, 145.6, 134.7, 134.2, 133.7, 132.0, 129.1, 128.3, 128.1, 126.7, 126.1, 125.3, 125.2, 124.1, 123.7, 109.5, 57.5, 40.1, 31.7.

HRMS (ESI⁺) C₂₀H₁₈NS [M+H]⁺: found 304.1151, required 304.1154.



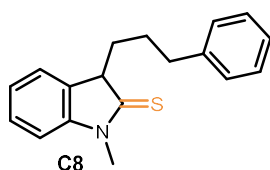
3-(Cyclohexylmethyl)-1-methylindoline-2-thione (C7)

Synthesized according to the general procedure **B** using 1-methylindolin-2-one (1 equiv., 1 mmol, 147 mg) and cyclohexanecarboxaldehyde (1.1 equiv., 1.1 mmol, 133 μL). The crude mixture was purified by flash column chromatography on silica gel (hexane/EtOAc 20:1) to afford catalyst **C7** as a yellow solid (165 mg, 64% yield over all 3 steps).

¹H NMR (500 MHz, CDCl₃): δ 7.37 – 7.30 (m, 2H), 7.17 (td, *J* = 7.5, 1.0 Hz, 1H), 7.01 (d, *J* = 7.9 Hz, 1H), 3.85 (dd, *J* = 9.0, 4.9 Hz, 1H), 3.64 (s, 3H), 2.19 (ddd, *J* = 13.9, 9.2, 4.8 Hz, 1H), 1.93 – 1.85 (m, 1H), 1.80 – 1.57 (m, 6H), 1.33 – 1.14 (m, 3H), 1.11 – 0.97 (m, 2H).

¹³C NMR (126 MHz, CDCl₃): δ 207.2, 145.7, 134.6, 128.0, 124.3, 124.1, 109.7, 55.4, 42.8, 35.1, 34.3, 32.5, 31.6, 26.6, 26.4, 26.3.

HRMS (ESI⁺) C₁₆H₂₂NS [M+H]⁺: found 260.1473, required 260.1467.



1-Methyl-3-(3-phenylpropyl)indoline-2-thione (C8)

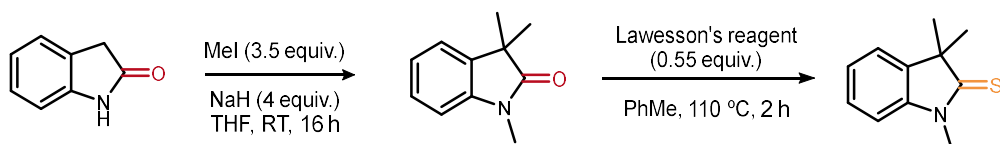
Synthesized according to the general procedure **B** using 1-methylindolin-2-one (1 equiv., 1 mmol, 147 mg) and 3-phenylpropionaldehyde (1.1 equiv., 1.1 mmol, 146 μL). The crude mixture was purified by flash column chromatography on silica gel (hexane/EtOAc 20:1) to afford catalyst **C8** as a yellow solid (123 mg, 44% yield over all 3 steps).

¹H NMR (500 MHz, CDCl₃): δ 7.35 (t, *J* = 7.8 Hz, 1H), 7.30 (d, *J* = 7.6 Hz, 1H), 7.28 – 7.24 (m, 2H), 7.21 – 7.16 (m, 2H), 7.15 – 7.11 (m, 2H), 7.00 (d, *J* = 7.9 Hz, 1H), 3.88 (t, *J* = 5.7 Hz, 1H), 3.65 (s, 3H), 2.69 – 2.56 (m, 2H), 2.37 – 2.26 (m, 1H), 2.26 – 2.16 (m, 1H), 1.70 – 1.58 (m, 1H), 1.44 – 1.34 (m, 1H).

¹³C NMR (126 MHz, CDCl₃): δ 205.9, 146.0, 142.1, 133.7, 128.5, 128.4, 128.2, 125.9, 124.3, 123.9, 109.6, 57.6, 36.1, 33.8, 31.5, 27.0.

HRMS (ESI⁺) C₁₈H₂₀NS [M+H]⁺: found 282.1318, required 282.1311.

Procedure for the synthesis of catalyst C3:



In a round bottom flask equipped with a stirring bar, oxindole (1 equiv., 15 mmol, 2 g) was dissolved in THF (48 mL), then NaH (4 equiv., 60 mmol, 2.4 g, 60% dispersion in oil) was added. The solution was cooled to 0 °C and MeI (3.5 equiv., 52.6 mmol, 3.27 mL) was added. The reaction mixture was stirred at ambient temperature overnight and quenched afterwards with water. The product was extracted with EtOAc, dried over anhydrous MgSO₄, and concentrated in vacuo. The crude product was purified by flash column chromatography on silica gel (hexane/EtOAc 20:1) to afford the intermediate 1,3,3-trimethylindolin-2-one as a colourless oil (1.43 g, 8.16 mmol, 54% yield). Such intermediate was placed in a round bottom flask equipped with a stirring bar, then the Lawesson's reagent (0.5 equiv., 4.08 mmol, 1.65 g), and toluene (17 mL) were added. The mixture was purged with argon and then stirred at 110 °C for 2 h. The solution was concentrated in vacuo and the crude mixture was purified by flash column chromatography on silica gel (EtOAc/hexane 10:1) to afford catalyst **C3** as a yellow oil (1.2 g, 78%).

¹H NMR (500 MHz, CDCl₃): δ 7.36 – 7.29 (m, 2H), 7.19 (td, J = 7.5, 0.9 Hz, 1H), 7.05 (d, J = 7.7 Hz, 1H), 3.66 (s, 3H), 1.44 (s, 6H).

¹³C NMR (101 MHz, CDCl₃): δ 212.2, 144.1, 140.6, 127.9, 124.4, 122.9, 109.7, 55.1, 31.6, 28.2.

Matching reported literature data.⁴⁰

5.2 Experimental Procedures and Compound Characterization for the Birch Reduction of Benzene Derivatives

Photochemical Reaction Set-up

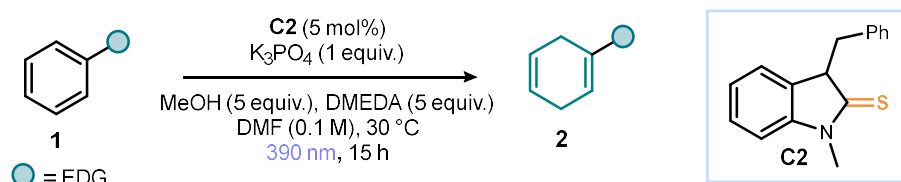
The reactions were performed under irradiation by two *Kessil* lamps (PR160L-390 nm, 100% intensity) using a 3D-printed photoreactor reported in literature (Figure 5.1).²⁸ The temperature in the reactor was set to 30 °C.

⁴⁰Wang, C.; Liu, L. NHC-catalyzed oxindole synthesis via single electron transfer. *Org. Chem. Front.* **2021**, *8*, 1454–1460.



Figure 5.1. Reaction set-up using a temperature-controlled 3D-printed photoreactor under irradiation at 390 nm by two Kessil lamps.

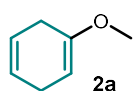
General procedure for Birch reduction of aromatic compounds (C):



Photocatalyst **C2** (2.6 mg, 0.01 mmol, 0.05 equiv.), arenes **1** (if solid, 0.2 mmol, 1 equiv.) and K_3PO_4 (42 mg, 0.2 mmol, 1 equiv.) were added sequentially to a 7 mL glass vial equipped with a stirring bar. The vial was sealed with a screw-top cap with septum and then three times vacuumed for 2 minutes and backfilled with argon. Oxygen free DMF (2 mL, 0.1 M) was added and the solution was stirred until the catalyst was completely dissolved. Then, MeOH (41 μL , 1.0 mmol, 5 equiv.), arenes (if liquid, 0.2 mmol, 1 equiv.) and DMEDA (104 μL , 1.0 mmol, 5 equiv.) were added via syringe. The vial was placed in the photoreactor and the reaction mixture was stirred (600 rpm) at 30 $^{\circ}\text{C}$ (reactor temperature) under 390 nm irradiation (2x PR160L-390 nm, 100% light intensity) for 16 hours.

After the reaction was completed, the mixture was filtered and the solvent was removed under reduced pressure (40 $^{\circ}\text{C}$, <15 mbar). The crude residue was purified by column chromatography to afford the corresponding product **2**.

For NMR analyses of products **2a-2d** and **2g**: Mesitylene or CH_2Br_2 was added as the internal standard (0.3 mmol, 1 equiv.) to the crude reaction mixture, followed by the addition of H_2O . The solution was extracted twice with 0.7 mL of CDCl_3 , dried over anhydrous MgSO_4 and then analysed via ^1H NMR.



1-Methoxycyclohexa-1,4-diene (2a)

Synthesized according to the general procedure **C** using anisole (33 μ L, 0.3 mmol). The yield was determined by adding mesitylene (1 equiv.) as internal standard to the reaction mixture (NMR yield: 64%).

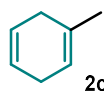
Matching reported literature data.⁴¹



Cyclohexa-1,4-diene (2b)

Synthesized according to the general procedure **C** using benzene (27 μ L, 0.3 mmol). The yield was determined by adding mesitylene (1 equiv.) as internal standard to the reaction mixture (NMR yield: 53%).

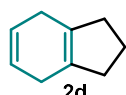
Matching reported literature data.⁴²



1-Methylcyclohexa-1,4-diene (2c)

Synthesized according to the general procedure **C** using toluene (32 μ L, 0.3 mmol). The yield was determined by adding mesitylene (1 equiv.) as internal standard to the reaction mixture (NMR yield: 52%).

Matching reported literature data.⁴³



2,3,4,7-Tetrahydro-1H-indene (2d)

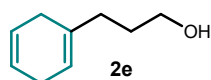
Synthesized according to the general procedure **C** using indane (37 μ L, 0.3 mmol). The yield was determined by adding mesitylene (1 equiv.) as internal standard to the reaction mixture (NMR yield: 58%).

Matching reported literature data.¹⁶

⁴¹O'Byrne, A.; Murray, C.; Keegan, D.; Palacio, C.; Evans, P.; Morgan, B. S. The Thio-Adduct Facilitated, Enzymatic Kinetic Resolution of 4-hydroxycyclopentenone and 4-hydroxycyclohexenone. *Org. Biomol. Chem.* **2010**, 8, 539–545.

⁴²Abraham, R. J.; Canton, M.; Griffiths, L. Proton chemical shifts in NMR: Part 17. Chemical shifts in alkenes and anisotropic and steric effects of the double bond. *Magn. Reson. Chem.* **2001**, 39, 421–431.

⁴³O'Mahony, M. J.; More O'Ferrall, R. A.; Boyd, D. R.; Lam, C. M.; O'Donoghue, A. C. Substituent effects on the dehydration of arene hydrates in aqueous solution. *J. Phys. Org. Chem.* **2013**, 26, 989–996.



3-(Cyclohexa-1,4-dien-1-yl)propan-1-ol (**2e**)

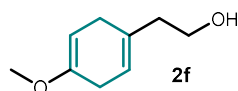
Synthesized according to the general procedure **C** (reaction time 48 h) using 3-phenylpropan-1-ol (477 mg, 3.5 mmol). The crude mixture was purified by flash column chromatography using silica gel impregnated with 2% w/w AgNO₃ (hexane/AcOEt, 2:1) to afford **2e** as a yellow liquid (52% yield, 242 mg).

¹H NMR (600 MHz, CDCl₃): δ 5.73 – 5.65 (m, 2H), 5.46 – 5.42 (m, 1H), 3.63 (t, *J* = 6.5 Hz, 2H), 2.71 – 2.64 (m, 2H), 2.61 – 2.56 (m, 2H), 2.05 – 2.00 (m, 3H), 1.71 – 1.65 (m, 2H).

¹³C NMR (151 MHz, CDCl₃): δ 134.6, 124.4, 124.3, 118.8, 62.8, 33.8, 30.3, 29.0, 26.7.

HRMS (ESI⁺) C₉H₁₄O [M]⁺: found, 138.1045 required 138.1039.

Matching reported literature data.¹⁶



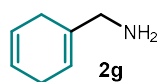
2-(4-Methoxycyclohexa-1,4-dien-1-yl)ethan-1-ol (**2f**)

Synthesized according to the general procedure **C** using 2-(4-methoxyphenyl)ethan-1-ol (30.4 mg, 0.2 mmol). The crude mixture was purified by flash column chromatography on silica gel (hexane/EtOAc 3:1 to 3:2) to afford **2f** as a colourless liquid (60% yield, 18.5 mg).

¹H NMR (600 MHz, CDCl₃): δ 5.53 – 5.48 (m, 1H), 4.65 – 4.60 (m, 1H), 3.70 (t, *J* = 6.2 Hz, 2H), 3.55 (s, 3H), 2.80 – 2.72 (m, 4H), 2.28 (t, *J* = 6.3 Hz, 2H).

¹³C NMR (151 MHz, CDCl₃): δ 153.0, 132.0, 120.6, 90.3, 60.4, 54.0, 39.9, 29.3, 29.2.

Matching reported literature data.¹⁶

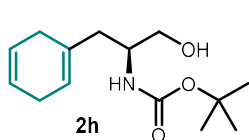


Cyclohexa-1,4-dien-1-ylmethanamine (**2g**)

Synthesized according to the general procedure **C** using phenylmethanamine (21.4 mg, 0.2 mmol). The yield was determined by adding CH₂Br₂ (1 equiv.) as internal standard to the reaction mixture (NMR yield: 52%).

Matching reported literature data.⁴⁴

⁴⁴Burrows, J.; Kamo, S.; Koide, K. Scalable Birch reduction with lithium and ethylenediamine in tetrahydrofuran. *Science*, **2021**, 374, 741–746.



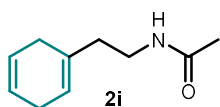
***tert*-Butyl-(*S*)-(1-(cyclohexa-1,4-dien-1-yl)-3-hydroxypropan-2-yl)carbamate (**2h**)**

Synthesized according to the general procedure **C** using *tert*-butyl-(*S*)-(1-hydroxy-3-phenylpropan-2-yl)carbamate (50.3 mg, 0.2 mmol). The crude mixture was purified by flash column chromatography on silica gel (hexane/EtOAc 9:1 to 8:2) to afford **2h** as a white solid (55% yield, 27.9 mg).

¹H NMR (600 MHz, CDCl₃): δ 5.73 – 5.66 (m, 2H), 5.53 – 5.48 (m, 1H), 4.62 (br s, 1H), 3.77 (br s, 1H), 3.70 – 3.65 (m, 1H), 3.60 – 3.54 (m, 1H), 2.85 – 2.45 (m, 5H), 2.19 (dd, *J* = 14.1, 6.4 Hz, 1H), 2.10 (dd, *J* = 14.0, 8.6 Hz, 1H), 1.44 (s, 9H).

¹³C NMR (151 MHz, CDCl₃): δ 156.8, 131.3, 124.1, 124.0, 122.3, 79.9, 66.3, 50.6, 39.8, 28.8, 28.4, 26.9.

HRMS (MALDI-TOF⁺) C₁₄H₂₃NO₃Na [M+Na]⁺: found 276.1576, required 276.1570.



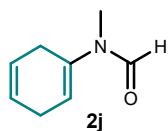
***N*-(2-(Cyclohexa-1,4-dien-1-yl)ethyl)acetamide (**2i**)**

Synthesized according to the general procedure **C** using *N*-(2-phenylethyl)acetamide (49.0 mg, 0.3 mmol, 1 equiv.). The crude mixture was purified by flash column chromatography on silica gel loaded with 2% AgNO₃ (EtOAc/DCM 2:1) to afford **2i** as a white solid (29.4 mg, 57% yield).

¹H NMR (500 MHz, CDCl₃): δ 5.75 – 5.67 (m, 2H), 5.52 – 5.47 (m, 1H), 5.44 (br s, 1H), 3.35 (td, *J* = 6.8, 5.5 Hz, 2H), 2.75 – 2.67 (m, 2H), 2.63 – 2.56 (m, 2H), 2.20 – 2.14 (m, 2H), 1.96 (s, 3H).

¹³C NMR (126 MHz, CDCl₃): δ 170.1, 132.1, 124.3, 124.1, 121.0, 37.1, 37.0, 28.7, 26.9, 23.5.

Matching reported literature data.⁴⁵



***N*-(Cyclohexa-1,4-dien-1-yl)-*N*-methylformamide (**2j**)**

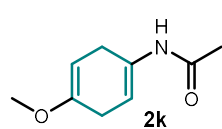
Synthesized according to the general procedure **C** using *N*-methyl-*N*-phenylformamide (27 mg, 0.2 mmol). The crude mixture was purified by flash column chromatography using silica gel impregnated with 2% w/w AgNO₃ (hexane/EtOAc, 3:1) to afford **2j** as a colourless liquid (44% yield, 12 mg).

⁴⁵Kondo, K.; Kubota, K.; Ito, H. Mechanochemistry enabling highly efficient Birch reduction using sodium lumps and D-(+)-glucose. *Chem. Sci.* **2024**, *15*, 4452–4457.

¹H NMR (600 MHz, CDCl₃): δ 8.30 (s, 1H), 5.77 – 5.69 (m, 2H), 5.46 – 5.42 (m, 1H), 3.01 (d, *J* = 0.6 Hz, 3H), 2.91 – 2.80 (m, 4H).

¹³C NMR (151 MHz, CDCl₃): δ 161.2, 135.3, 124.0, 122.7, 114.6, 29.3, 27.5, 26.7.

HRMS (ESI⁺) C₈H₁₂NO [M+H]⁺: found 138.0919, required 138.0913.



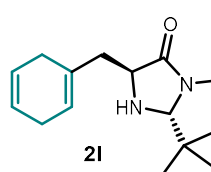
***N*-(4-Methoxycyclohexa-1,4-dien-1-yl)acetamide (2k)**

Synthesized according to the general procedure C using *N*-(4-methoxyphenyl)acetamide (33.0 mg, 0.2 mmol). The desired product was detected in 26% NMR yield using CH₂Br₂ as an internal standard (0.2 mmol). The crude mixture was purified by flash column chromatography on silica gel (hexane/EtOAc 6:4 to 4:6) but further purification was required. The fractions containing starting material and product were combined and concentrated, and subjected to further purification by reverse phase preparative HPLC on a Synergi 4u Hydro -RP 80A Prep Column (10 mm x 250 mm, 130 Å, 4 μm) (30% to 70% CH₃CN in H₂O). The pure fractions were combined and directly evaporated to afford **2k** as a white solid.

¹H NMR (600 MHz, CDCl₃): δ 6.33 (s, 1H), 6.10 – 6.05 (m, 1H), 4.56 (t, *J* = 3.6 Hz, 1H), 3.54 (s, 3H), 2.93 (td, *J* = 7.4, 3.1 Hz, 2H), 2.83 (td, *J* = 7.5, 3.7 Hz, 2H), 2.04 (s, 3H).

¹³C NMR (151 MHz, CDCl₃): δ 168.5, 153.0, 130.5, 108.95, 89.0, 54.2, 28.9, 28.3, 24.7.

HRMS (ESI⁺) C₉H₁₃NO₂Na [M+Na]⁺: found 190.0844, required 190.0838.



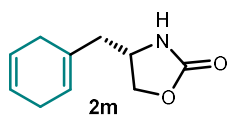
(2*R*,5*S*)-2-(*tert*-Butyl)-5-(cyclohexa-1,4-dien-1-ylmethyl)-3-methylimidazolidin-4-one (2l)

Synthesized according to the general procedure C using (2*R*,5*S*)-5-benzyl-2-0(*tert*-butyl)-3-methylimidazolidin-4-one (45.4 μL, 49.3 mg, 0.3 mmol, 1 equiv.). The crude mixture was purified by flash column chromatography on silica gel (hexane/EtOAc 2:1) to afford **2l** as a white/yellow solid (24 mg, 49% yield).

¹H NMR (500 MHz, CDCl₃): δ 5.94 (s, 1H), 5.89 – 5.80 (m, 2H), 4.25 (d, *J* = 1.5 Hz, 1H), 3.89 (dd, *J* = 10.1, 3.8 Hz, 1H), 3.32 (s, 1H), 2.96 (s, 3H), 2.90 – 2.72 (m, 3H), 2.61 (d, *J* = 14.5 Hz, 1H), 2.58 – 2.45 (m, 1H), 2.15 (dd, *J* = 14.6, 10.0 Hz, 1H), 1.04 (s, 9H).

¹³C NMR (126 MHz, CDCl₃): δ 174.8, 133.2, 123.2, 122.9, 121.1, 83.9, 56.6, 41.3, 37.0, 31.5, 28.5, 27.5, 25.6.

HRMS (ESI⁺) C₁₅H₂₅N₂O [M+H]⁺: found 249.1958, required 249.1961.



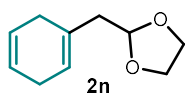
(S)-4-(Cyclohexa-1,4-dien-1-ylmethyl)oxazolidin-2-one (2m)

Synthesized according to the general procedure **C** using (S)-4-Benzyl-2-oxazolidinone (53.2 mg, 0.3 mmol). The crude mixture was purified by flash column chromatography on silica gel (hexanes/EtOAc 2:1) to afford **2m** as a white solid (29 mg, 54% yield).

¹H NMR (500 MHz, CDCl₃): δ 5.75 – 5.65 (m, 2H), 5.56 – 5.50 (m, 1H), 5.34 (br s, 1H), 4.49 (t, *J* = 8.2 Hz, 1H), 4.05 (dd, *J* = 8.4, 5.6 Hz, 1H), 4.00 (tt, *J* = 8.1, 5.9 Hz, 1H), 2.75 – 2.66 (m, 2H), 2.67 – 2.49 (m, 2H), 2.23 (qd, *J* = 14.0, 6.9 Hz, 2H).

¹³C NMR (126 MHz, CDCl₃): δ 159.3, 130.0, 124.4, 123.6, 132.0, 70.1, 50.3, 43.5, 29.2, 26.8.

HRMS (ESI⁺) C₁₀H₁₃NO₂Na [M+Na]⁺: found 202.0844, required 202.0838.



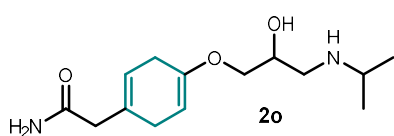
2-(Cyclohexa-1,4-dien-1-ylmethyl)-1,3-dioxolane (2n)

Synthesized according to the general procedure **C** using 2-benzyl-1,3-dioxolane (32.8 mg, 0.2 mmol). The crude mixture was purified by flash column chromatography on silica gel (hexane/EtOAc 99:1 to 97:3) to afford **2n** as a yellowish oil (43% yield, 14.3 mg).

¹H NMR (600 MHz, CDCl₃): δ 5.73 – 5.65 (m, 2H), 5.59 – 5.55 (m, 1H), 4.95 (t, *J* = 5.1 Hz, 1H), 4.03 – 3.94 (m, 2H), 3.90 – 3.81 (m, 2H), 2.72 – 2.62 (m, 4H), 2.33 (d, *J* = 5.1 Hz, 2H).

¹³C NMR (151 MHz, CDCl₃): δ 130.3, 124.2, 124.0, 122.0, 103.7, 64.9, 42.3, 29.8, 26.9.

HRMS (ESI⁺) C₁₀H₁₄O₂Na [M+Na]⁺: found 189.0891, required 189.0886.



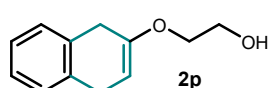
2-(4-(2-Hydroxy-3-(isopropylamino)propoxy)cyclohexa-1,4-dien-1-yl)acetamide (2o)

Synthesized according to the general procedure **C** using *Atenolol* (50.5 mg, 0.2 mmol). The crude mixture was subjected to removal of volatiles, and the resulting residue was washed with DCM and hexane, to afford **2o** as a pale yellow solid (54% yield, 27.5 mg).

¹H NMR (600 MHz, DMSO-*d*₆): δ 7.26 (s, 1H), 6.80 (s, 1H), 5.46 – 5.41 (m, 1H), 4.96 (br s, 1H), 4.61 (t, *J* = 2.9 Hz, 1H), 3.76 (m, 1H), 3.62 (dd, *J* = 9.9, 5.0 Hz, 1H), 3.56 (dd, *J* = 9.9, 6.0 Hz, 1H), 2.82 – 2.75 (m, 1H), 2.74 (s, 2H), 2.66 (m, 5H), 2.55 – 2.51 (m, 2H), 0.99 (dd, *J* = 6.4, 1.6 Hz, 6H).

¹³C NMR (151 MHz, DMSO-*d*₆): δ 172.0, 151.2, 130.6, 120.2, 91.0, 69.2, 67.7, 49.7, 48.5, 43.4, 29.1, 28.9, 22.3.

HRMS (ESI⁺) C₁₄H₂₄N₂O₃Na [M+Na]⁺: found 291.1685, required 291.1679.



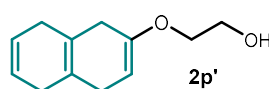
2-((1,4-Dihydronaphthalen-2-yl)oxy)ethan-1-ol (2p)

Synthesized according to the general procedure C using 2-(naphthalen-2-yloxy)ethanol (18.8 mg, 0.1 mmol). The crude mixture was purified by flash column chromatography on silica gel (hexane/EtOAc 95:5 to 85:15) to afford **2p** as a white solid (47% yield, 9 mg).

¹H NMR (600 MHz, CDCl₃): δ 7.19 – 7.11 (m, 4H), 4.86 (t, *J* = 3.6 Hz, 1H), 3.91 – 3.88 (m, 4H), 3.52 – 3.48 (m, 2H), 3.48 – 3.44 (m, 2H), 2.03 – 1.95 (m, 1H).

¹³C NMR (151 MHz, CDCl₃): δ 152.2, 134.0, 133.5, 128.3, 128.0, 125.9, 125.8, 91.8, 67.7, 61.4, 32.1, 29.4.

HRMS (ESI⁺) C₁₂H₁₅O₂ [M+H]⁺: found 191.1028, required 191.1067.



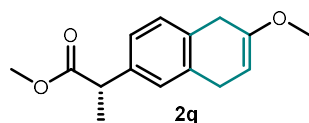
2-((1,4,5,8-Tetrahydronaphthalen-2-yl)oxy)ethan-1-ol (2p')

Synthesized according to the general procedure C using 2-(Naphthalen-2-yloxy)ethanol (18.8 mg, 0.1 mmol). The crude mixture was purified by flash column chromatography on silica gel (hexane/EtOAc 95:5 to 85:15) to afford **2p'** as a green liquid (21% yield, 4 mg).

¹H NMR (600 MHz, CDCl₃): δ 5.78 – 5.67 (m, 2H), 4.67 (t, *J* = 3.3 Hz, 1H), 3.88 – 3.84 (m, 2H), 3.84 – 3.80 (m, 2H), 2.69 – 2.64 (m, 2H), 2.64 – 2.60 (m, 2H), 2.58 (s, 4H), 1.91 (t, *J* = 6.1 Hz, 1H).

¹³C NMR (151 MHz, CDCl₃): δ 152.3, 124.9, 124.5, 124.0, 122.9, 92.2, 67.9, 61.9, 33.6, 31.7, 31.2, 30.7.

HRMS (ESI⁺) C₁₂H₁₇O₂ [M+H]⁺: found 193.1228, required 193.1223.



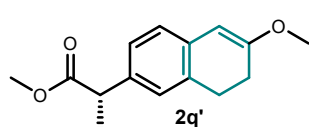
Methyl (*S*)-2-(6-methoxy-5,8-dihydronaphthalen-2-yl)propanoate (2q)

Synthesized according to the general procedure C using methyl (*S*)-2-(6-methoxynaphthalen-2-yl)propanoate (48.9 mg, 0.2 mmol). The crude mixture was purified

by flash column chromatography on silica gel (hexane/EtOAc 20:1) to afford **2q** as a white solid (60% yield, 30 mg).

¹H NMR (400 MHz, CDCl₃): δ 7.09 (dd, *J* = 3.4, 1.7 Hz, 3H), 4.81 (tt, *J* = 3.8, 1.2 Hz, 1H), 3.71 – 3.67 (m, 1H), 3.66 (s, 3H), 3.61 (s, 3H), 3.49 (q, *J* = 4.4 Hz, 2H), 3.40 (t, *J* = 4.8 Hz, 2H), 1.49 (d, *J* = 7.2 Hz, 3H).

¹³C NMR (101 MHz, CDCl₃): δ 175.1, 153.3, 138.2, 134.6, 132.7, 128.6, 126.9, 125.0, 90.5, 54.2, 52.0, 45.1, 31.9, 29.5, 18.7.



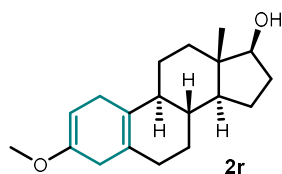
Methyl (*S*)-2-(6-methoxy-7,8-dihydronaphthalen-2-yl)propanoate (2q'**)**

Synthesized according to the general procedure **C** using methyl (*S*)-2-(6-methoxynaphthalen-2-yl)propanoate (48.9 mg, 0.2 mmol). The desired product was detected in 22% NMR yield using CH₂Br₂ as an internal standard (0.2 mmol). Isomerization of **2q** under oxygen atmosphere to **2q'** allowed the isolation and characterization of the product. It was purified by flash column chromatography on silica gel (hexane/EtOAc 20:1) to afford **2q'** as a white solid.

¹H NMR (400 MHz, CDCl₃): δ 7.05 – 6.98 (m, 2H), 6.90 (d, *J* = 7.7 Hz, 1H), 5.52 (s, 1H), 3.69 (s, 3H), 3.68 – 3.62 (m, 4H), 2.87 (t, *J* = 8.2 Hz, 2H), 2.39 (t, *J* = 8.1 Hz, 2H), 1.47 (d, *J* = 7.1 Hz, 3H).

¹³C NMR (151 MHz, CDCl₃): δ 175.5, 160.5, 136.7, 134.7, 132.5, 126.3, 125.7, 125.0, 96.0, 55.0, 52.2, 45.2, 28.8, 27.4, 18.8.

HRMS (MALDI-TOF⁺) C₁₅H₁₈O₃ [M+H]⁺: found 269.1154, required 269.1149.



(8*R*,9*S*,13*S*,14*S*)-3-Methoxy-13-methyl-4,6,7,8,9,11,12,13,14,15,16,17-dodecahydro-1*H*-cyclopenta[*a*]phenanthren-17-ol (2r**)**

Synthesized according to the general procedure **C** using (8*R*,9*S*,13*S*,14*S*)-3-methoxy-13-methyl-7,8,9,11,12,13,14,15,16,17-decahydro-6*H*-cyclopenta[*a*]phenanthren-17-ol (28.6 mg, 0.1 mmol). The crude mixture was purified by flash column chromatography on silica gel (hexane/EtOAc 8:2 to 6:1) to afford **2r** as a white solid (14% yield, 4.0 mg).

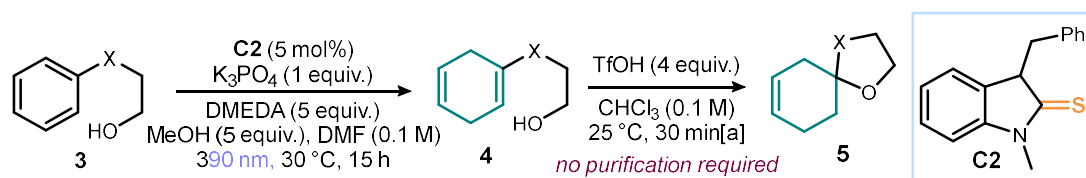
¹H NMR (600 MHz, CDCl₃): δ 4.67 – 4.62 (m, 1H), 3.72 – 3.64 (m, 1H), 3.55 (s, 3H), 2.91 – 2.84 (m, 1H), 2.71 – 2.57 (m, 2H), 2.57 – 2.49 (m, 1H), 2.13 – 2.03 (m, 2H), 1.91 – 1.81 (m, 3H), 1.73 – 1.68 (m, 1H), 1.66 – 1.59 (m, 2H), 1.49 – 1.08 (m, 8H), 0.76 (s, 3H).

¹³C NMR (151 MHz, CDCl₃): δ 152.8, 128.1, 125.1, 90.8, 82.1, 54.0, 50.1, 45.6, 43.5, 39.1, 37.1, 34.3, 30.8, 30.6, 28.5, 26.9, 25.5, 23.2, 11.4.

HRMS (MALDI-TOF⁺) C₁₉H₂₉O₂ [M+H]⁺: found 289.2168, required 289.2162.

5.3 Experimental Procedures and Compound Characterization for Spirocyclization

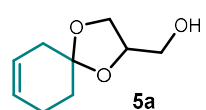
General procedure for spirocyclization (D):



The arene reduction was performed according to general procedure C (see section 5.2). Afterwards, the reaction mixture was filtered through a syringe filter (Acrodisc[®]) to remove solids, then the solvent and excess DMEDA were removed under reduced pressure (40 °C, <15 mbar). In a 4 mL vial equipped with a stirring bar, the remaining residue, containing the crude 1,4-dihydro product **4**, was dissolved in CHCl₃ (0.1 M). The vial was sealed with a screw-top cap with septum and TfOH (4 equiv.) was added via syringe. The reaction mixture was stirred for 30 minutes.

After the reaction was completed, the mixture was filtered and then the solvent was removed under reduced pressure. The crude residue was purified by column chromatography to afford the corresponding product **5** with the reported yields.

For NMR analyses of product **5b**: CH₂Br₂ was added as the internal standard (0.3 mmol, 1 equiv.) to the crude reaction mixture, followed by addition of H₂O. The solution was extracted twice with 0.7 mL of CDCl₃, dried over anhydrous MgSO₄ and then analysed via ¹H NMR.



(1,4-Dioxaspiro[4.5]dec-7-en-2-yl)methanol (5a)

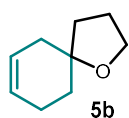
Synthesized according to the general procedure D using 3-phenoxypropane-1,2-diol (50.5 mg, 0.3 mmol). The crude mixture was purified by flash column chromatography

on silica gel (hexane/EtOAc 95:5) to afford **5a** in a diastereomeric mixture (1:1) as a colourless oil (23% yield, 13.6 mg over both steps).

Diastereomeric mixture (1:1):

¹H NMR (600 MHz, CDCl₃): δ 5.75 – 5.67 (m, 2H, d₁+d₂), 5.64 – 5.58 (m, 2H, d₁+d₂), 4.33 – 4.23 (m, 2H, d₁+d₂), 4.08 (td, J = 8.2, 6.5 Hz, 2H, d₁+d₂), 3.85 (ddd, J = 8.2, 6.5, 4.5 Hz, 2H, d₁+d₂), 3.77 (dd, J = 11.7, 3.7 Hz, 2H, d₁+d₂), 3.61 (ddd, J = 11.8, 5.0, 0.6 Hz, 2H, d₁+d₂), 2.39 – 2.18 (m, 8H, d₁+d₂), 1.86 – 1.69 (m, 4H, d₁+d₂).

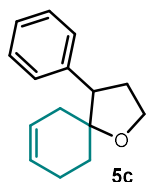
¹³C NMR (151 MHz, CDCl₃): δ 126.49, 126.47, 124.07, 124.04, 108.85, 108.76, 76.03, 75.89, 65.47, 65.41, 62.92, 62.86, 36.53, 35.48, 32.12, 30.52, 24.57, 24.40.



1-Oxaspiro[4.5]dec-7-ene (5b)

Synthesized according to the general procedure **D** using 3-phenylpropan-1-ol (27 mg, 0.2 mmol). The yield was determined by adding CH₂Br₂ (1 equiv.) as internal standard to the reaction mixture (NMR yield: 36% over both steps).

Matching reported literature data.⁴⁶



3,4-Dihydro-1H-spiro[naphthalene-2,2'-[1,3]dioxolane] (5c)

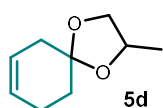
Synthesized according to the general procedure **D** using 3,3-diphenylpropan-1-ol (63.7 mg, 0.3 mmol). The crude mixture was purified by flash column chromatography on silica gel (hexane) to afford **5c** in a diastereomeric mixture (2:1) as a colourless oil (16% yield, 10.3 mg over both steps).

Diastereomeric mixture (2:1):

¹H NMR (600 MHz, CDCl₃): δ 7.33 – 7.27 (m, 2H d₁ + 1H d₂), 7.26 – 7.16 (m, 3H d₁ + 1.5H d₂), 5.72 – 5.53 (m, 2H d₁), 5.46 (ddtd, J = 10.0, 4.5, 2.7, 1.6 Hz, 1H d₂), 4.16 (td, J = 8.8, 4.5 Hz, 1H d₁), 4.13 – 4.07 (m, 0.5H d₂), 4.02 – 3.95 (m, 1H d₁ + 0.5H d₂), 3.11 – 3.05 (m, 1H d₁ + 0.5H d₂), 2.46 (dtd, J = 12.8, 8.3, 4.5 Hz, 1H d₁), 2.39 – 2.25 (m, 2H d₁ + 1.5H d₂), 2.15 – 2.05 (m, 2H d₁), 1.92 – 1.86 (m, 0.5H d₂), 1.85 – 1.78 (m, 1H d₁ + 0.5H d₂), 1.77 (m, 0.5H d₂), 1.74 – 1.68 (m, 1H d₁), 1.68 – 1.62 (m, 1H d₁), 1.61 – 1.58 (m, 0.5H d₂), 0.99 – 0.93 (m, 0.5H d₂).

⁴⁶McElroy, T.; Thomas, J. B.; Brine, G. A.; Navarro, H. A.; Deschamps, J.; Carroll F. I. A Practical Synthesis of the Kappa Opioid Receptor Selective Agonist (+)-5*R*,7*S*,8*S*-*N*-Methyl-*N*-[7-(1-pyrrolidiny)-1-oxaspiro[4,5]dec-8-yl]benzeneacetamide (U69,593). *Synlett* **2008**, 6, 943–947.

¹³C NMR (151 MHz, CDCl₃): δ 141.66, 140.08, 128.54, 128.39, 128.13, 128.12, 127.08, 126.65, 126.50, 126.46, 126.24, 124.66, 124.59, 82.74, 82.09, 65.20, 65.17, 53.67, 53.64, 36.28, 32.56, 32.44, 31.86, 31.85, 29.69, 28.02, 23.35, 22.45.



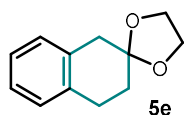
2-Methyl-1,4-dioxaspiro[4.5]dec-7-ene (5d)

Synthesized according to the general procedure **D** using 1-phenoxypropan-2-ol (45.7 mg, 0.3 mmol). The crude mixture was purified by flash column chromatography on silica gel (hexane) to afford **5d** in a diastereomeric mixture (1:1) as a colourless oil (32% yield, 14.9 mg over both steps).

¹H NMR (600 MHz, CDCl₃): δ 5.75 – 5.66 (m, 2H), 5.64 – 5.56 (m, 1H), 4.33 – 4.22 (m, 1H), 4.09 (ddd, *J* = 9.0, 7.9, 5.7 Hz, 1H), 3.48 (td, *J* = 7.8, 4.1 Hz, 1H), 2.35 – 2.20 (m, 4H), 1.82 – 1.73 (m, 2H), 1.30 (dd, *J* = 6.1, 2.0 Hz, 3H).

¹³C NMR (151 MHz, CDCl₃): δ 126.6, 126.5, 124.4, 124.3, 108.1, 108.1, 72.0, 71.8, 70.7, 70.6, 37.0, 36.0, 32.5, 31.2, 24.6, 24.5, 18.6, 18.6.

HRMS (ESI⁺) C₁₁H₁₄O₂Na [M+Na]⁺: found 177.0891, required 177.0886.



3,4-Dihydro-1H-spiro[naphthalene-2,2'-[1,3]dioxolane] (5e)

Synthesized according to the general procedure **D** using 2-(naphthalen-2-yloxy)-ethanol (56.5 mg, 0.3 mmol). The crude mixture was purified by flash column chromatography on silica gel (hexane) to afford **5e** as a colourless oil (37% yield, 24.7 mg over both steps).

¹H NMR (600 MHz, CDCl₃): δ 7.15 – 7.02 (m, 4H), 4.08 – 4.00 (m, 4H), 3.01 – 2.96 (m, 4H), 1.99 – 1.92 (m, 2H).

¹³C NMR (151 MHz, CDCl₃): δ 135.2, 134.4, 129.3, 128.5, 126.0, 125.8, 108.3, 64.5, 39.1, 31.8, 29.7, 28.0.

5.4 Photophysical Studies

Sample Preparation:

- Neutral catalyst **C2**

A 25 mL glass vial containing catalyst **C2** (0.01 mmol) was sealed with a septum, vacuumed and backfilled with argon for 3 times, then degassed DMF (5 mL, HPLC

grade) was added via syringe ($2 \cdot 10^{-3}$ M solution). 40 μ L of the stock solution were taken and diluted further with DMF (4 mL) to obtain a $2 \cdot 10^{-5}$ M solution (20 μ L were taken for a $1 \cdot 10^{-5}$ M solution). 3 mL of the solution were transferred into an argon filled quartz cuvette (10 x 10 mm light path) equipped with a septum.

- Deprotonated catalyst **I**

A 25 mL glass vial containing K_3PO_4 (130 mg) was sealed with a septum, vacuumed and backfilled with argon for 3 times, then degassed DMF (16 mL, HPLC grade) was added via syringe. Addition of 160 μ L of a freshly prepared neutral catalyst **C2** solution ($2 \cdot 10^{-3}$ M) gave a $2 \cdot 10^{-5}$ M solution (80 μ L were taken for a $1 \cdot 10^{-5}$ M solution). The vial was sealed with Parafilm and stirred at ambient temperature for 0.5 hour. 3 mL of the solution were transferred into an argon filled quartz cuvette (10 x 10 mm light path) equipped with a septum.

Absorption Measurements

UV-Vis measurements were carried out on an Agilent Cary 60 UV-Vis spectrophotometer equipped with two silicon diode detectors, double beam optics and Xenon pulse light.

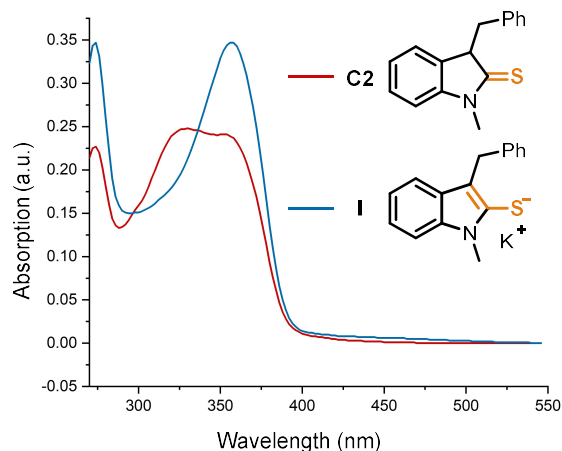


Figure 5.2. Absorption spectra recorded for catalyst **C2** in DMF without (red line) and with (blue line) K_3PO_4 in a $2 \cdot 10^{-5}$ M solution.

Emission Spectrum

Fluorescence measurements were carried out on an Aminco-Bowman Series 2 Luminescence spectrofluorimeter equipped with a high voltage PMT detector and continuum Xe light source. The emission spectrum of the deprotonated catalyst **I** (formed in situ upon addition of K_3PO_4

to **C2** in degassed DMF according to the standard procedure) was recorded from 370 nm to 600 nm after excitation with a 355 nm laser (Figure 5.3).

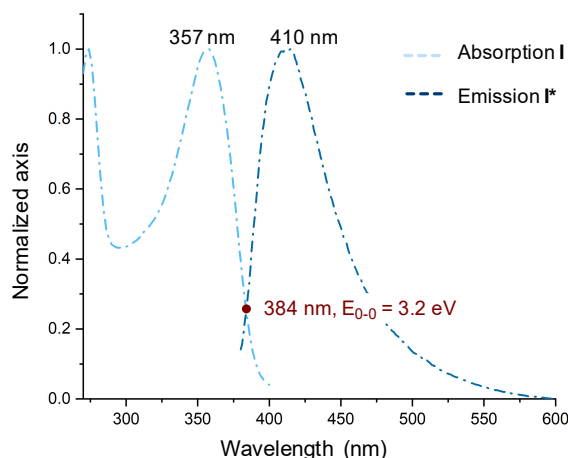


Figure 5.3. Normalized absorption and emission spectra of the active catalyst **I** (formed upon deprotonation of **C2**) in DMF in a $2 \cdot 10^{-5}$ M solution.

Stern-Volmer Quenching Studies

Fluorescence measurements were carried out on an Aminco-Bowman Series 2 Luminescence spectrofluorimeter equipped with a high voltage PMT detector and continuum Xe light source. A 1.0 M solution of the quencher substrate **1a** in degassed DMF was prepared and 20 μ L of this stock solution were added to the solution of the active catalyst **C2**, prepared according to the standard procedure. The addition of the anisole (**1a**) solution (the quencher) was repeated for five times. After each addition, the solution was mixed and the emission spectra of the excited catalyst was acquired from 380 nm to 600 nm (the excitation wavelength was fixed at 370 nm) (Figure 5.4). A solvent blank was subtracted from all the measurements.

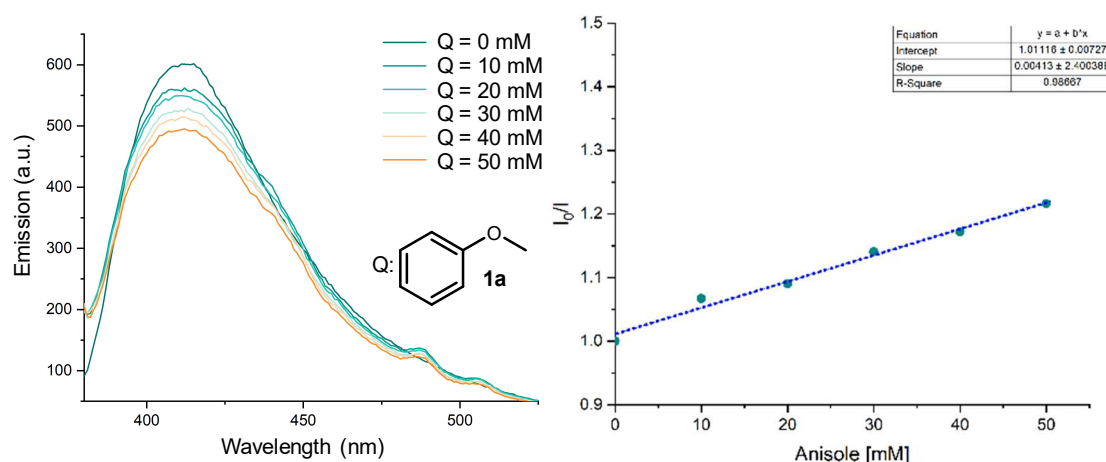


Figure 5.4. Stern-Volmer quenching studies of the deprotonated catalyst **C2** with anisole **1a**.

The Stern-Volmer plot shows a linear correlation between the amounts of anisole (**1a**) and the ratio I_0/I , following the relationship: $I_0/I = 1 + K_{SV}[Q]$ (Q = Quencher).

For **1a** as quencher, a Stern-Volmer quenching constant of 0.00413 M^{-1} was calculated.

5.5 Electrochemical Studies

Cyclic voltammetry (CV) measurements were carried out on a Princeton Applied Research PARSTAT 2273 instrument with a glassy carbon disk electrode (diameter: 3 mm) as working electrode. A silver wire coated with AgCl immersed in a 3.0 M aqueous solution of KCl and separated from the analyte by a fritted glass disk was employed as the reference electrode and a Pt wire counter-electrode completed the electrochemical setup. The scan rate was 100 mV/s unless otherwise stated. The substrates were measured at a concentration of 0.01 M in DMF with TBAPF₆ (0.1 M) as electrolyte (Figure 5.5). The preparation of the deprotonated catalyst solutions was carried out as described in the photophysical studies section 5.4 (at a concentration of 0.01 M).

Potentials are quoted with the following notation: E_p^C (E_{Red}) refers to the cathodic peak potential, E_p^A (E_{Ox}) refers to the anodic peak potential.

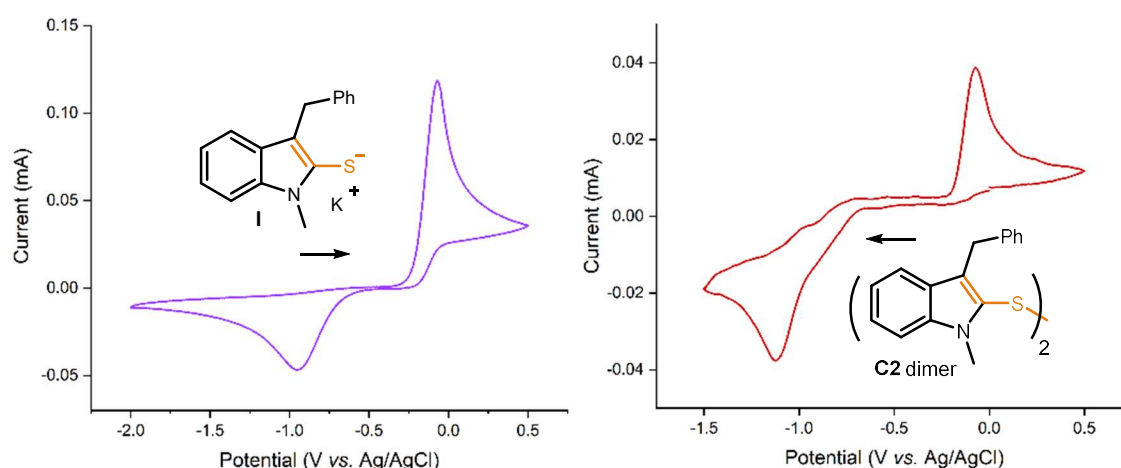


Figure 5.5. (left) CV of the deprotonated catalyst **I** in DMF starting with the oxidation, irreversible oxidation $E_p^A = -0.07 \text{ V}$ and irreversible reduction $E_p^C = -0.95 \text{ V}$ vs. Ag/AgCl. **(right)** CV of the dimer of catalyst **C2** in DMF starting with the reduction, irreversible oxidation $E_p^A = -0.07 \text{ V}$ vs. Ag/AgCl.

5.6 Evaluation of the Excited-State Potential of the Deprotonated Photocatalyst C2

Using the data collected from the CV studies (Figure 5.5) and from the absorption and emission spectra (Figure 5.3) of the deprotonated catalyst **C2** (anion **I**) and **C2**, we could estimate the redox potential of the excited state with the following equation:⁴⁷

$$E(\mathbf{Pc}^*/\mathbf{Pc}^{-*}) = E(\mathbf{Pc}^*/\mathbf{Pc}^-) - E_{0-0}(\mathbf{Pc}^{-*})/(\mathbf{Pc}^-)$$

Since the electrochemical oxidation of **I** is irreversible (Figure 5.5), the irreversible peak potential E_p anode was used for $E(\mathbf{Pc}^*/\mathbf{Pc}^-)$. The oxidation potential was calculated to be -0.07 V vs. SCE (in ACN). $E_{0-0}(\mathbf{Pc}^{-*})/(\mathbf{Pc}^-)$ was determined spectroscopically from the intersection of the normalized absorbance and emission spectra to have a value of 3.31 eV.

The redox potential of excited-state **I** is:

$$E(\mathbf{Pc}^*/\mathbf{Pc}^{-*}) = (-0.07) - 3.23 = -3.30 \text{ V vs. Ag/AgCl}$$

5.7 Evidence of Hydrogen Bonding Interaction between DMEDA and K₃PO₄

To a 7 mL glass vial, DMEDA (0.1 mmol, 11 μ L, 1 equiv.), K₃PO₄ (0.1 mmol, 21 mg, 1 equiv.) and DMSO-*d*₆ (1 mL) were added. The solution was stirred at ambient temperature for 15 min and then the ¹H NMR spectrum was recorded (Figure 5.6). Upon the addition of K₃PO₄, the symmetric peak signals of DMEDA split into two signals, likely due to hydrogen bonding to only one N–H, leading to the desymmetrization of the molecule.

⁴⁷Buzzetti, L.; Crisenza, G. E. M.; Melchiorre, P. Mechanistic Studies in Photocatalysis. *Angew. Chem. Int. Ed.* **2019**, *58*, 3730–3747.

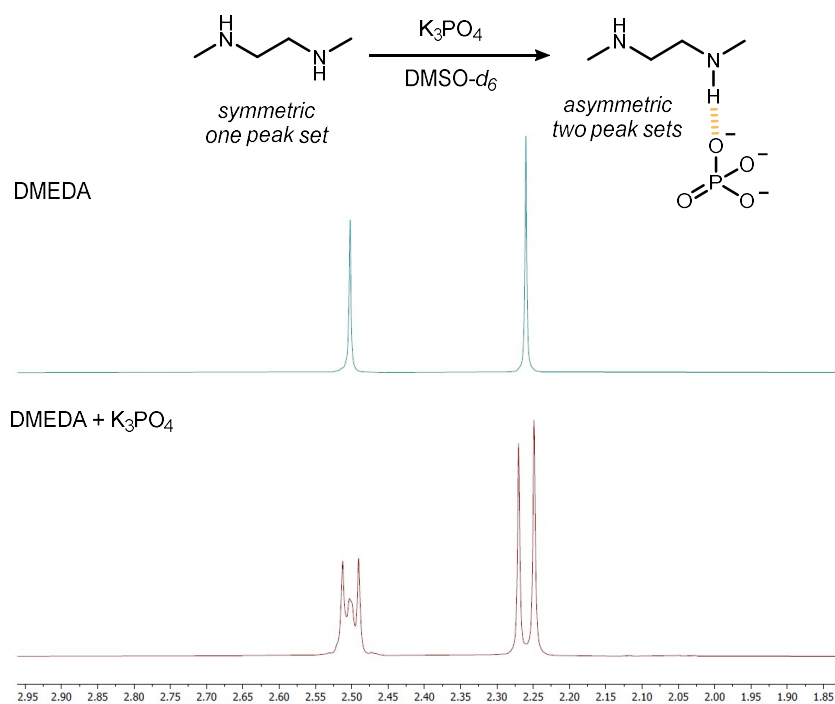
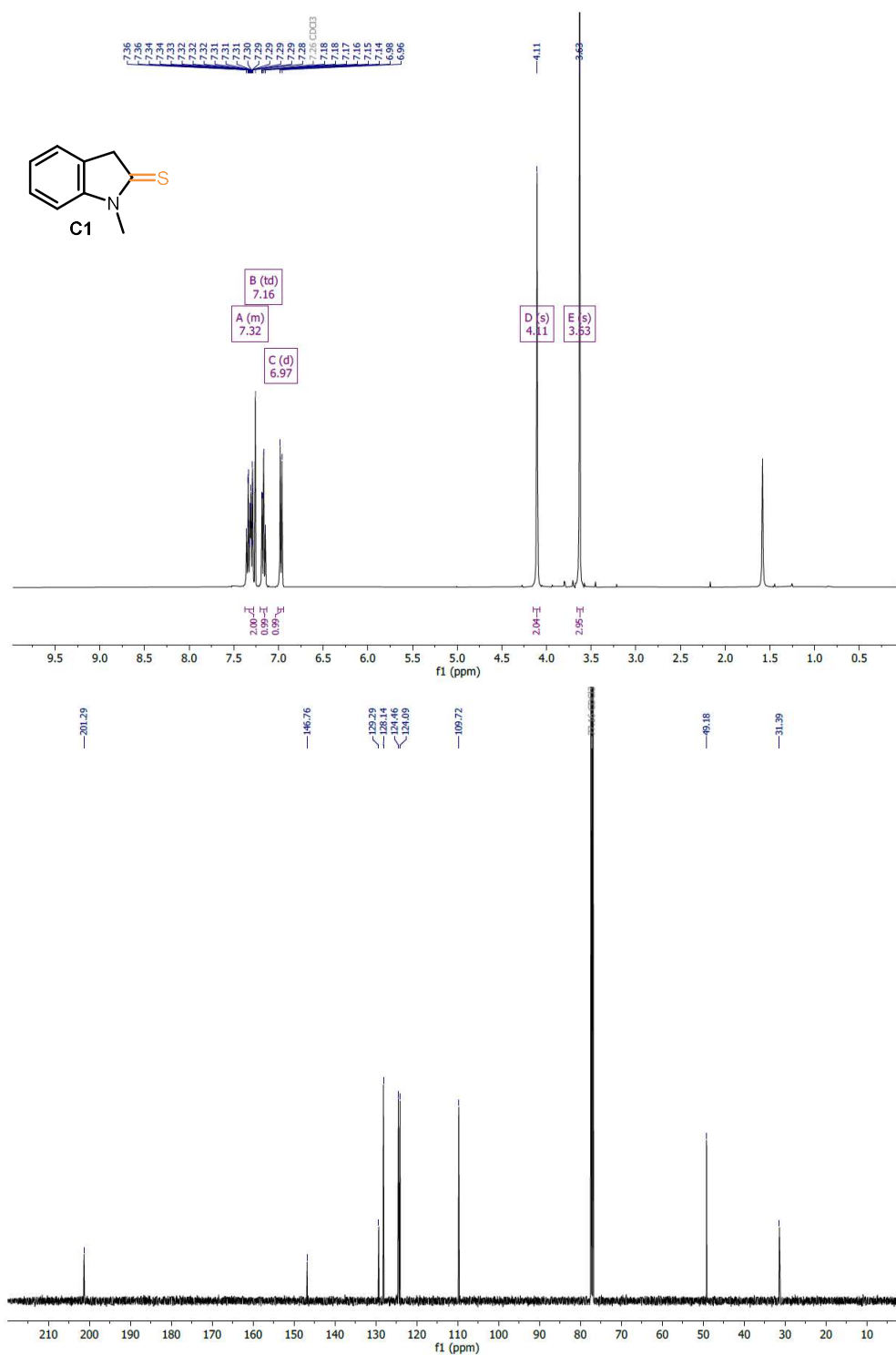
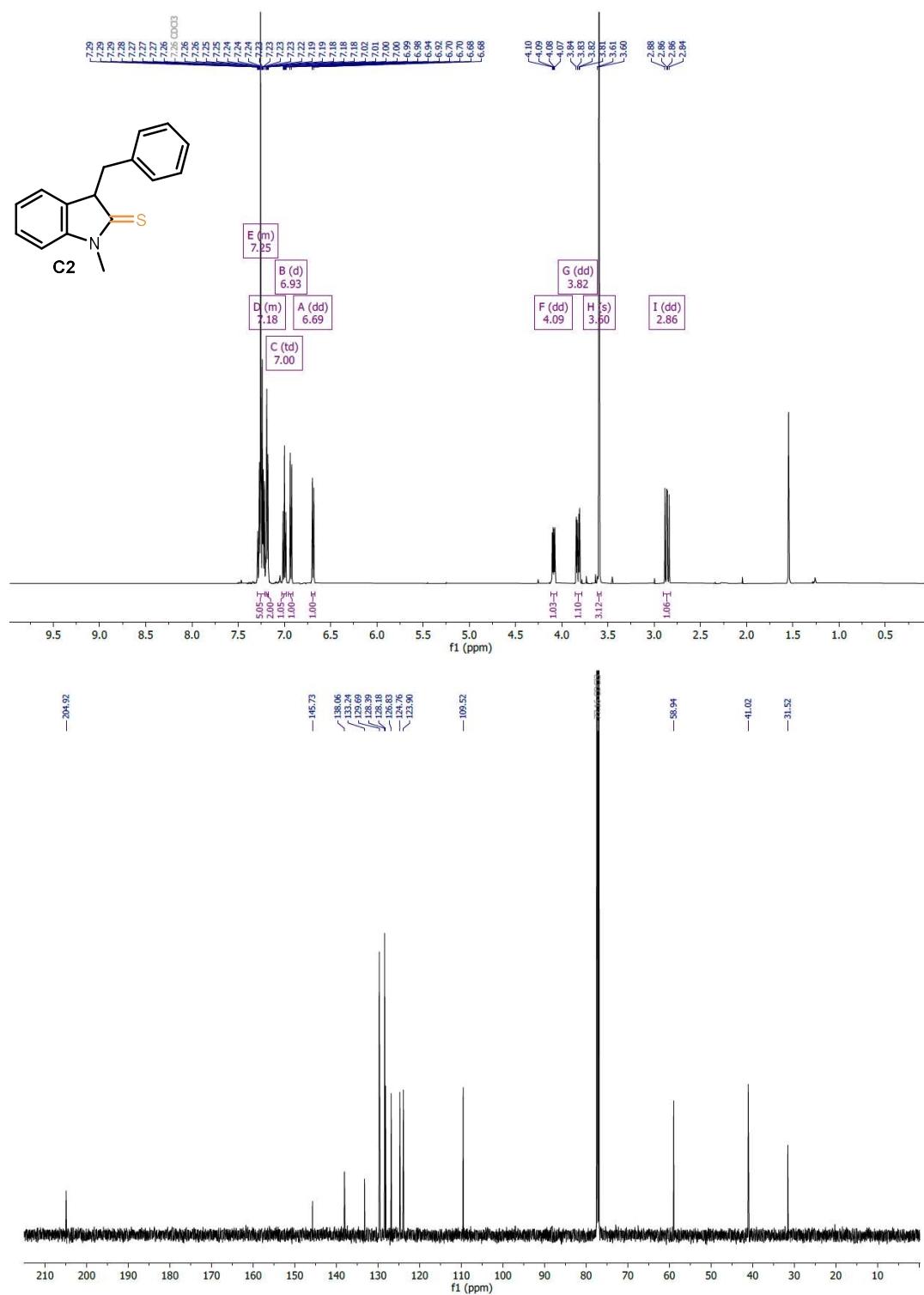
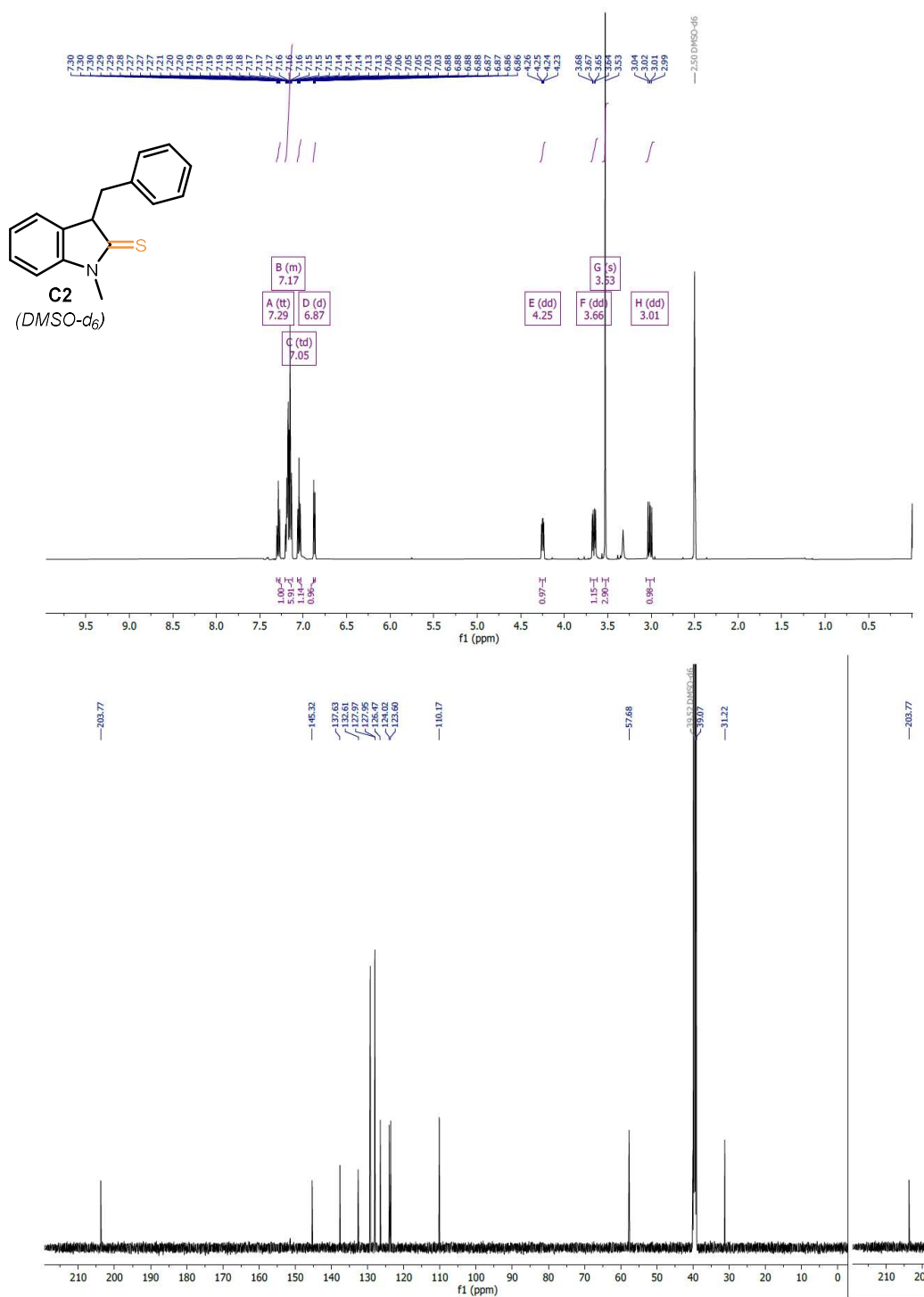


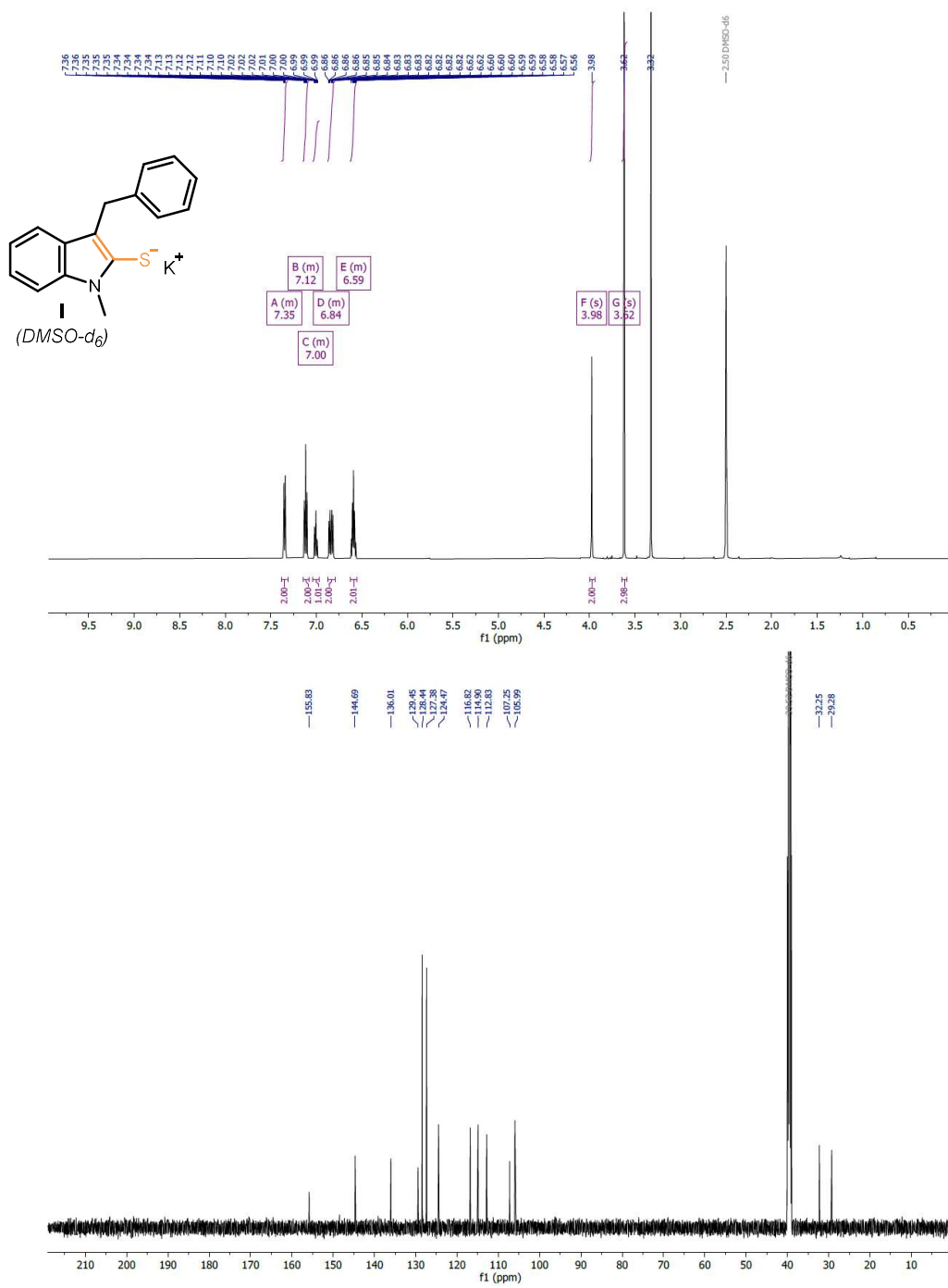
Figure 5.6. Hydrogen bonding interaction between DMEDA and K_3PO_4 .

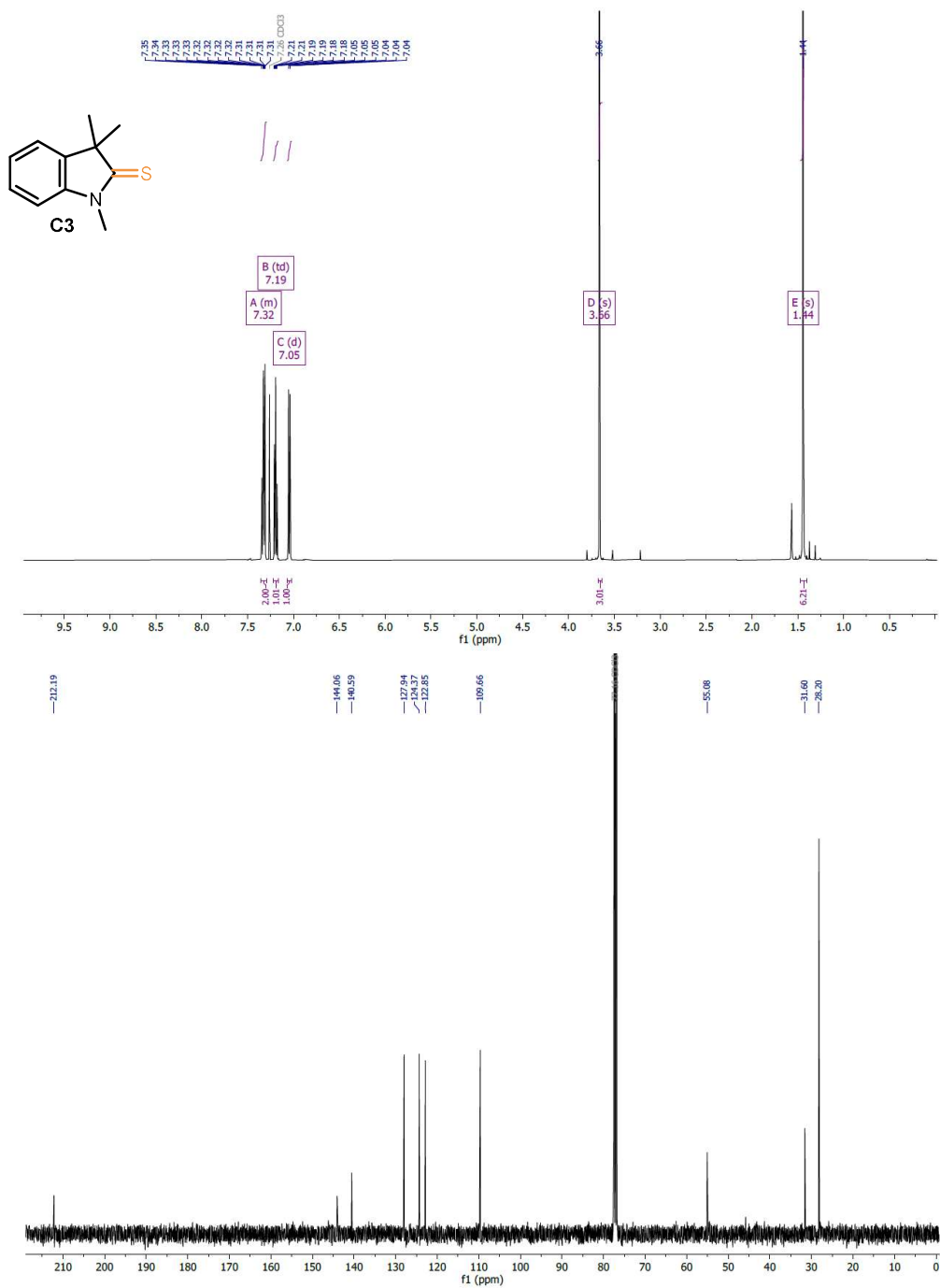
5.8 NMR Spectra

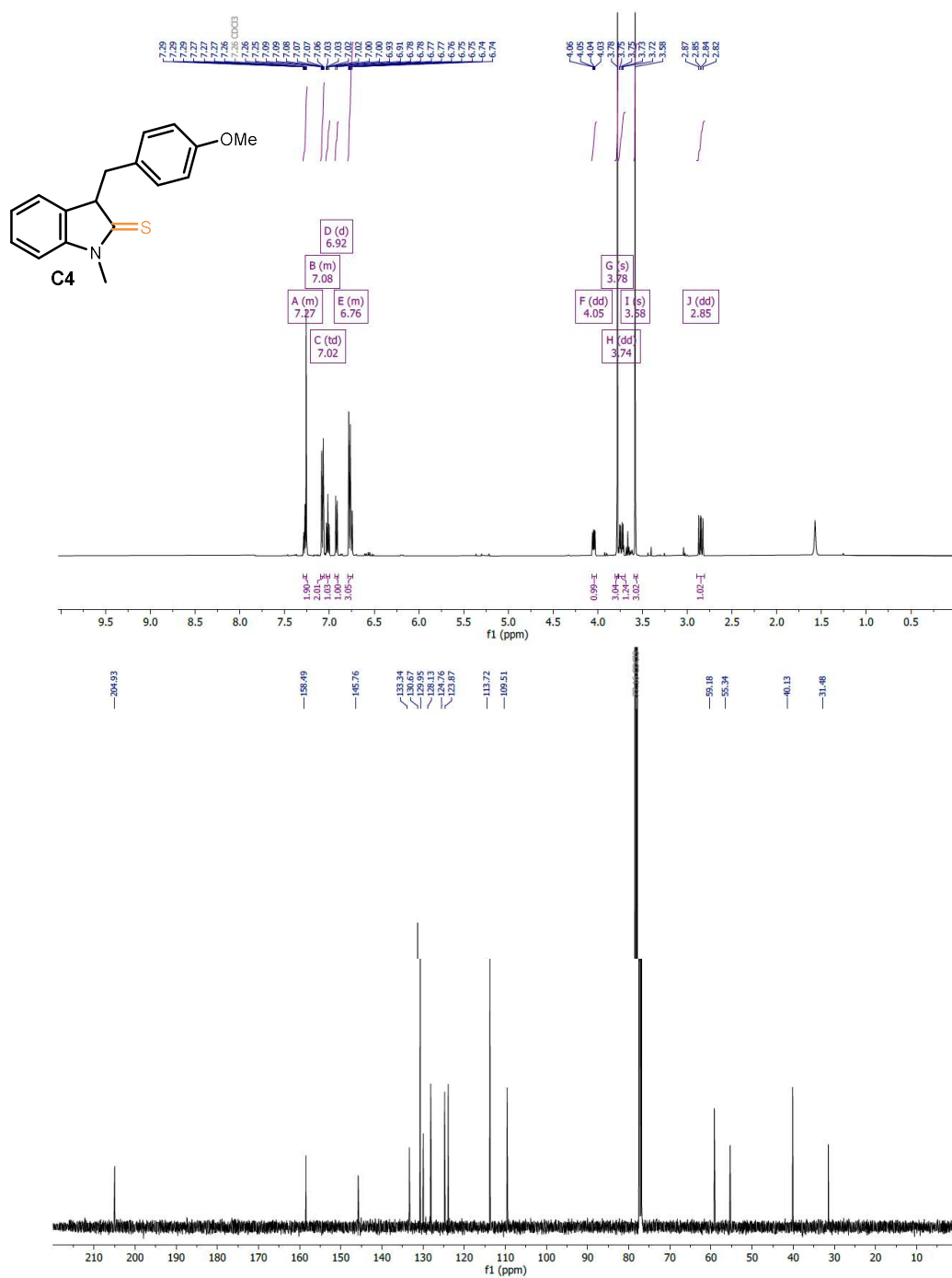


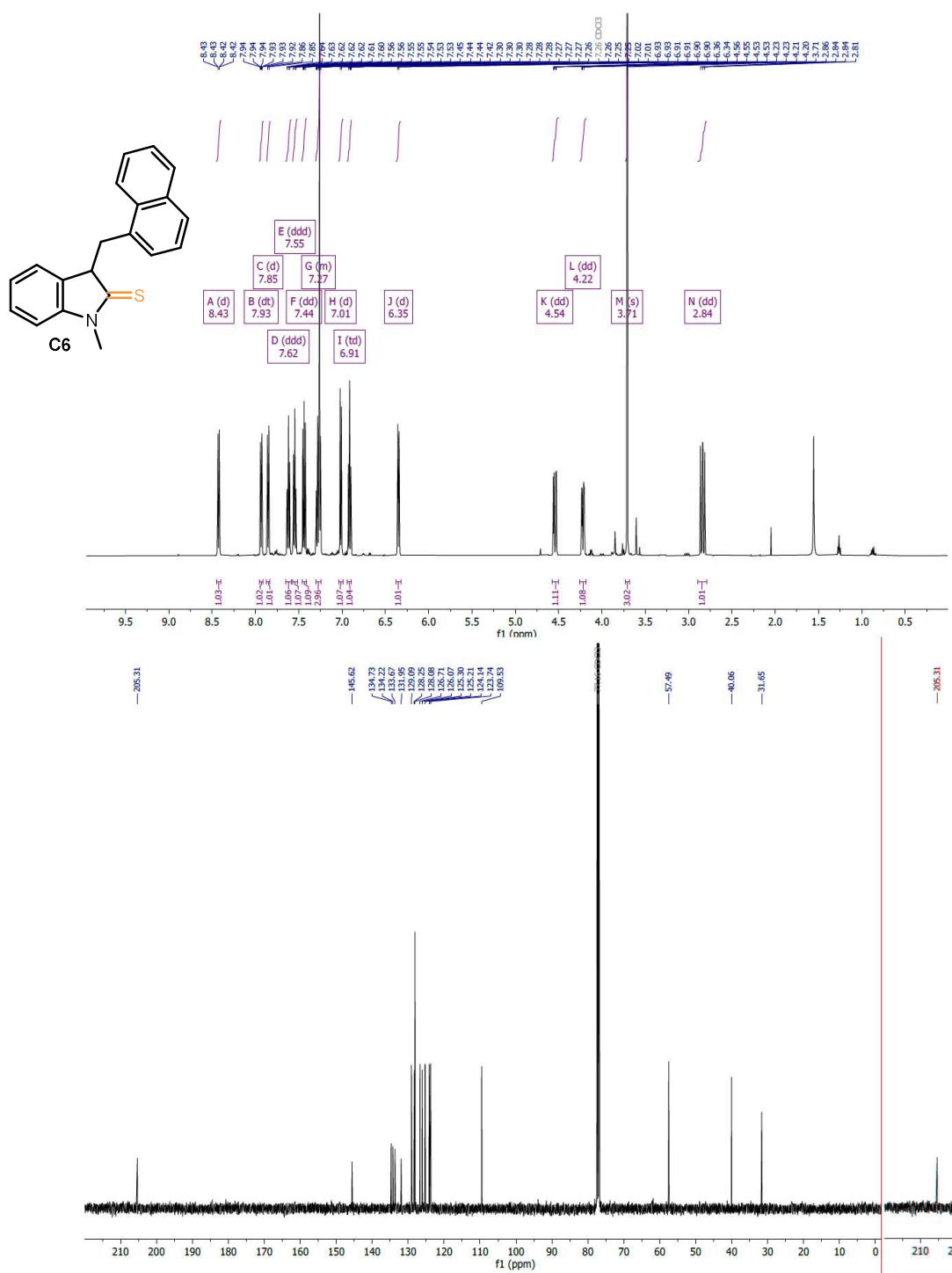


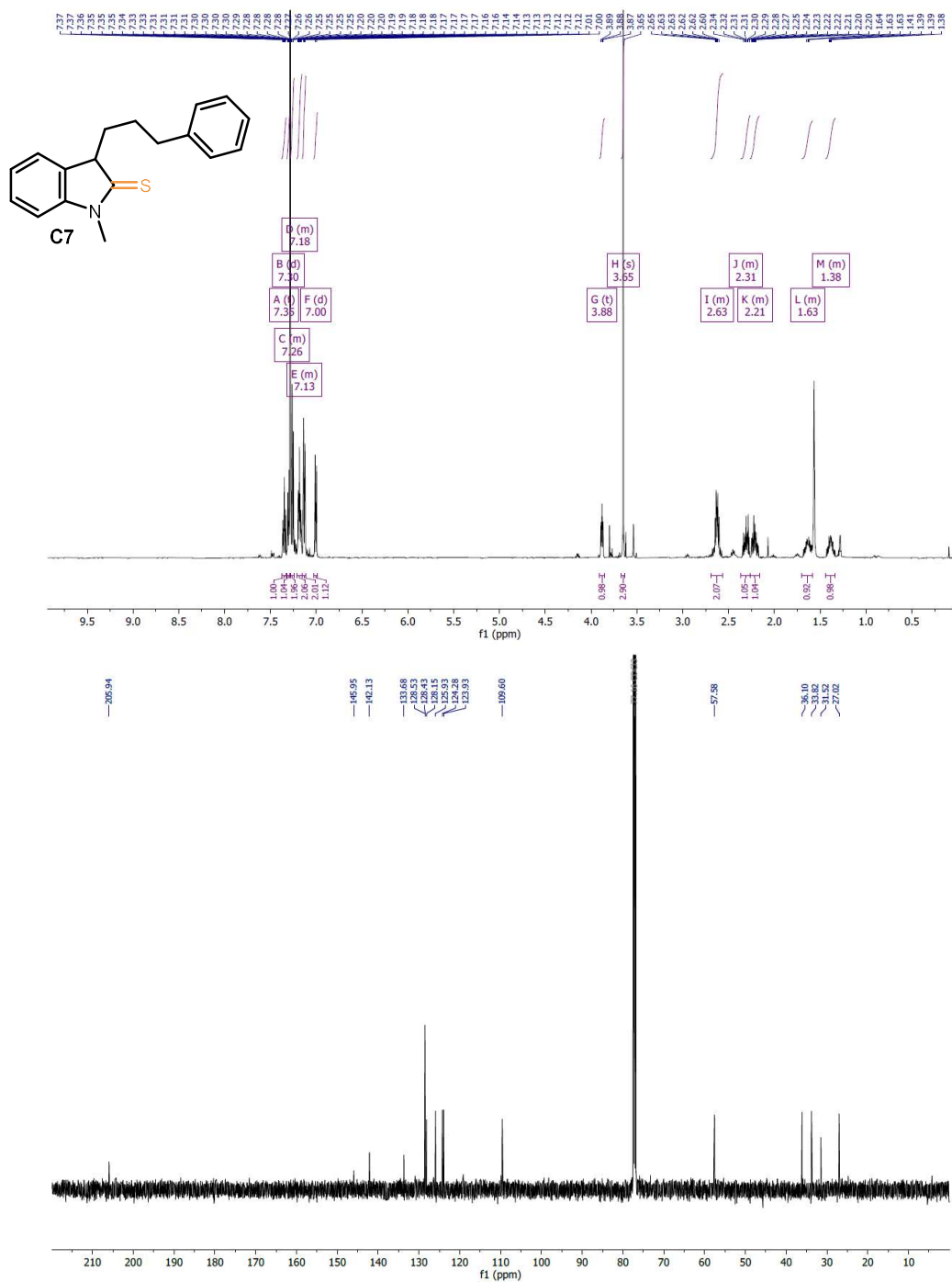


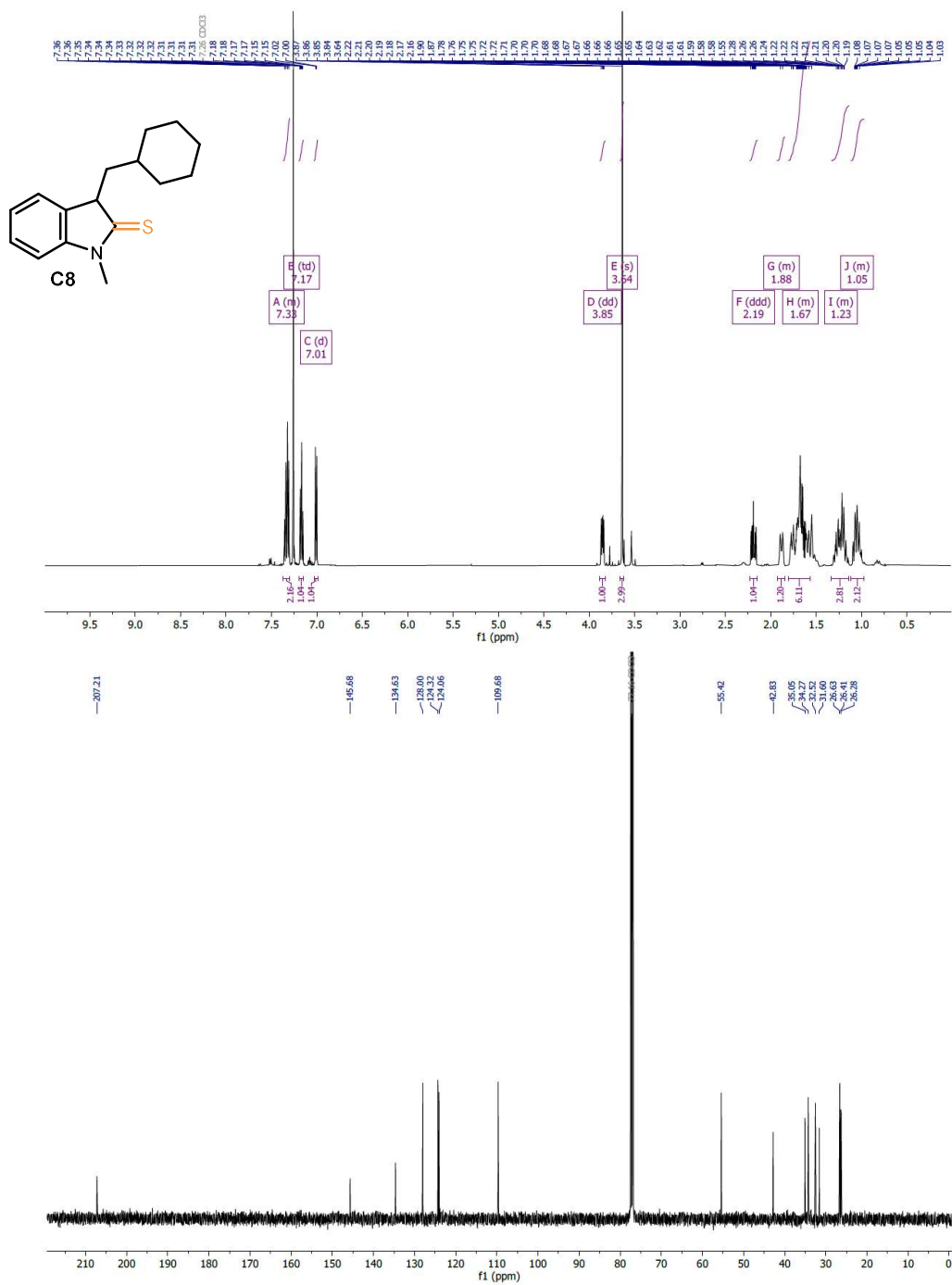


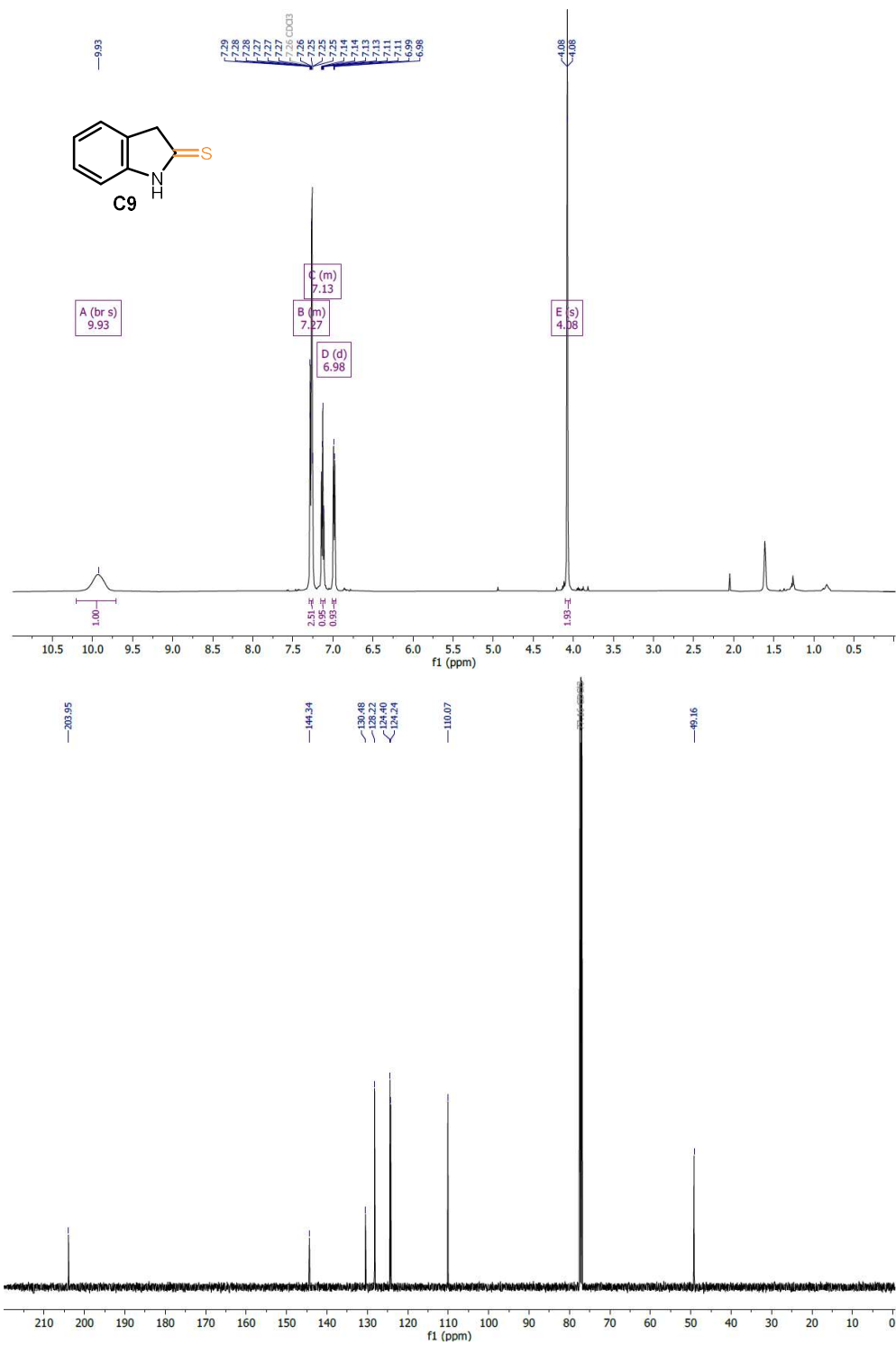


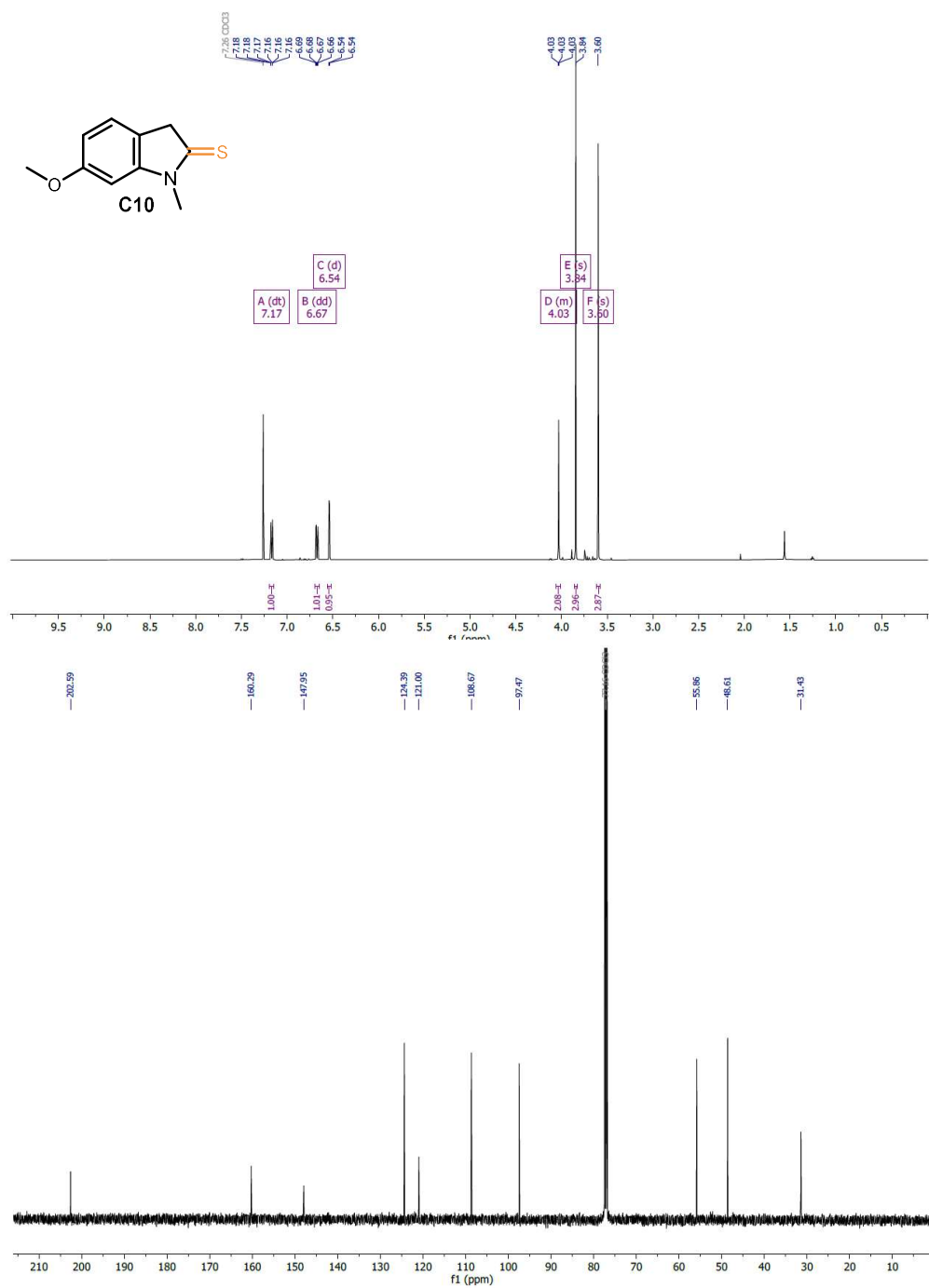


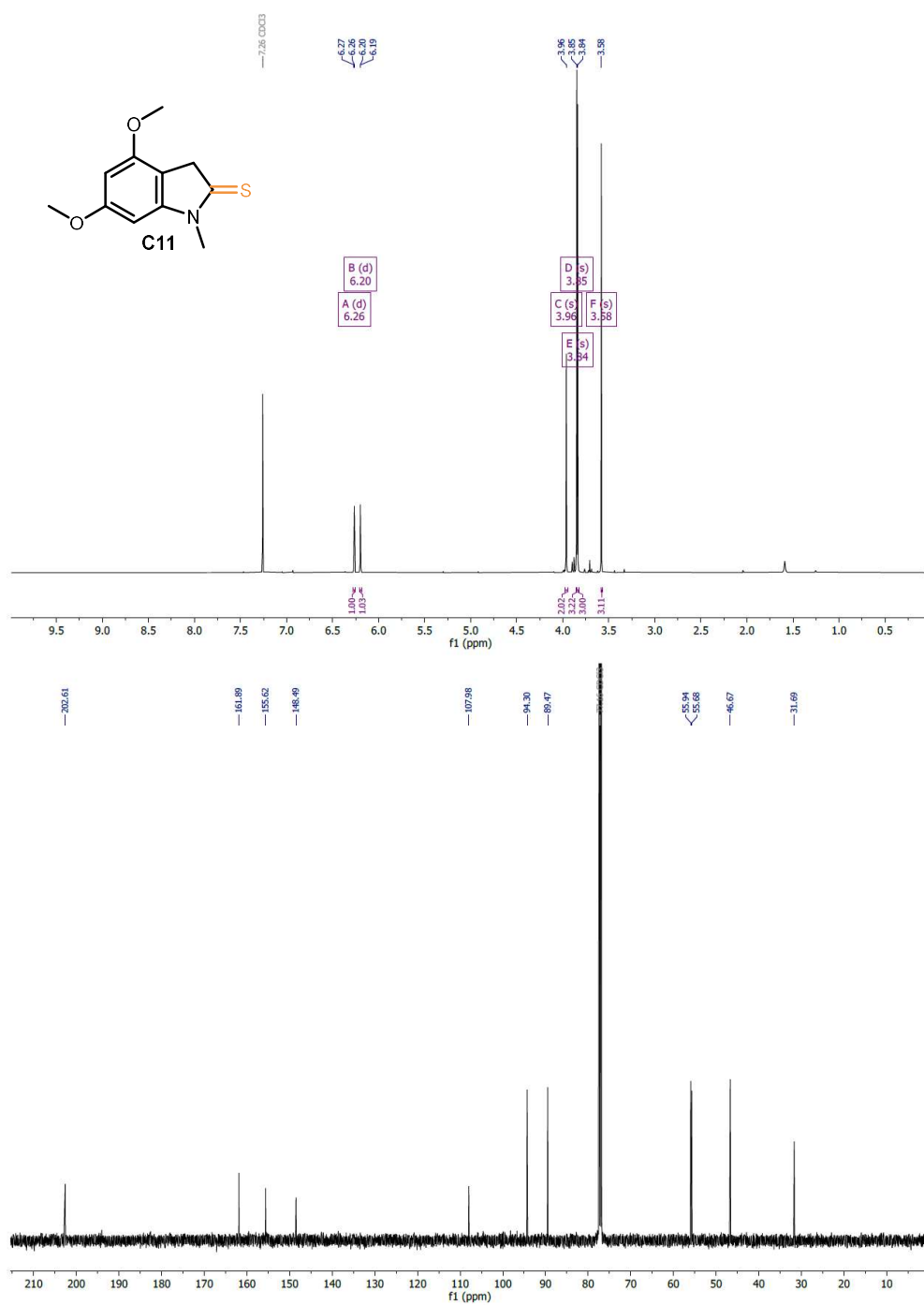


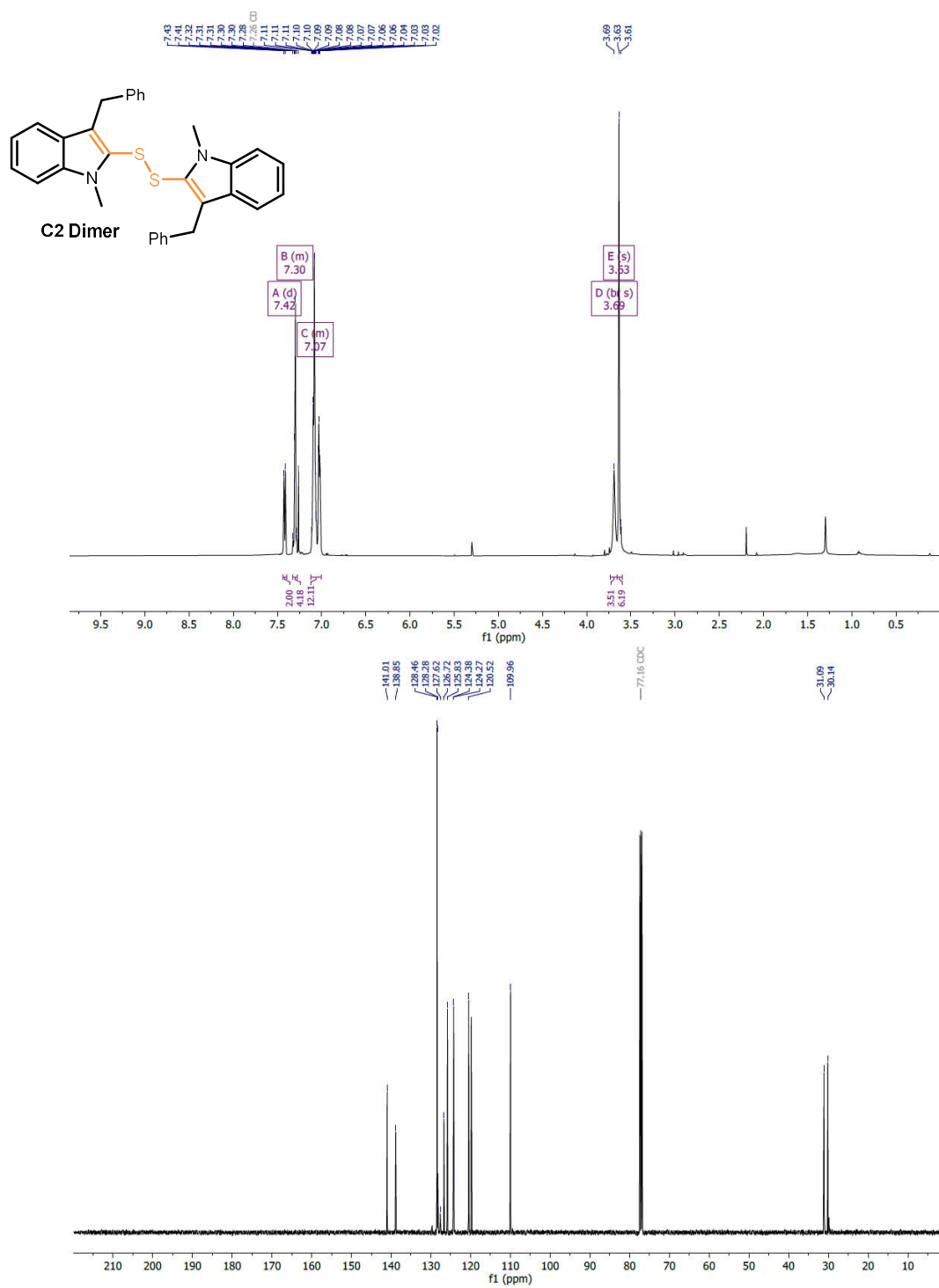


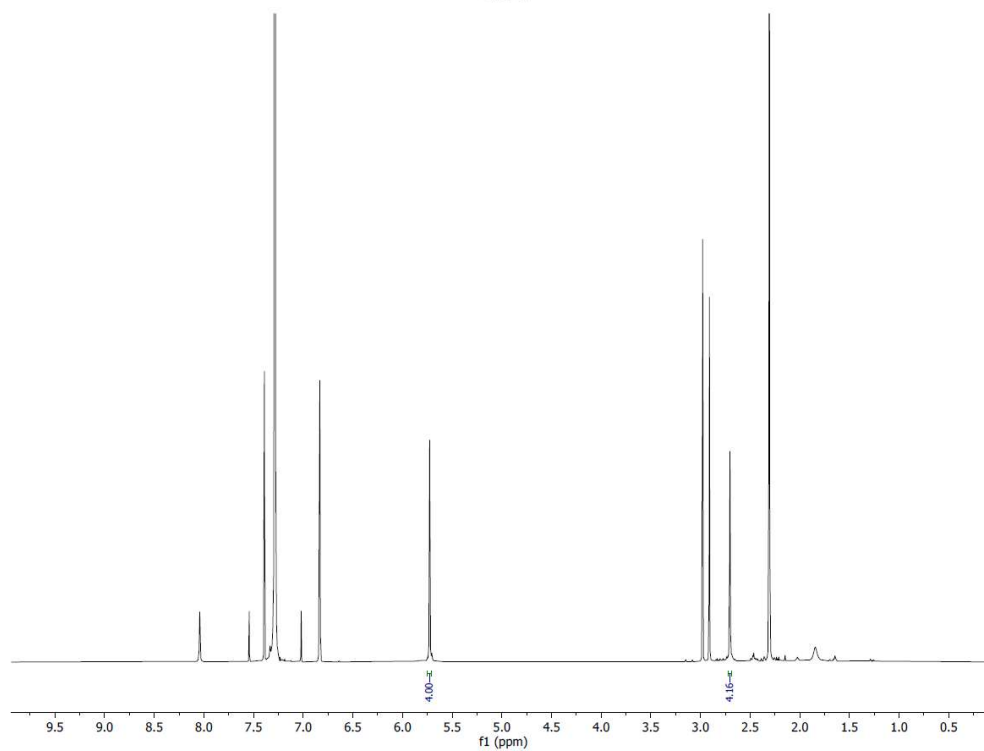
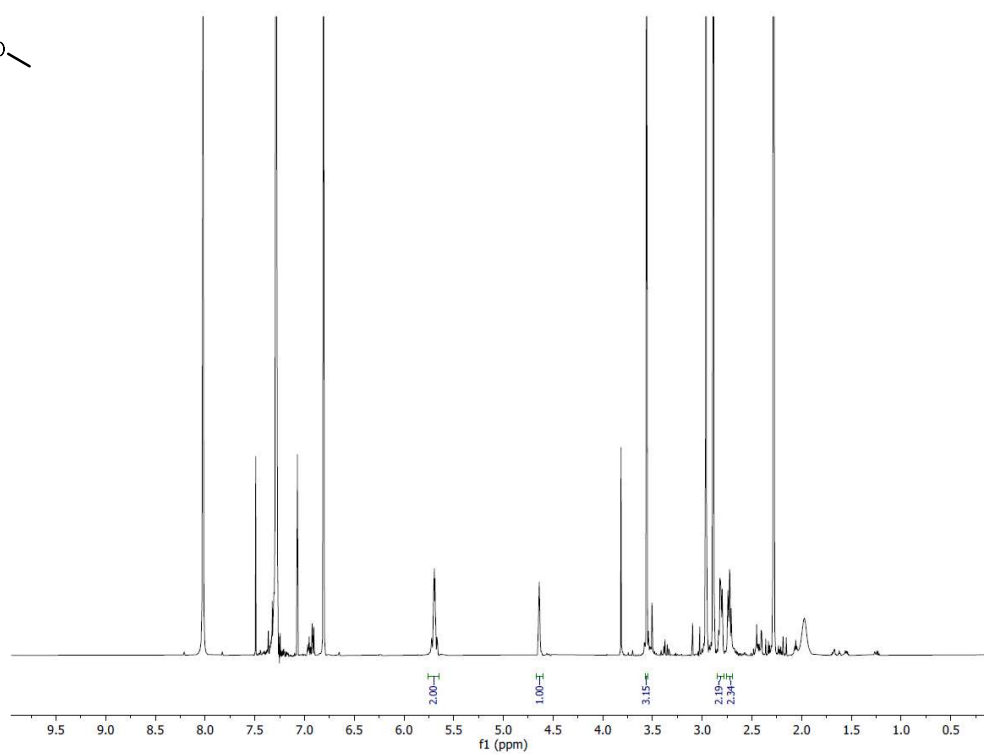
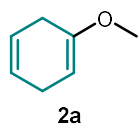


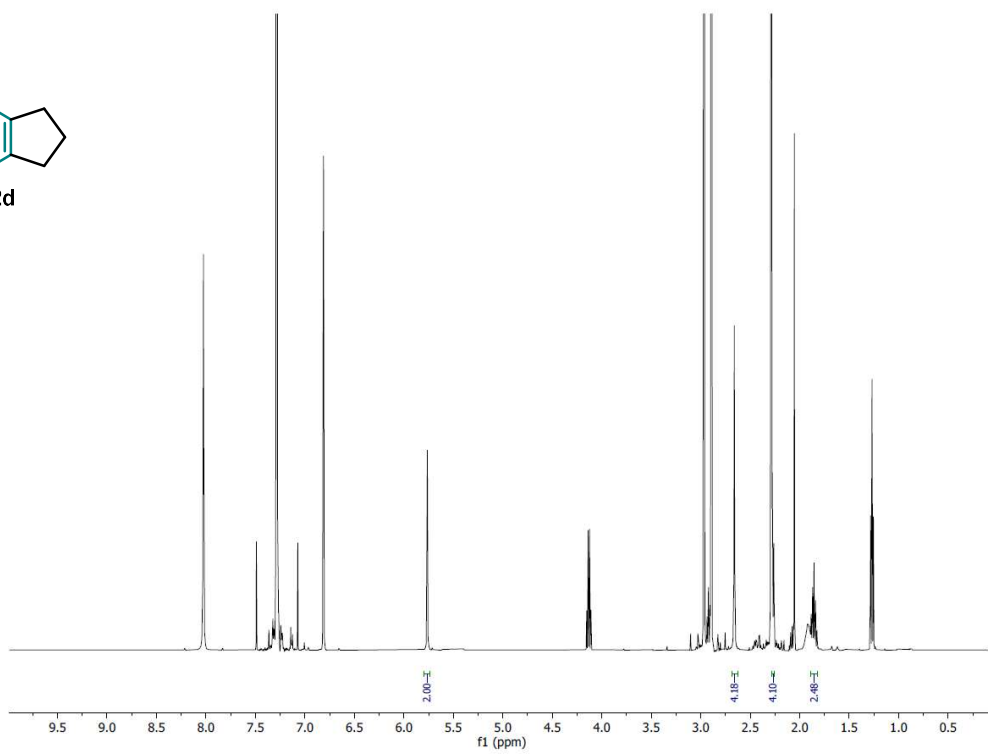
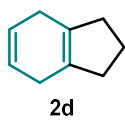
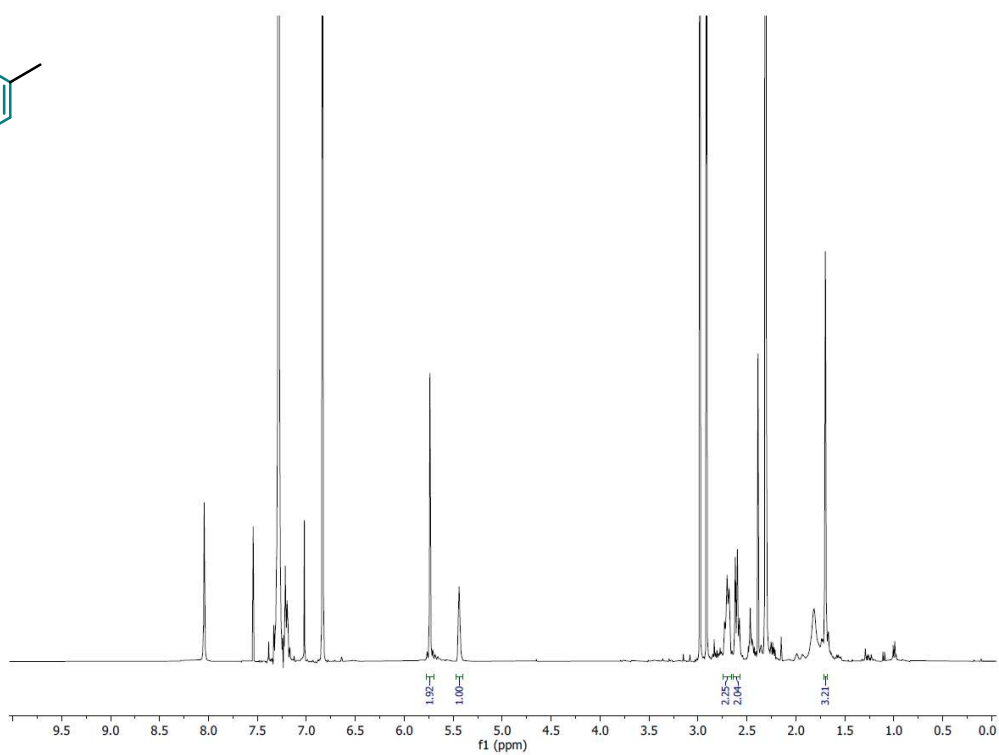
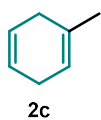


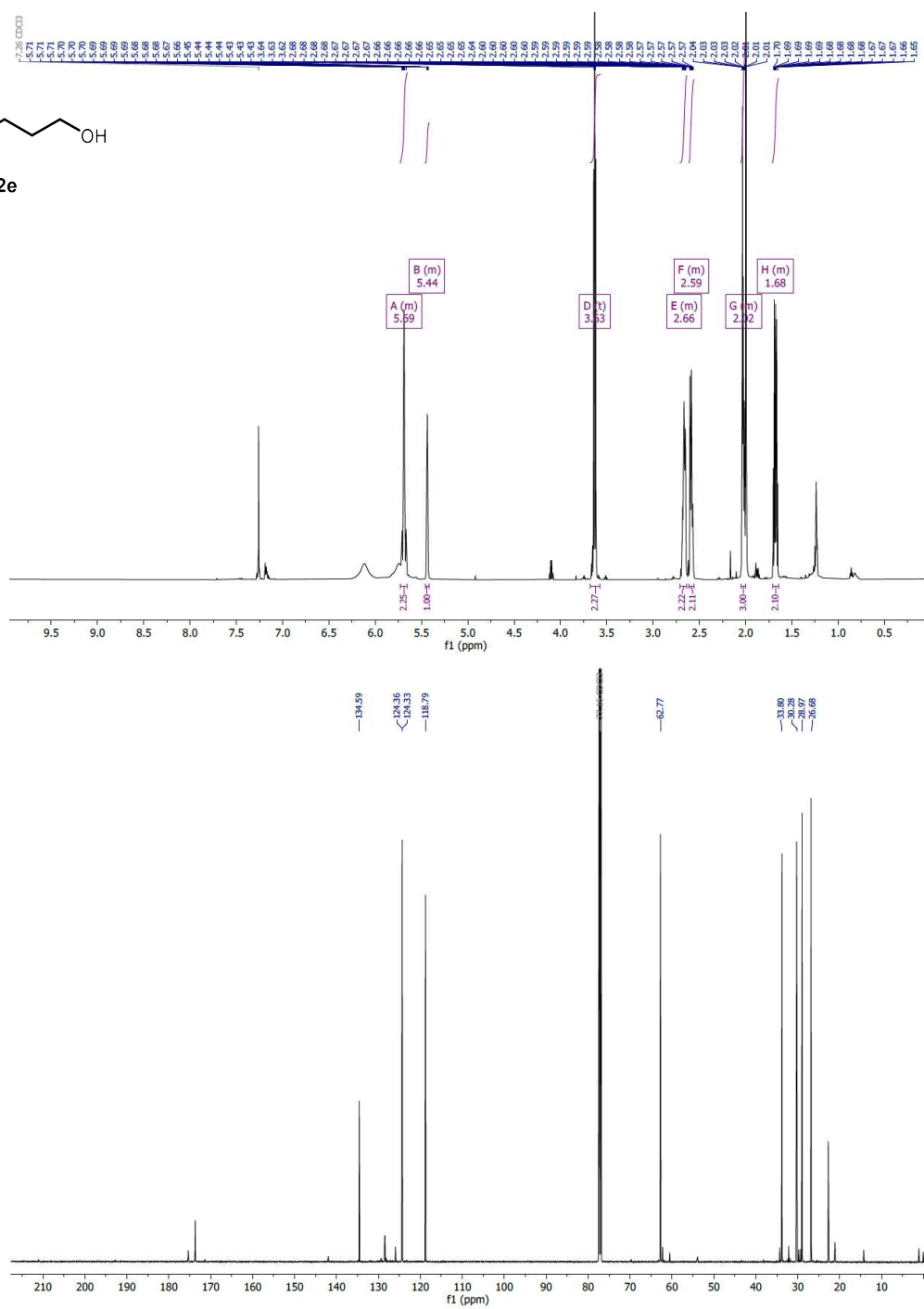
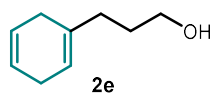


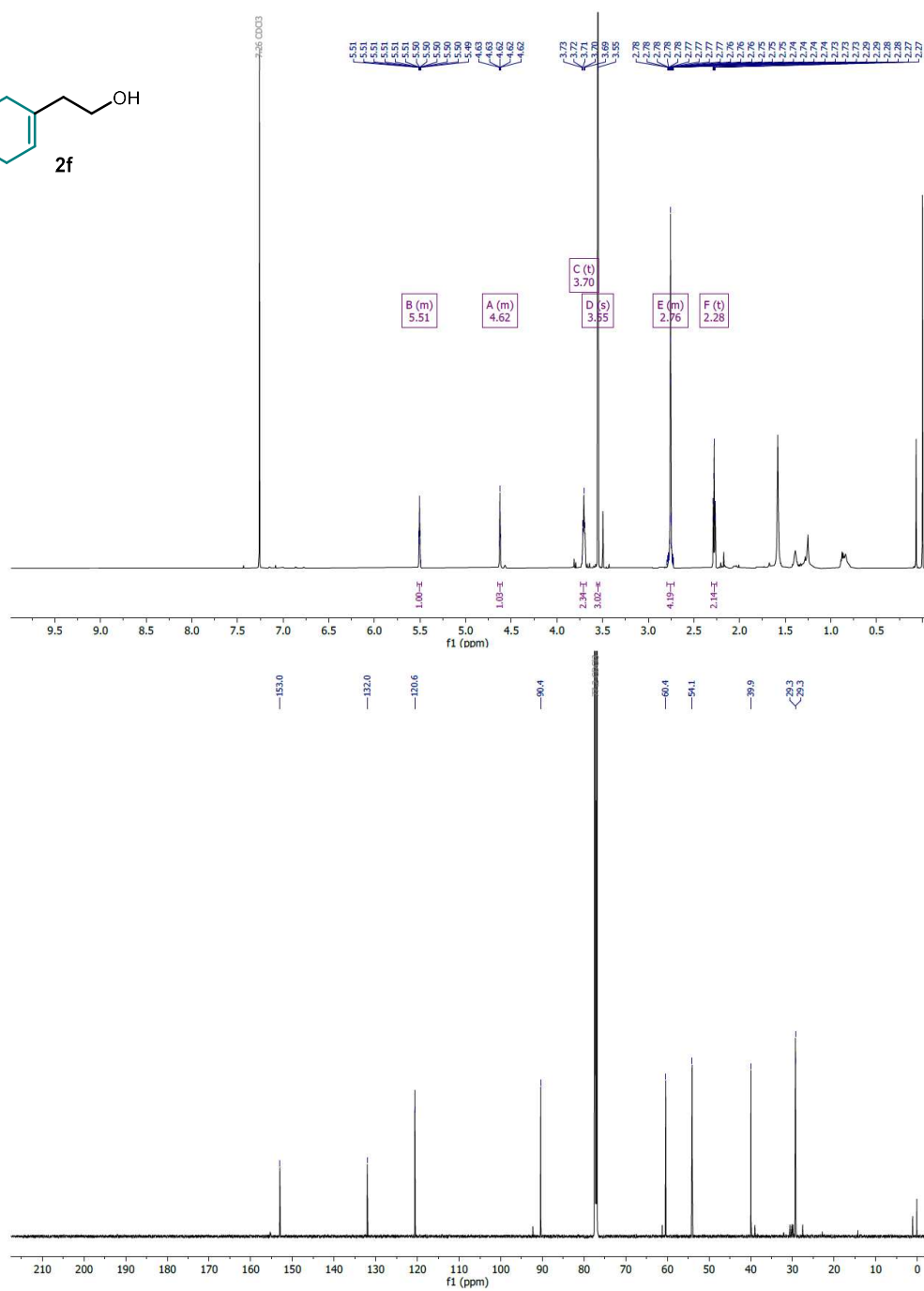
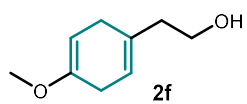


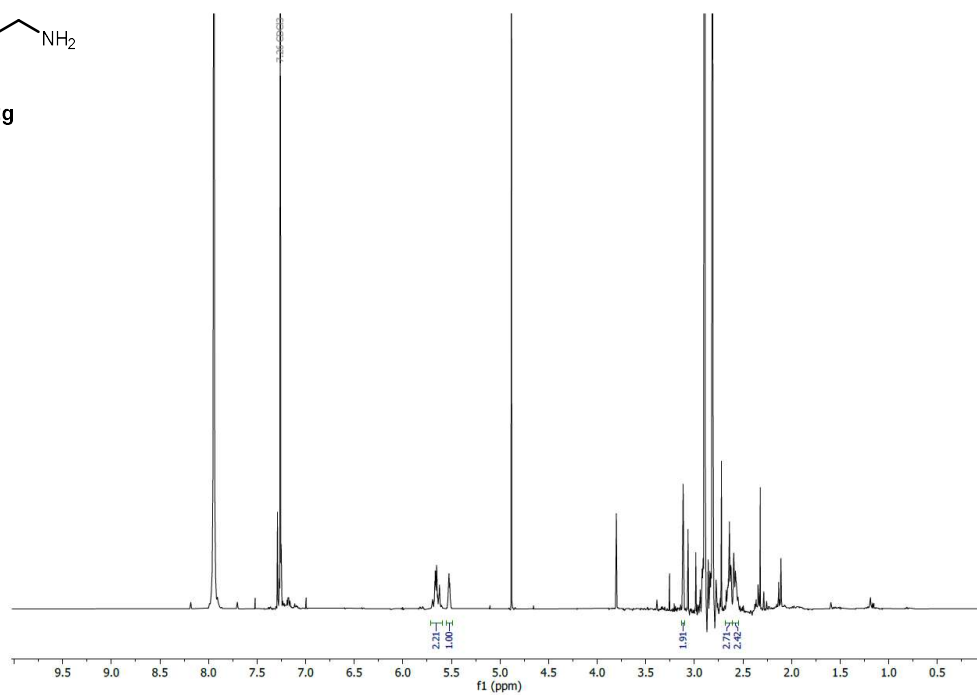
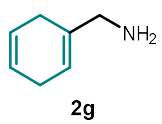


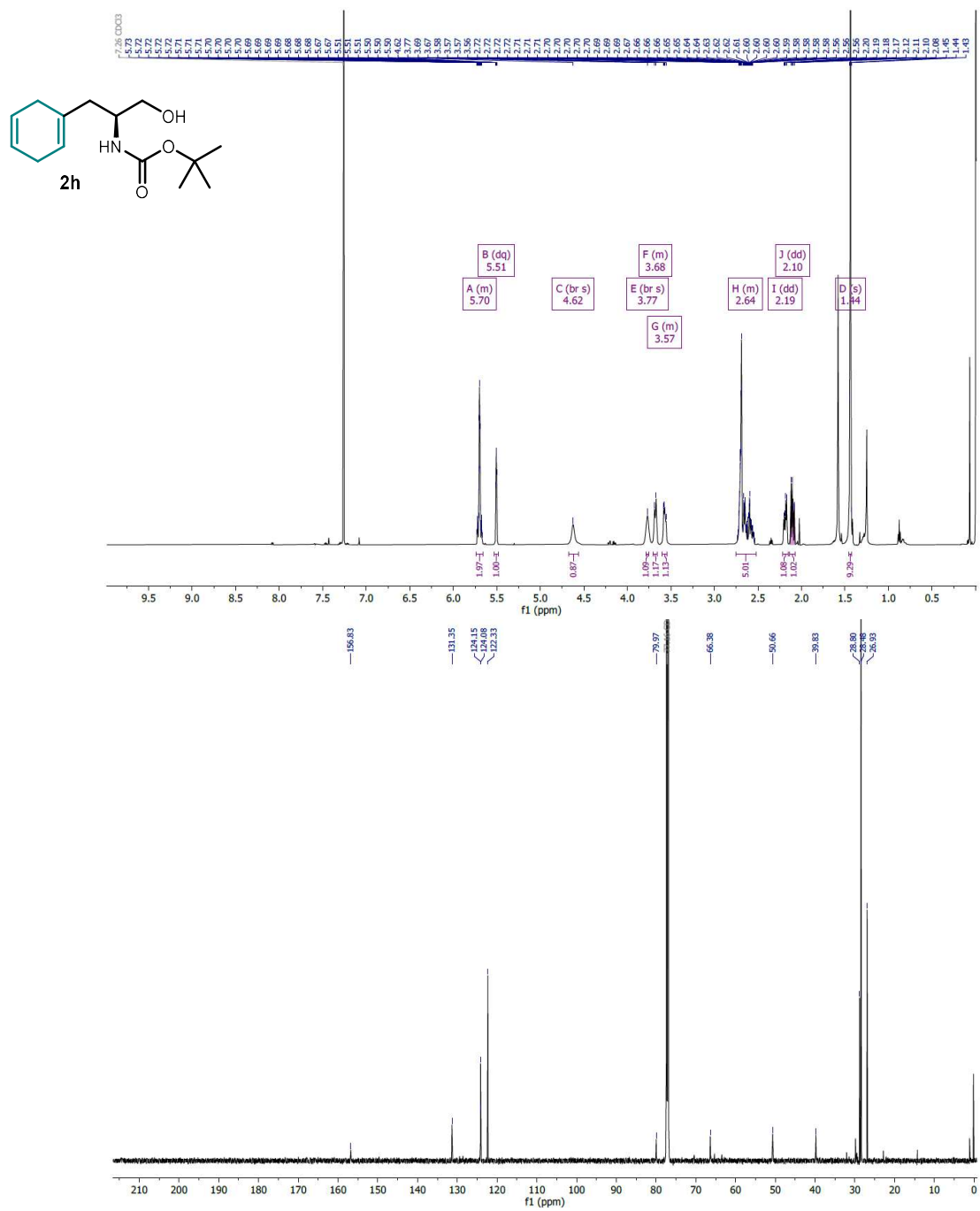


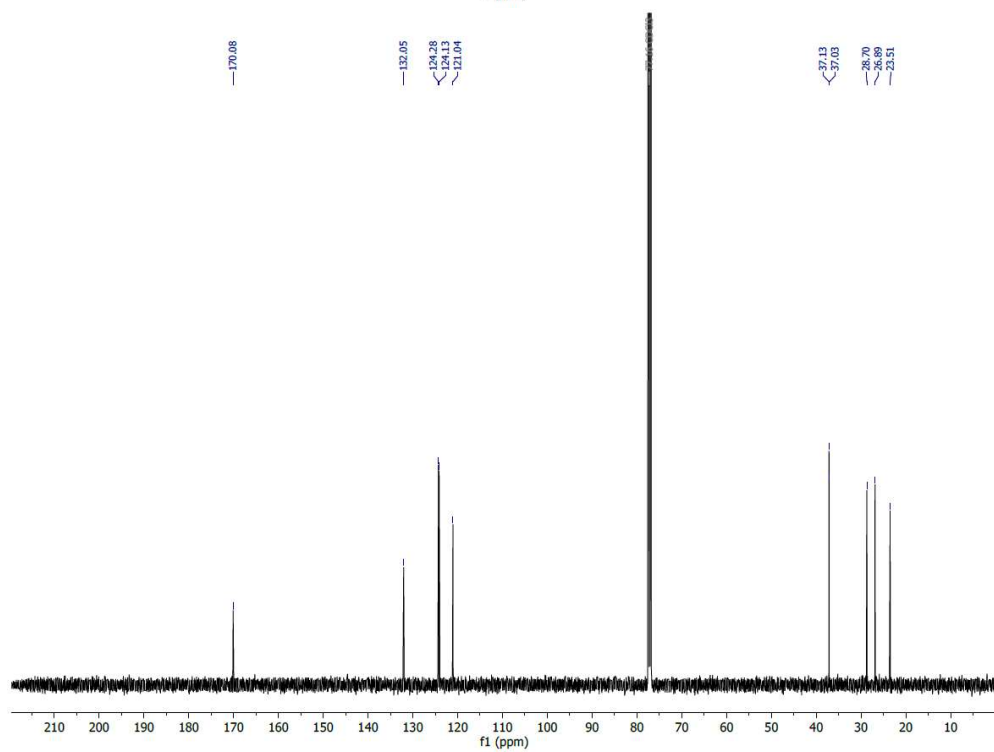
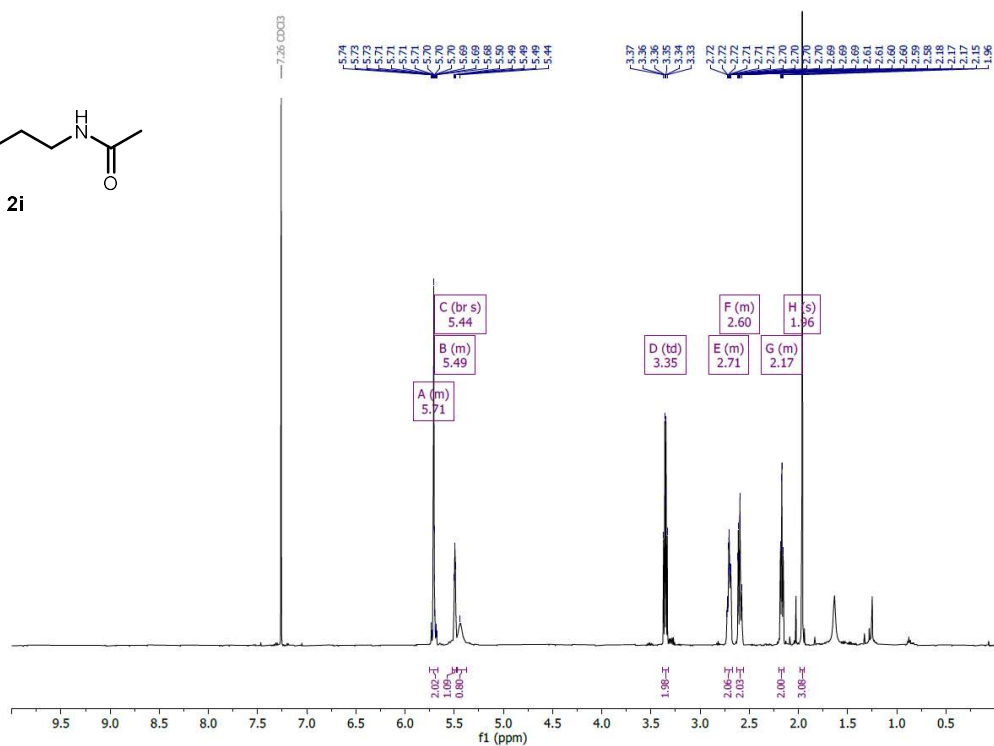
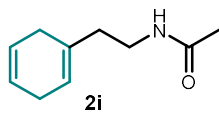


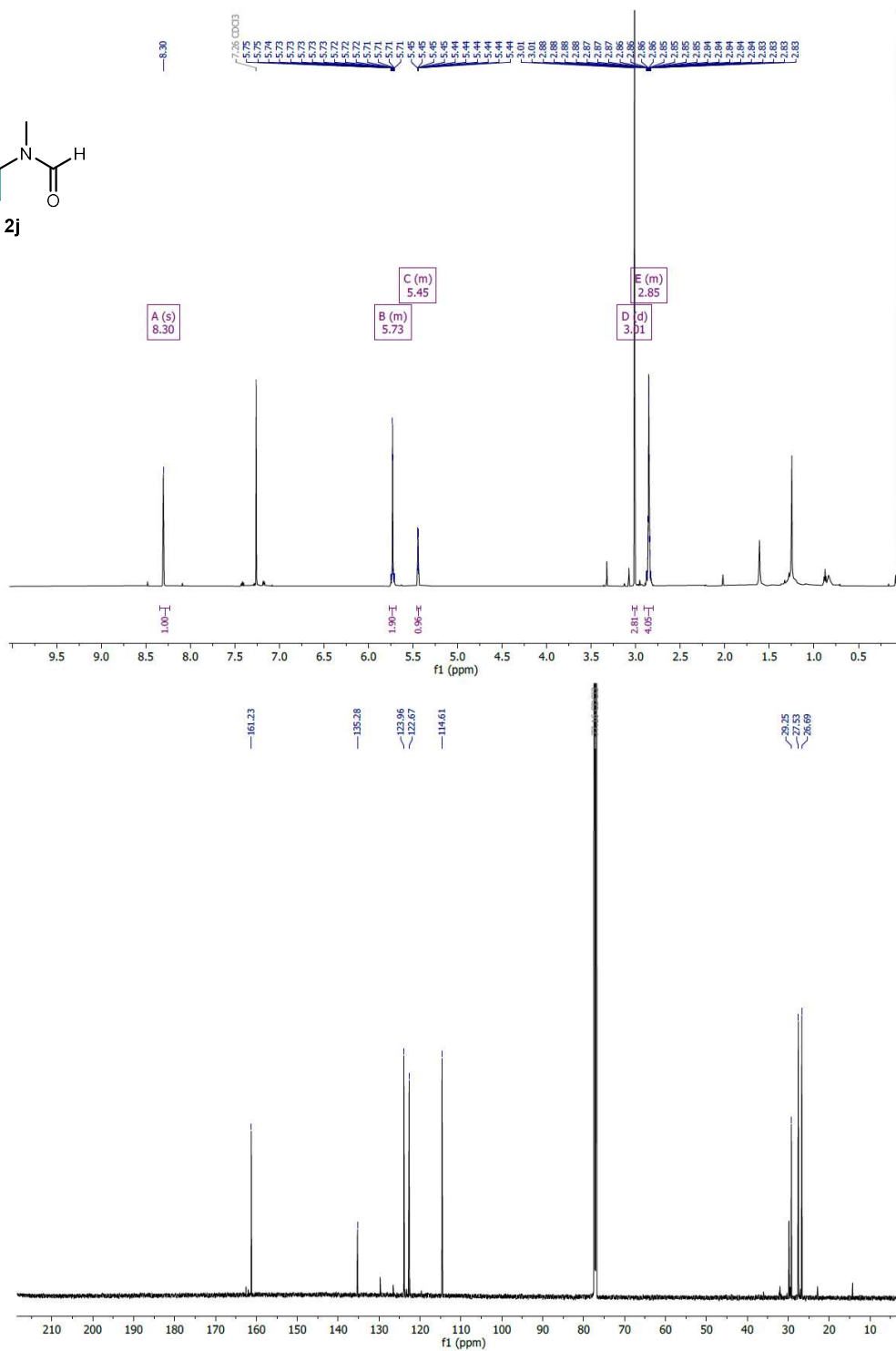
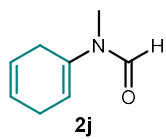


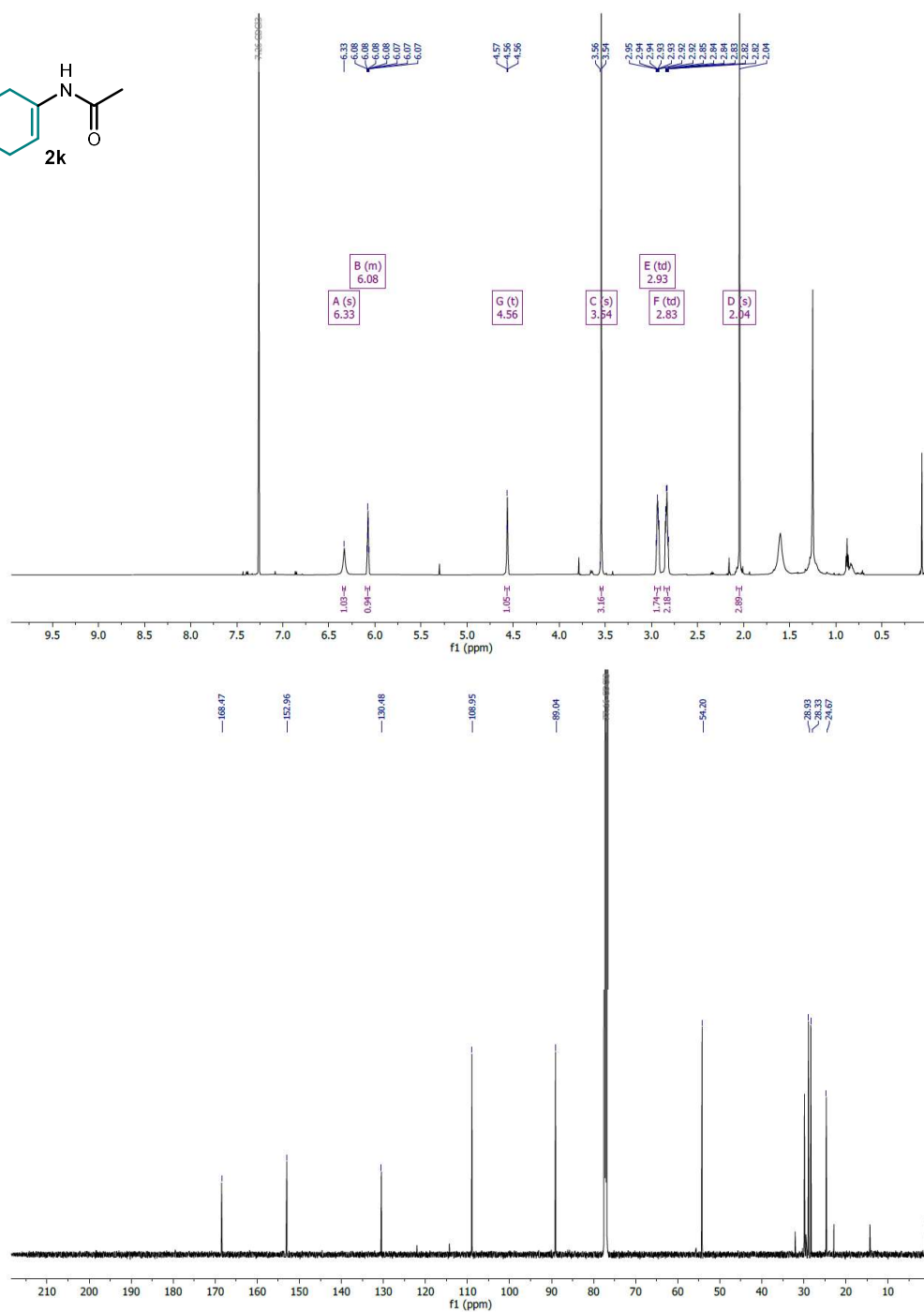
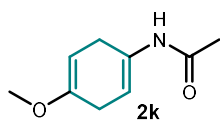


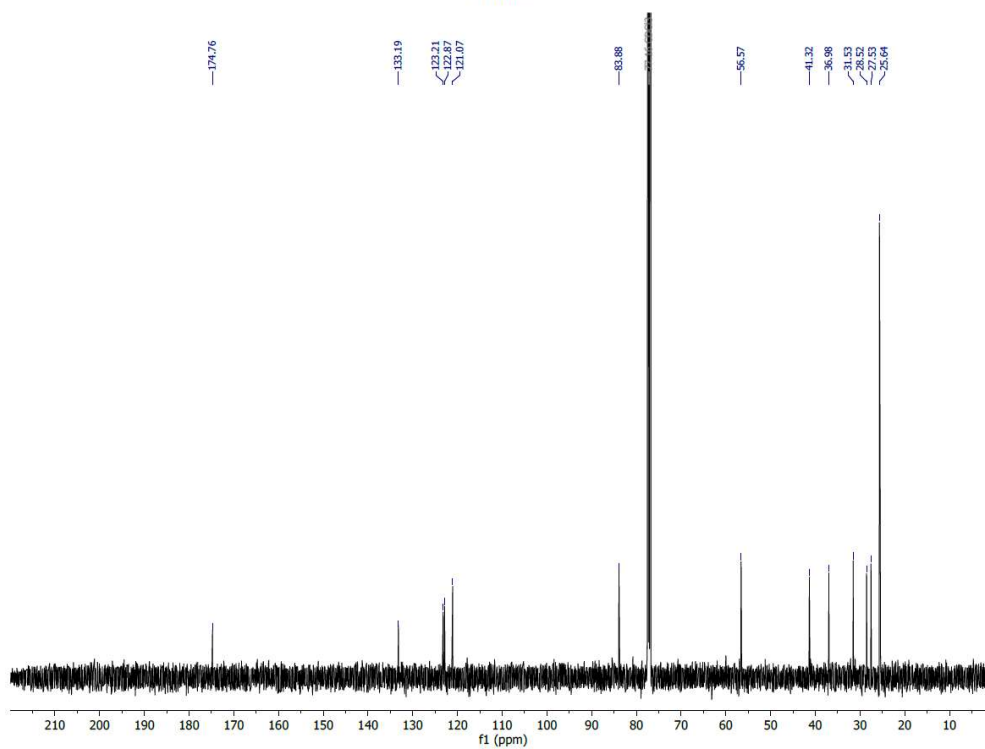
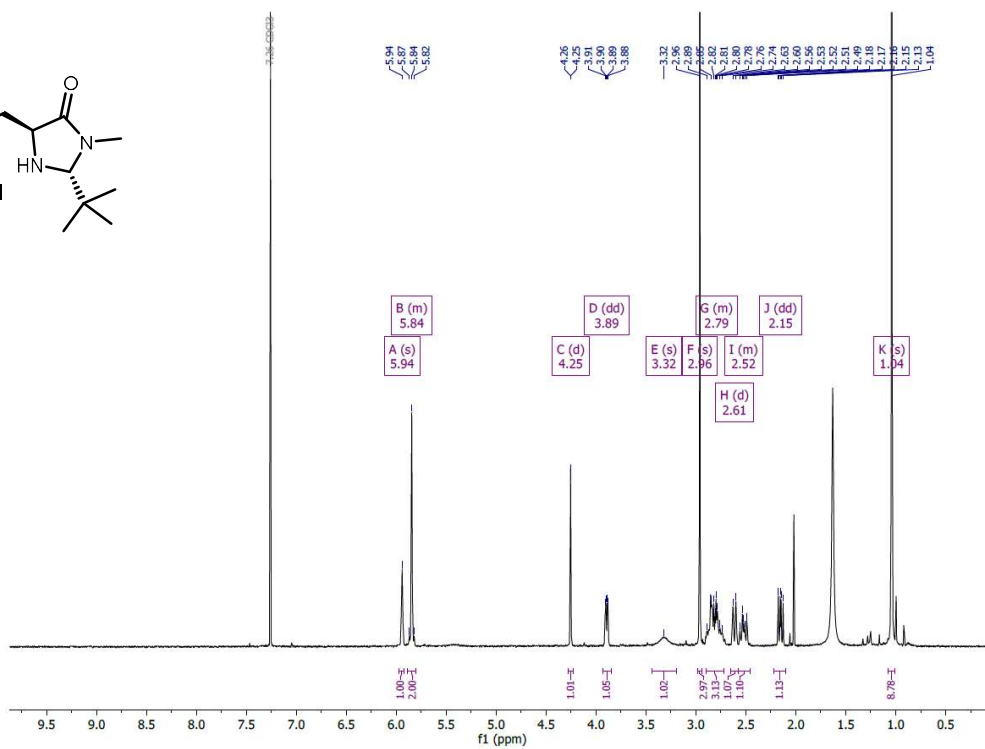
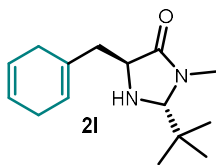


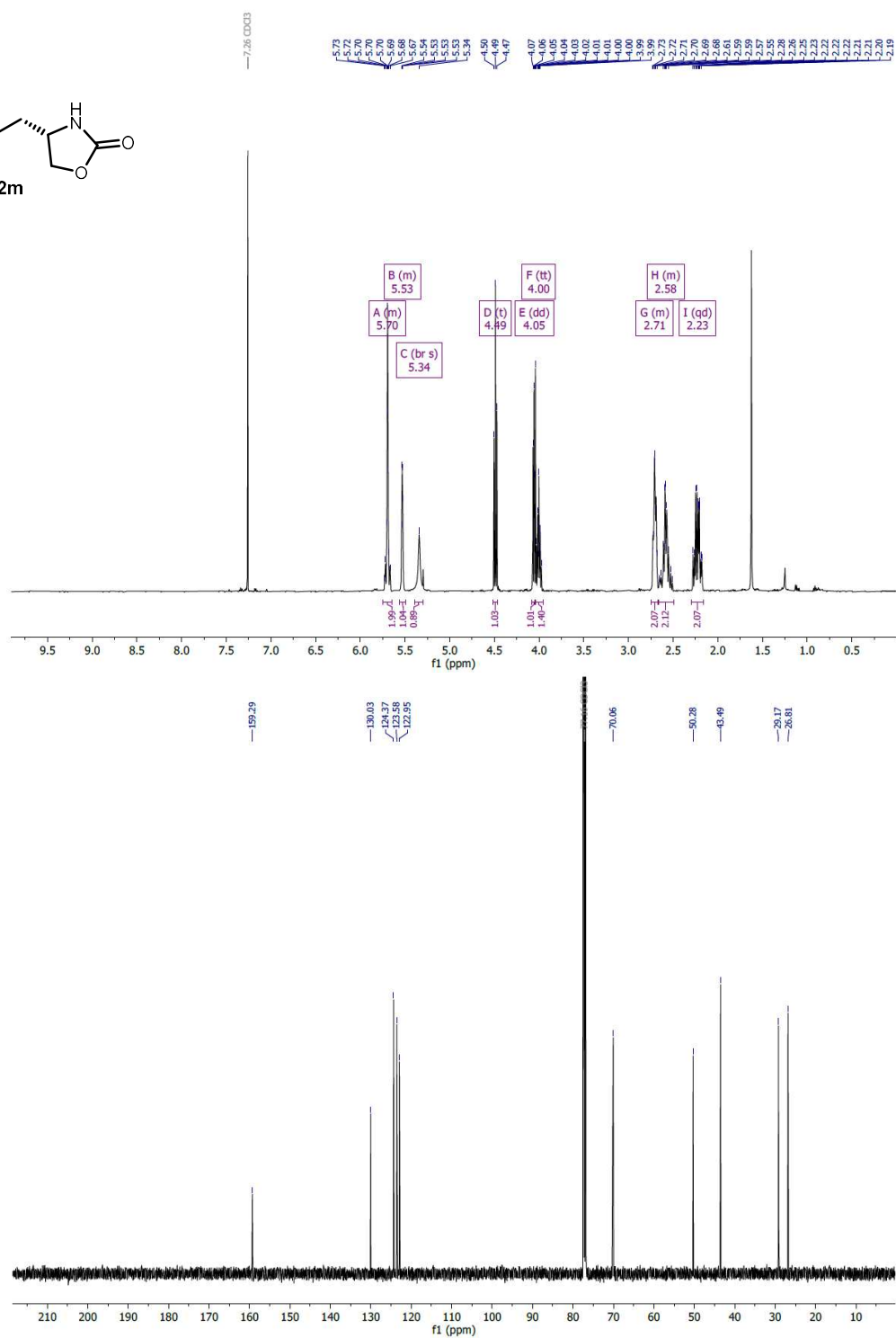
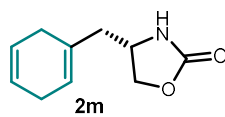


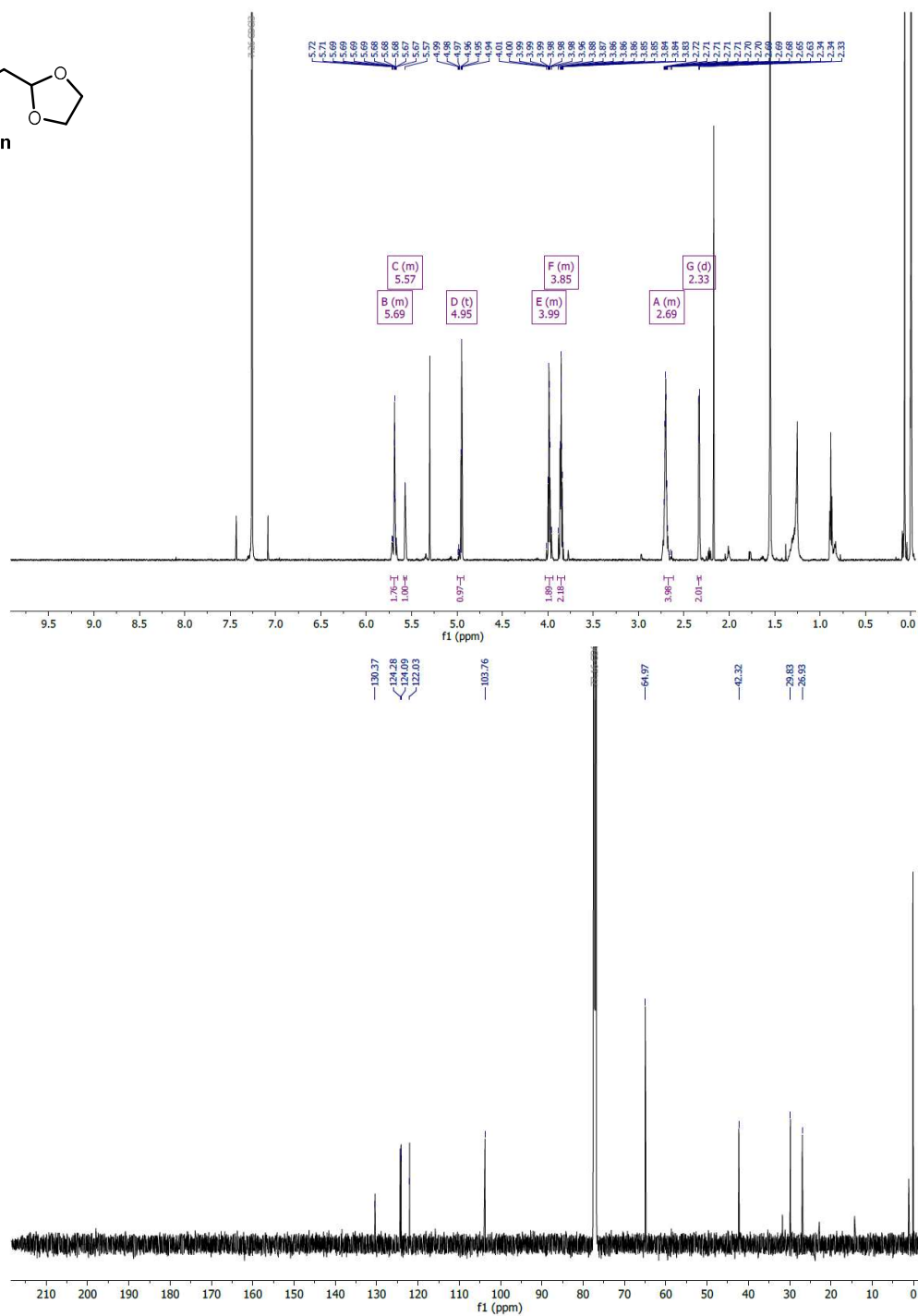
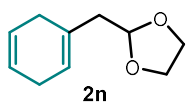


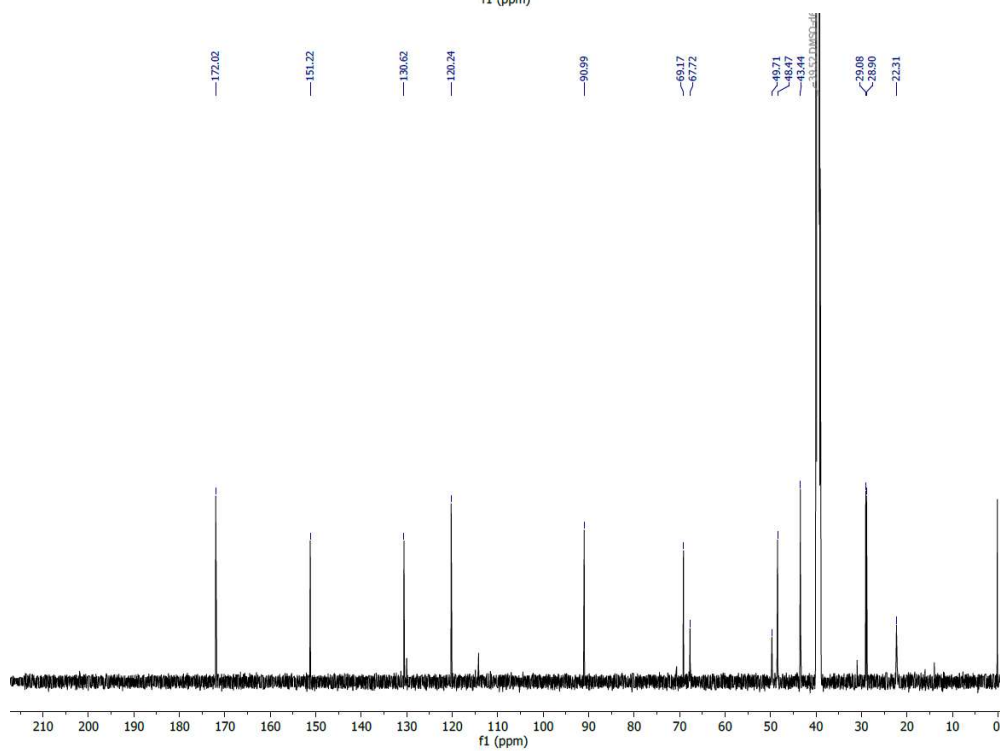
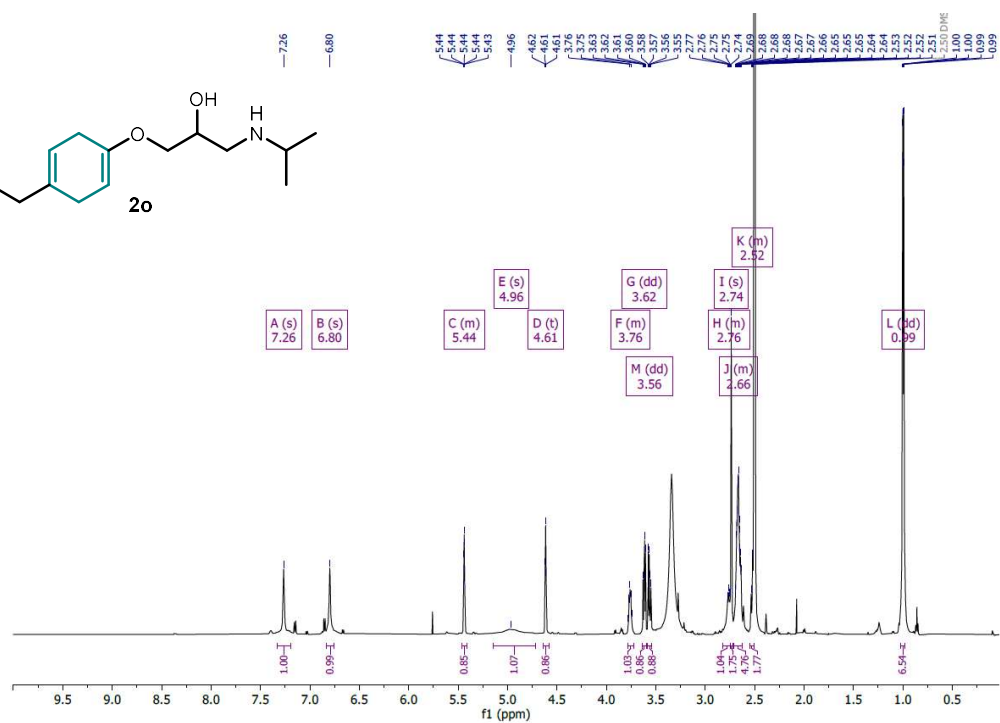
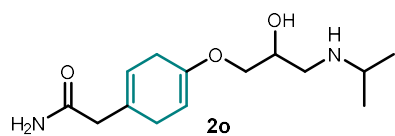


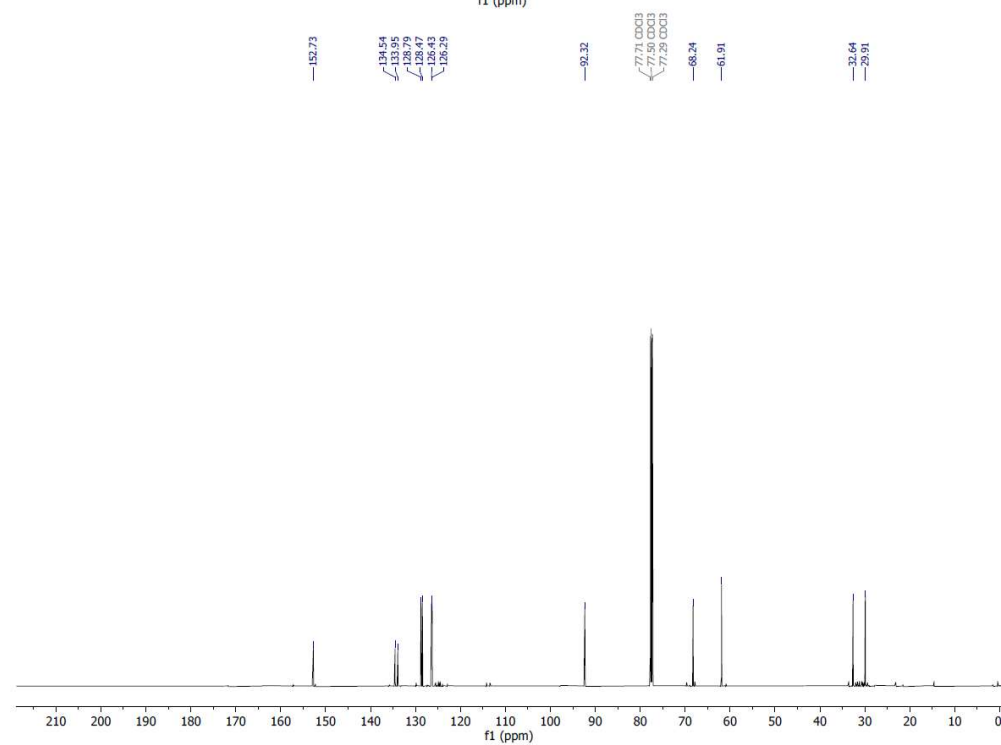
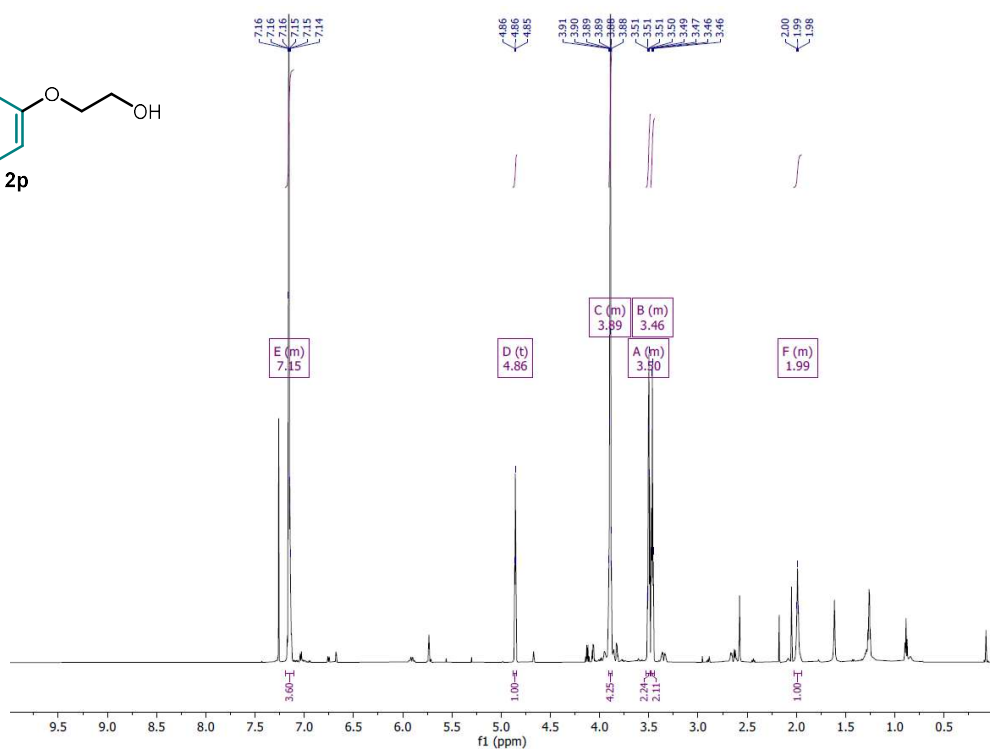
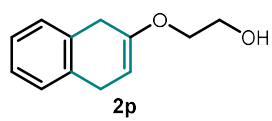


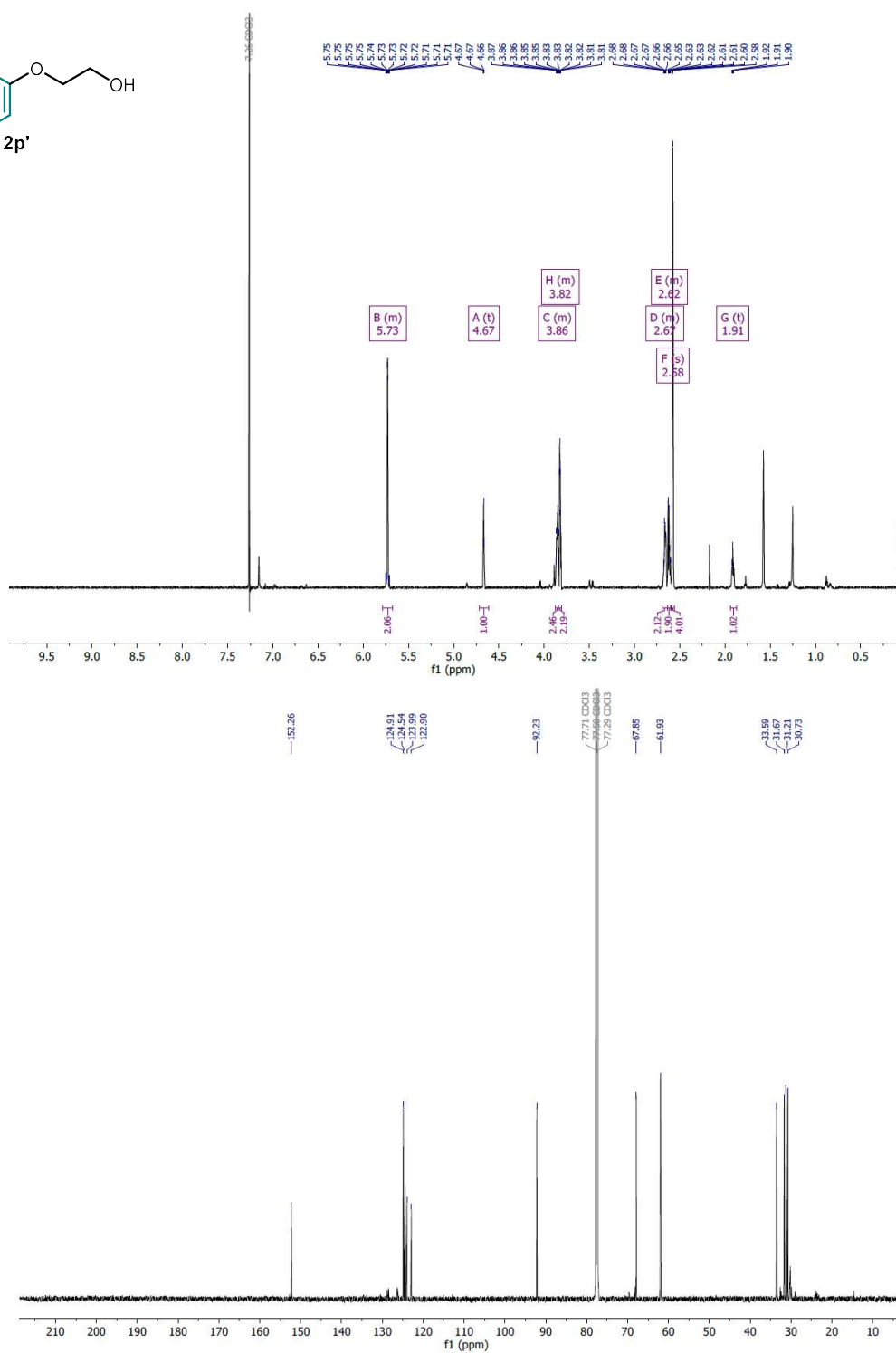
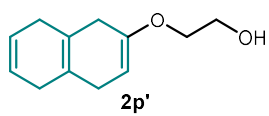


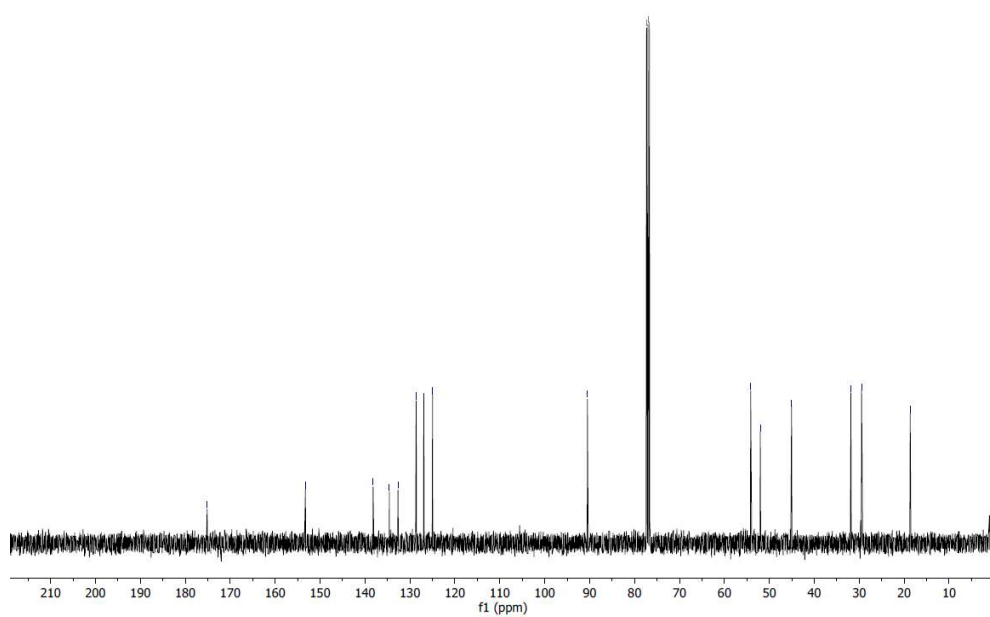
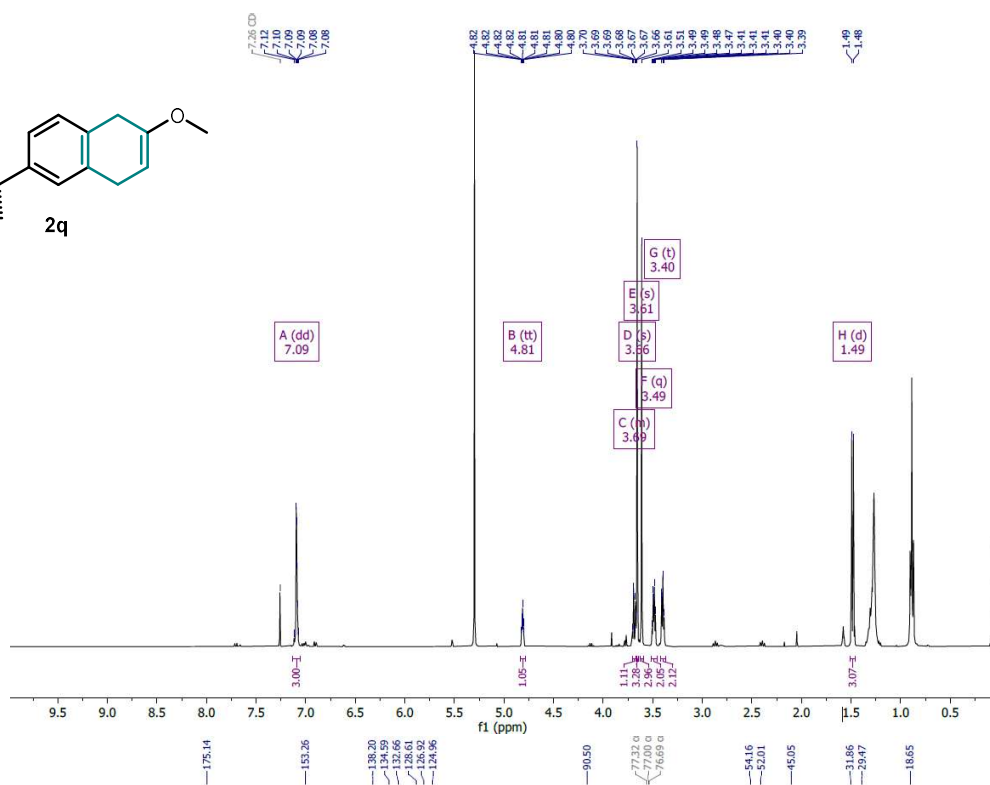
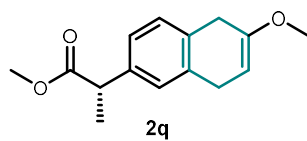


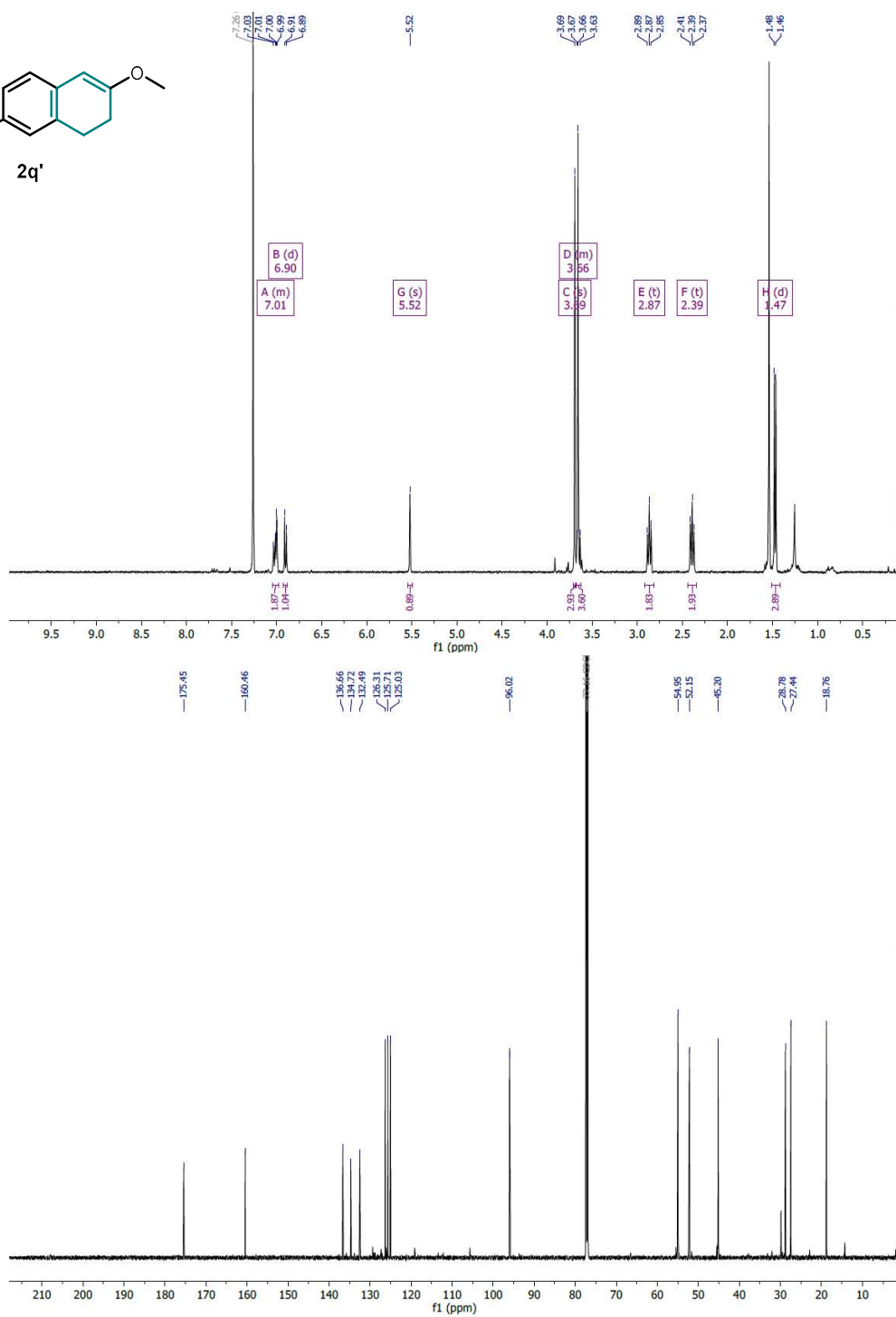
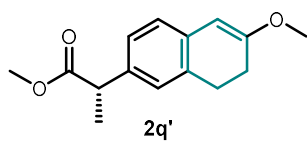


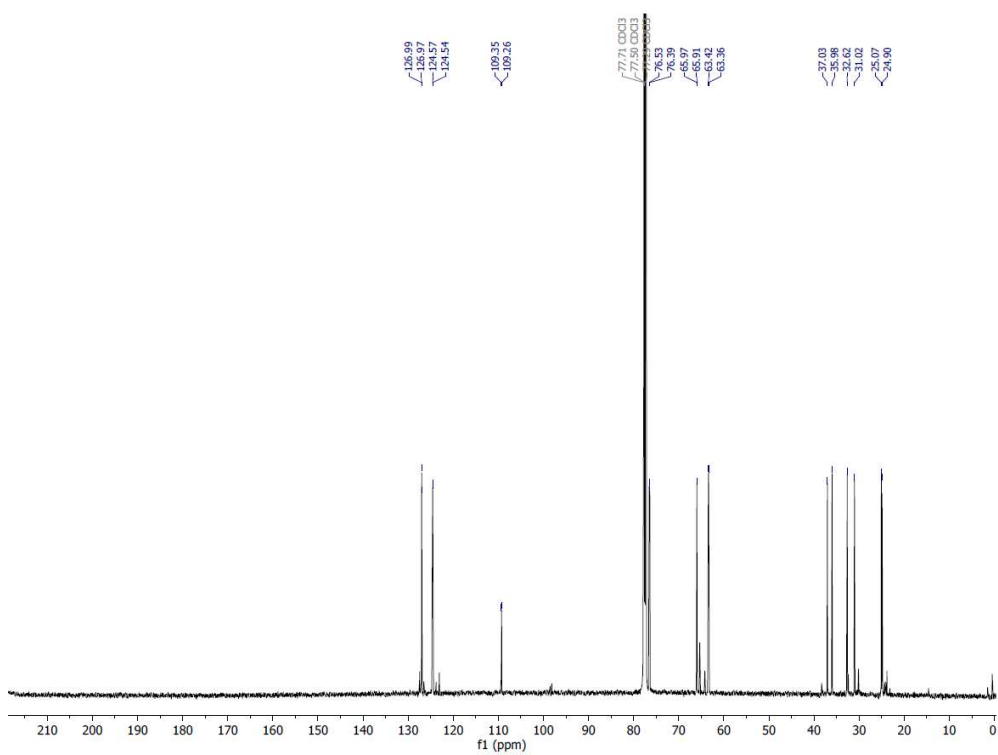
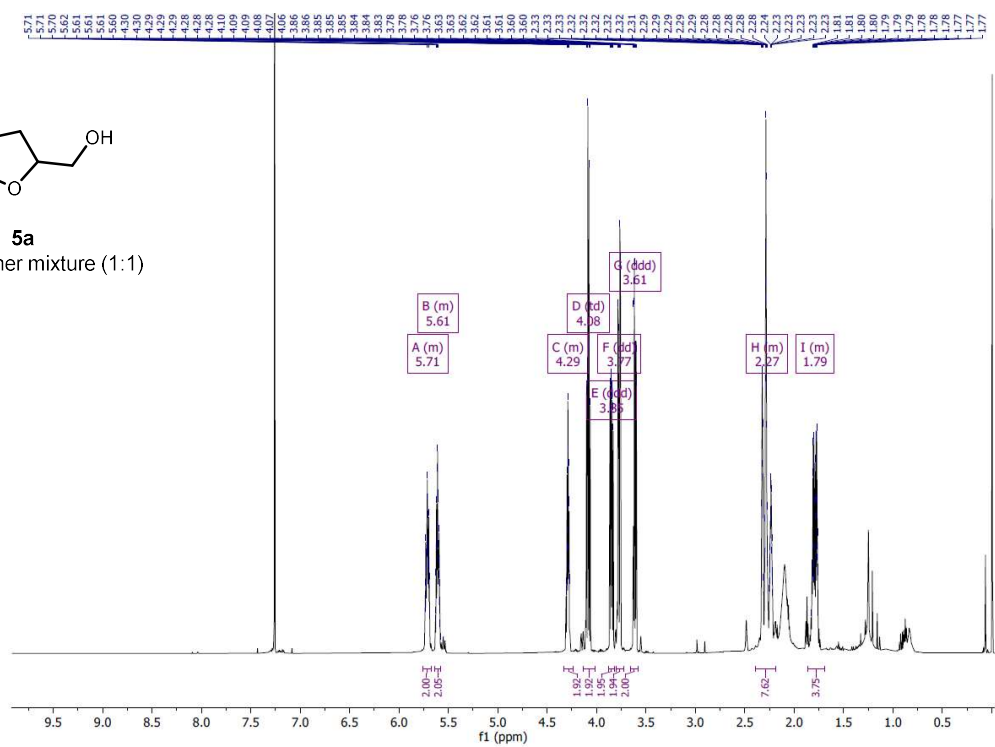
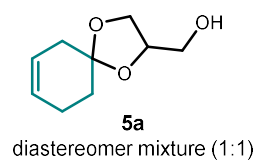


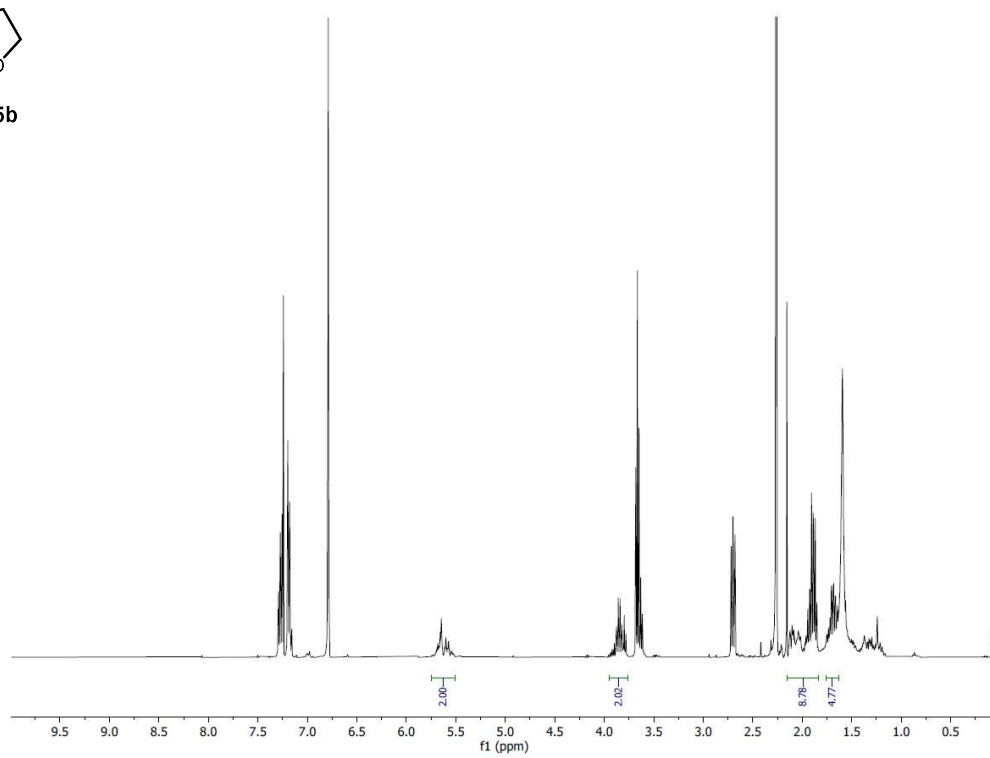
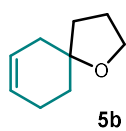


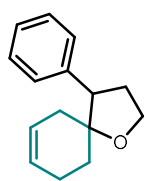




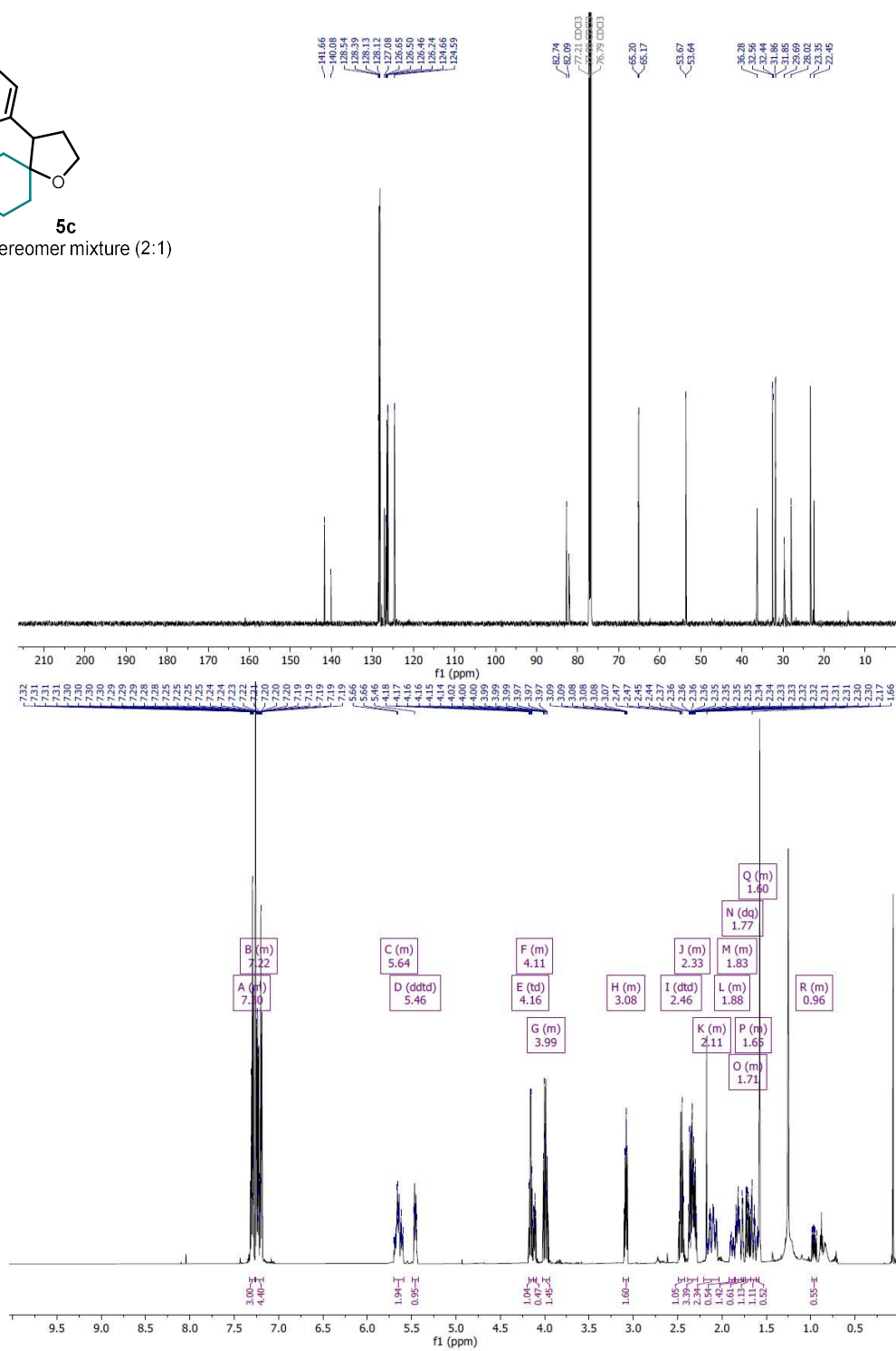


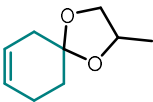






5c
diastereomer mixture (2:1)





5d

 diastereomer mixture (1:1)

